THE UNIVERSITY *of* EDINBURGH

Investigating Mechanisms of Synaptic Loss in Progressive Supranuclear Palsy

By Lois Keavey

Neuroscience (Biomedical Sciences – Centre for Discovery Brain Sciences)(MSc by Research)

The University of Edinburgh

2023

Contents

Acknowledgments

I would like to thank Professor Tara Spires-Jones for providing me with the opportunity to undertake this project, and for her continued support throughout. I would also like to express immense gratitude for all the guidance, support and inspiration given to me by Dr Robert McGeachan, who provided me with invaluable advice, as well as Jamie Rose and Elizabeth Simzer, all of whom contributed both their time and expertise to aid me in my research. I would also like to thank Kris Holt, Lewis Taylor, Dr Declan King, Dr Kat Bowles and Dr Filipa Henderson Sousa for giving me the opportunity to discuss and progress my ideas, as well as the entirety of the Spires-Jones lab for their support.

Abstract

Tau protein is generally considered to exist natively as an unfolded protein, functioning to stabilise microtubules in axons. Posttranslational modifications such as phosphorylation can influence its aggregation and oligomerisation, resulting in the formation of pathological forms of tau such as hyperphosphorylated and oligomeric tau, and neurofibrillary tangles. In tauopathies such as Progressive Supranuclear Palsy (PSP), patients experience difficulties with balance, ocular disturbance and dysphagia, as well as cognitive decline. Tau sequentially appears in a spatiotemporal pattern through functionally connected regions of the brain, with earlier presentation in the substantia nigra, and later in the frontal cortex in PSP. In this project we have utilised a sub-diffraction limit microscopy technique called array tomography, and immunohistochemical staining of paraffin embedded human post-mortem tissue. Through analysis of colocalization of pathological tau, pre-synapses, reactive astrocytes and microglia in the substantia nigra and frontal cortex, we investigated the accumulation of pathological tau at synapses, gliosis and synaptic engulfment by glia in PSP compared to age and sex matched controls. Results from array tomography suggest there is increased accumulation of hyperphosphorylated tau at pre-synapses in substantia nigra (type 3 ANOVA, $p<0.05$), plus increased colocalization of reactive astrocytes with pre-synapses in this region (type 3 ANOVA $p<0.05$). Human paraffin staining suggested that though no direct difference was observed between PSP and control cohorts, differences in colocalization of tau and pre-synapses with reactive astrocytes and microglia between PSP and control brains were found to be effects of the different brain regions studied, and disease progression with age. Diaminobenzidine (DAB) staining with AT8 allowed observation of increased burden of hyperphosphorylated tau in PSP compared to controls in both frontal cortex and substantia nigra (type 3 ANOVA $p<0.05$) and observation of the variation of tau burden across both PSP and control cases. Linear mixed effects models (type 3 ANOVA) were used for all analyses. By illustrating the accumulation of pathological tau at pre-synapses and reactive astrocytes, we have built upon previous evidence of tau accumulation within the PSP brain, supporting the hypothesis that synaptic accumulation of tau may lead to dysfunction, and loss of synapses.

Lay Summary

Tau is a protein that helps keep cells in the brain called neurons structurally stable. Chemical changes to tau protein can cause it to stick to other individual tau proteins to form clumps, which can then also stick together to form larger tangles. These changes to tau protein cause it to become toxic to the brain. It is thought that this toxic tau can spread through the brain across connections between neurons, known as synapses. Astrocytes and microglia are cells that are free to move throughout the brain, and act to combat injury or infection in the brain. It is also thought that these cells may have a role in the spread of toxic tau across different parts of the brain, as well as destroying synapses between neurons that contain toxic tau. Diseases where we see these changes to tau and the negative effects it has on the brain are called tauopathies, such as Alzheimer's Disease and Progressive Supranuclear Palsy, also called PSP. Patients with PSP suffer from loss of balance, and issues with eyesight and swallowing. In this project we collected human brain tissue taken after death of patients with PSP and those with normal brains. Using imaging techniques that allow us to see high levels of detail, we aimed to investigate whether toxic tau is collecting in synapses more in PSP brains compared to normal brains. We also aimed to explore if there was a difference in how many astrocytes and microglia might be involved in destroying synapses between PSP and normal brains, by observing differences in how many astrocytes and microglia are seen overlapping with toxic tau and synapses. We found that one kind of toxic tau collected significantly more in the first part of the synapse connection (also called the pre-synapse) in PSP compared to normal brains. We also saw more astrocytes overlapping with pre-synapses in these PSP cases than in normal brains. Additionally, there appeared to be differences in how much toxic tau overlapped with microglia and astrocytes between the two parts of the brain we focused on. This work shows us that toxic tau does collect in synapses and astrocytes, and may help us to understand how synapses lose their function and are removed from the brain in PSP.

Introduction

i. Tauopathies and Progressive Supranuclear Palsy

Tauopathies are a group of neurodegenerative disorders, generally characterized by the inclusion of pathological tau protein in neurons and sometimes glia, the resulting phenotypes of which are varied and complex. Movement, cognition, language, and behaviour can all be affected by synaptic destruction and neuronal loss as a result of accumulation of pathological tau (Zhang *et al.,* 2022). Alzheimer's disease (AD), potentially the most well-known tauopathy is characterized by the accumulation of both amyloid-β peptide, and tau protein, resulting in gradual, progressive cognitive impairment and dementia affecting 43.8 million people worldwide in 2016 (Ittner and Götz, 2011; Li *et al.,* 2022). Other tauopathies include progressive supranuclear palsy (PSP), frontotemporal dementia (FTD) and corticobasal degeneration (CBD) (Fig. 1). Of the 55.2 million people worldwide currently suffering from dementia, 2.6% are thought to be caused by FTD, and incidence of PSP and CBD have been assessed at 2.6 and 0.4 per 100,000 people per year (Zhang *et al.,* 2022).

PSP patients experience difficulties with balance (postural instability), akinesia (loss of control of the limbs), dysphagia, amongst other lingual and cognitive disorders, and visual and ocular disturbances (Alster *et al.,* 2020a; Pîrscoveanu *et al.,* 2017). However, PSP can present with varying, but distinct characteristic clinical phenotypes (Dickson *et al.,* 2007). Patients diagnosed with PSP (average age of onset in mid-60s) typically experience a slow disease course, typically living for 5-7 years after the onset of symptoms, though rapid progression is occasionally seen, with a duration of 2-3 years (Armstrong et al., 2014; Coughlin and Litvan, 2020). Those with PSP can also often develop dementia associated with cortical pathology such as neurofibrillary tangles (NFTs) and reactive glia (Armstrong et al., 2007; Bigio *et al.,* 1999). Furthermore, cases of PSP diagnosed pathologically can be difficult to recognize in their clinical presentation. Those diagnosed with PSP-Richardson's syndrome (PSP-RS) present with what is classed as the core clinical features of PSP, including early onset of falls and postural instability, as well as supranuclear vertical gaze palsy and cognitive dysfunction (Alster *et al.,* 2020a; Williams *et al.,* 2005). It is generally understood that anatomical regions affected earliest in PSP-RS include subcortical nuclei and certain brainstem nuclei, with earliest appearance of neuronal tau in the substantia nigra, globus pallidus and subthalamic nucleus. Analysis of heat maps and distribution patterns of neuronal, astroglial and oligodendroglial tau pathologies in postmortem brains has provided evidence of sequential distribution of tau pathologies across different brain regions in clinical subtypes of PSP (Fig. 3). The sequential spread following AD progression has been classified into 'Braak stages' I-IV, referencing brain regions burdened by the accumulation of pathological tau (Robbins *et al.,* 2021); a similar sequential patterning has been shown in PSP (Kovacs *et al.,* 2020). Accumulation of astroglial and oligodendroglial tau tend to follow similar patterns of spread, though these show earliest signs of accumulation in the striatum and globus pallidus, respectively (Kovacs *et al.,* 2020). Structural imaging biomarkers such as the 'hummingbird sign' resulting from midbrain atrophy (Massey *et al.,* 2012), and quantitative MRI signature 'magnetic resonance parkinsonism index' (Quattrone *et al.,* 2008), can be useful when identifying or differentiating PSP patients from different diagnoses with similar clinical phenotypes, though with varying specificity and

sensitivity; generally it is easier to visualize these structural changes when the disease is more progressed (Coughlin and Litvan, 2020).

Alternatively, those with PSP-parkinsonism (PSP-P), which can be confused with Parkinson's disease (PD) due to overlapping clinical presentation (particularly in early stages of development) show tremor and asymmetric onset, and initially some response to levodopa, a common anti-parkinsonism drug. Comparison of biochemical and genetic characteristics of 103 pathologically confirmed PSP cases identified 54% as having PSP-RS, and 32% with PSP-P, a statistic replicated in other studies (Alster *et al.,* 2020a; Williams *et al.,* 2005). Further studies have suggested around one third of PSP patients will ultimately gain a diagnosis of PSP-P, likely after initial presentation marked as PD. Furthermore, those with PSP-P show longer survival than those with PSP-RS, and may only develop clinical symptoms to match those associated with PSP-RS years later (Coughlin and Litvan, 2020). Other 'atypical' forms of PSP include frontal PSP (PSP-F), where patients present with symptoms such as behavioural changes and apathy, similar to those observed in frontotemporal dementia (FTD). These behavioural changes are often the earliest clinical manifestation of the PSP, affecting the frontal areas predominantly (Han *et al.,* 2010). In PSP-speech-language variant (PSP-SL), patients may present with progressive non-fluent aphasia with apraxia of speech (Josephs *et al.,* 2006a; Mochizuki *et al.,* 2003). A further complication of diagnosis lies with those who present with symptoms of corticobasal degeneration (CBD), such as limb apraxia, dystonia and myoclonus, and sensory deficits, a third of whom may be found to have pathology associated with PSP at autopsy, as opposed to CBD (Lee *et al.,* 2011). The clinical variation of PSP subtypes can result in difficulties in diagnosis, though efforts are being made to clarify diagnostic criteria between subtypes (Höglinger *et al.,* 2017). As brain regions affected earliest in disease progression in atypical PSP subtypes don't always align with those in PSP-RS, this may also add to the difficulties surrounding diagnosis and ultimately, treatment.

Beyond the macroscopic pathology including atrophy and loss of brain weight, PSP can be characterized on the microscopic level. NFTs, which can often appear globose, mostly affect the substantia nigra, subthalamic nucleus and globus pallidus, though they can also be present in other regions of the basal ganglia, brainstem and regions affected later in disease progression (Dickson *et al.,* 2007). Tau-positive heterogenous cytoplasmic granules, containing β-sheet structure (there have been conflicting reports as to this factor, though even partially folded tau monomers and filaments contain this structure) characterize initial accumulation of tau in neurons in the form of pre-tangles (Cowan and Mudher, 2013; Ferrer *et al.,* 2014). Tangles, or NFTs occur as compact accumulations of bundles of tau-positive fibrils (Ferrer *et al.,* 2014). Evidence of tangles *in vivo* has suggested aggregation of soluble, toxic forms of tau into filamentous and fibrillary forms may actually be protective in the short term, as caspase activation that could lead to cell death was reversed. Furthermore, caspase activation has been observed prior to formation of NFTs in soluble tau containing neurons in mouse models (Spires-Jones *et al.,* 2011). Tau pathology is linked with presence of reactive astrocytes and microglia, and other chronic neuroinflammatory processes (Vogels *et al.,* 2019). Tufted astrocytes, amongst other products of gliosis, are a characteristic feature of PSP, and are generally considered to be seen exclusively in PSP. Tufted astrocytes have morphological changes specific to tau inclusions (Ikeda *et al.,* 2016; Kovacs, 2020). They can be most commonly found in

Tauopathy	Primary/ Secondary	Tau pathology	Presentation and symptoms	Tau isoform
Alzheimer's Disease (AD)	Secondary (with amyloid-β pathology)	Neurofibrillary tangles	Memory loss, behavioural dysfunction, sleep pattern changes, apathy and anxiety	3R/4R
Argyrophilic grain disease (AGD)	Primary	Argyrophilic grains, oligodendrocytic coiled bodies and pre-tangles	Cognitive decline	4R
Chronic traumatic encephalopathy (CTE)	Primary	Neurofibrillary tangles and glial tangles	Memory loss, behavioural dysfunction	3R/4R
Corticobasal Degeneration (CBD)	Primary	Neurofibrillary tangles, coiled bodies, argyrophilic threads, astrocytic plaques	Asymmetrical limb apraxia, levodopa-resistant parkinsonism, cognitive deficits	4R
Frontotemporal Dementia (FTD) (+ Pick's Disease (PiD) + Parkinsonism linked to chromosome 17 (FTDP-17))	Primary	Neuronal and glial tau deposits (FTD and FTDP-17) Pick bodies (PiD)	Motor deficits, disinhibition and behavioural dysfunction, impaired executive abilities, aphasia	3R/4R, 3R (PiD), OR 4R
Primary age related tauopathy (PART)	Primary (sometimes with amyloid-β pathology)	Neurofibrillary tangles	Cognitive impairment (may be associated with AD, currently unknown)	3R/4R
Progressive Supranuclear Palsy (PSP)	Primary	Neurofibrillary tangles, neuropil threads, tau deposits in astrocytes, tufted astrocytes and oligodendroglial coiled bodies	Postural instability, dysphasia, akinesia, visual and ocular disturbances, cognitive decline	4R

Figure 1: A table including descriptions of tauopathies, including tau-related pathology and presentation (Carmo *et al.,* 2020; Crary *et al.,* 2014; Pippin and Gupta, 2023; Wszolek *et al.,* 2006; Zhang *et al.,* 2022)

the subthalamus, frontal cortex, striatum and medial thalamus, though they are present in other regions (Fig. 3) (Dickson *et al.,* 2007; Kovacs *et al.,* 2020; Yoshida, 2014). Hyperphosphorylated tau deposits can result in the formation of argyrophilic oligodendroglial coiled bodies, though these are also seen in other disorders as well as PSP (Dickson *et al.,* 2007; Ferrer *et al.,* 2014). Degeneration of motor neurons, though unusual, may be seen in those with PSP (Josephs *et al.,* 2006b). The phenotypic diversity of the disease makes developing therapies for treatment difficult, and currently there is no cure. Current pharmacological therapies aim to treat

symptoms, commonly showing only mild to moderate efficacy such as levodopa for bradykinesia and rigidity, and zolpidem for ocular motor deficits (Coughlin and Litvan, 2020). Non-pharmacological, multidisciplinary care such as physical therapy may also improve patient function and decrease the chance of falls (Clerici *et al.,* 2017).

PSP is a 'pure', primary tauopathy involving only tau pathology, as are FTD and CBD (Zhang *et al.,* 2022), however AD is a secondary tauopathy as it includes both tau and amyloid-β pathology (it is also an amyloidopathy) (Coughlin and Litvan, 2020). Due to overlapping pathology, PSP models can be useful for investigating tau accumulation in other tauopathies, and vice versa, with the ultimate aim to understand and treat each of these diseases. We must also maintain an awareness of both the similarities and differences in these tauopathies when undertaking research. Immunohistochemistry and western blots have been utilized to examine tau epitopes in AD and PSP, with results suggesting that despite differences in distribution and NFT ultrastructure (Hasegawa, 2019), the same collection of abnormal tau epitopes are generated in the two diseases (Schmidt *et al.,* 1996). Whilst PSP predominantly involves 4R tau, named so for the 4 repetitive sequences formed during splicing, in AD both 3R (with 3 repeats) and 4R tau are present (Martínez-Maldonado *et al.,* 2021). Furthermore, RNA-sequencing data from temporal cortex and cerebellum samples of PSP and AD patients found conserved, regionally specific transcriptomic changes. As the changes were observed in minimal to significant pathologically affected, but functionally connected brain regions, this suggests results are less likely to be driven by similarities in gross neuropathology or changes to cell proportion, more likely that transcriptomic changes are due to downstream events as a result of neurodegeneration as opposed to events initiating it (Wang *et al.,* 2022). In AD, gene expression alteration in younger patients involves immune-inflammatory responses, with changes related to synaptic transmission seen in older patients overall. Conversely, these two associated effects of gene expression changes occur at around the same time in PSP patients. Gene expression alteration associated with myelination are enriched in both PSP and AD (Iohan *et al.,* 2022). Research illustrating both the similarities and differences between PSP, AD and other tauopathies provides us with evidence that there are shared adverse biological consequences of the pathological changes observed in these diseases, however we must be careful to contextualize any conclusions we make with the individual natures of these diseases.

ii. Tau - the Protein, and How it Becomes Pathological

Tau is generally regarded as a natively unfolded protein, with posttranslational modifications such as phosphorylation influencing its aggregation and oligomerization (Fig. 2) (Wang and Mandelkow, 2016). Tau is also considered to be an axonal protein, with controlled polarized distribution to allow it to function appropriately to stabilize microtubules (Panda *et al.,* 1995). Tau protein has also been suggested to have roles in many physiological processes (Kent *et al.,* 2020) such as neurogenesis and synaptogenesis (Chen *et al.,* 2012), myelination promotion (Lopes *et al.,* 2016; Sotiropoulos *et al.,* 2014), insulin signalling (Marciniak *et al.,* 2017), permitting hyperexcitability (Pallas-Bazarra *et al.,* 2016), LTP and LTD (Ahmed *et al.,* 2014; Kimura *et al.,* 2014; Regan *et al.,* 2015), motor control (Lei *et al.,* 2012), and involvement in protecting DNA (Violet *et al.,* 2014). In humans, the *MAPT* (Microtubule Associated Protein Tau) gene encoding Tau protein is located on chromosome 17q21,

with two haplotypes formed by polymorphisms along the *MAPT* gene, H1 and H2, which have been associated with tauopathies such as corticobasal degeneration (Houlden *et al.,* 2001), the former being strongly associated with PSP due to its overexpression in this disorder (Avila *et al.,* 2004). Through alternative splicing of exons 2, 3 and 10 of the 16 that make up *MAPT* during transcription, distinct mRNAs result in the production of multiple Tau isoforms, as well as through posttranslational modifications such as phosphorylation. The two main domains of tau isoforms are the amino-terminal projection domain and carboxy-terminal microtubule-binding domain (Avila *et al.,* 2004). The latter contains 3 or 4 (tau 3R or 4R respectively) similar repetitive sequences, resulting from differential splicing of exon 10 of *MAPT*, with tau 4R showing a greater affinity for microtubule binding, with the potential to displace tau 3R, suggesting 'competition' between isoforms for microtubule binding may be involved in disease development (Lu and Kosik, 2001). In normal human brains, the amounts of 3R and 4R tau are equal but this can change in a neurodegenerative state; in PSP pathogenic lesions comprise primarily if not entirely of 4R tau accumulations

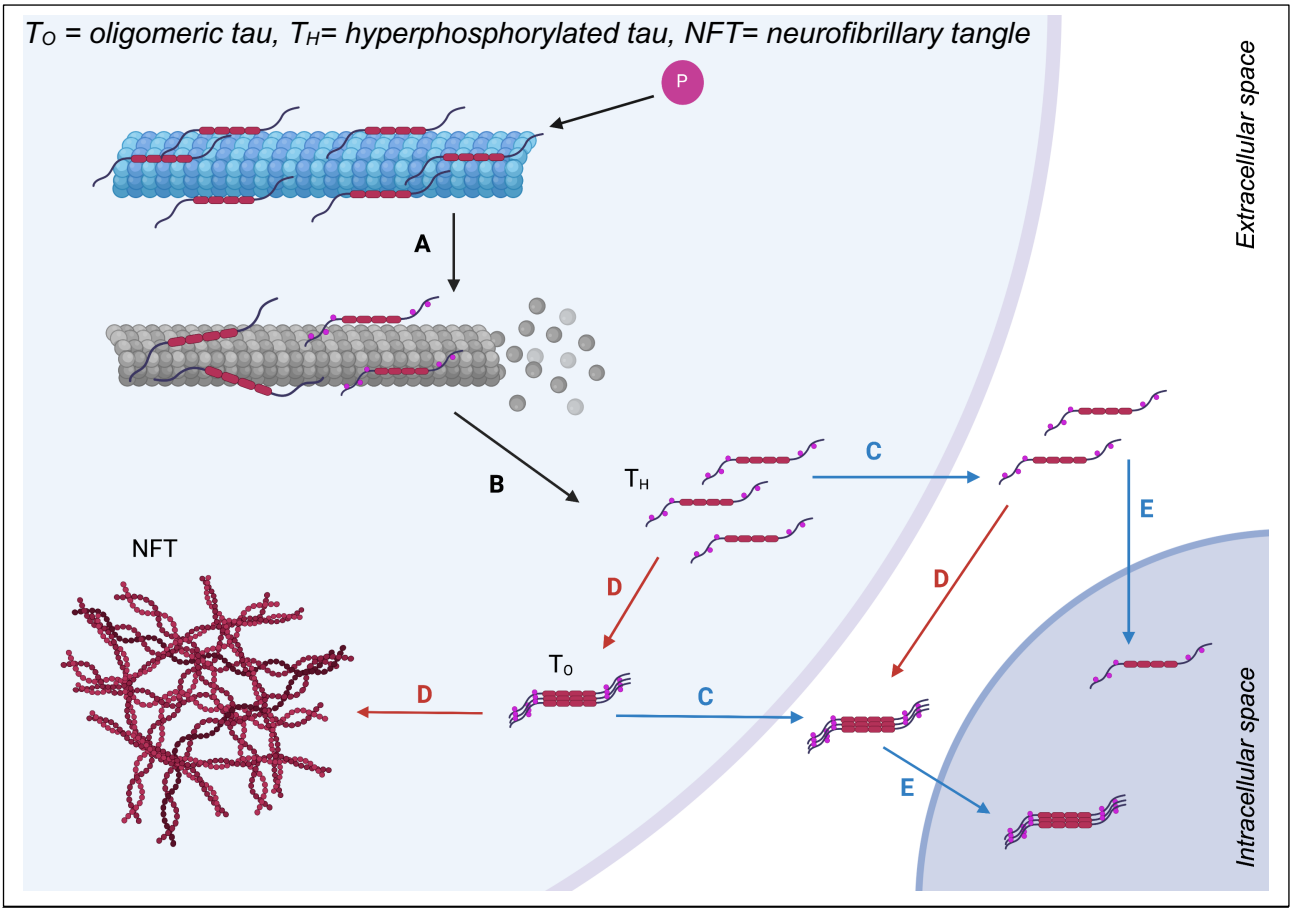

Figure 2: A) Tau bound to microtubules in neurons provides stability. Phosphorylation of tau causes B) dissociation from microtubules, causing them to lose stability and disintegrate, and hyperphosphorylated tau monomers (T_H) to be released to move freely through the neuron. Hyperphosphorylated tau can be transported across the neuron and aggregate. C) Soluble hyperphosphorylated and oligomeric tau (T_O) can be exported from the neuron into the extracellular space. D) Both intracellularly and extracellularly, hyperphosphorylated tau can aggregate to form oligomeric tau. Intracellularly, further aggregation can result in formation of fibrils and NFTs. E) Soluble tau epitopes can be taken up by new neurons. Created using BioRender.

(Coughlin and Litvan, 2020; Gao *et al.,* 2018). It has been suggested, however, that tau with low affinity for microtubules can be released into cytosol, where it would therefore be free to form aggregates (Gerson *et al.,* 2014). Post-translational modifications of tau such as hyperphosphorylation may induce this lesser affinity for microtubules, resulting in pathological tau that is free to self-aggregate, and weakened microtubules (Hanger *et al.,* 2009). Dogma surrounding associated tau dissociation from microtubules is supported by evidence that tau binds with tubulin in microtubules to provide stability and reduces the concentration of tubulin required for polymerisation, with hyperphosphorylation, truncation of C-terminal (Niewidok *et al.,* 2016) and mutations at microtubule-binding sites (Gilley *et al.,* 2012) reducing the binding capacity of tau to microtubules in AD models. However, pseudo-phosphorylation of tau, whilst able to induce a significant decrease in rate of binding to microtubules, does not impact the rate of tau dissociation from microtubules (Niewidok *et al.,* 2016), suggesting the timing of tau hyperphosphorylation with regards to its dissociation from microtubules is something that requires further study . Tau can be phosphorylated by several protein kinases, such as proline-directed protein kinases (PDPKs) and non-PDPKs, altered levels of both of which have been observed in AD brains (Chung, 2009). Phosphorylation of tau has also been reported to potentially cause mis-sorting of tau from axons to postsynaptic terminals and dendrites, as well as altering its degradation (Guillozet-Bongaarts *et al.,* 2006; Hoover *et al.,* 2010). Aggregation of tau monomers can lead to the formation of oligomers (or oligomeric tau), which are sometimes labelled the 'most toxic' form of tau due to their solubility, and ability to be internalized by brain cells. They have been shown to exist at increased levels in PSP brains compared to controls, and have been detected in AD brains, even before NFTs have been observed (Gao *et al.,* 2018; Gerson *et al.,* 2014; Puangmalai *et al.,* 2020). These small, soluble tau oligomers (of varying sizes according to polyacrylamide gel electrophoresis) provide an issue in comparing literature; oligomers containing anything between 2 and 8 tau molecules can be classed together, (Cowan and Mudher, 2013), however there is little evidence to suggest that these different oligomers all act or affect structures of the brain in the same way. Oligomeric tau has been shown to accumulate in neurones (Montalbano *et al.,* 2022), inhibits fast axonal transport (Ward *et al.,* 2012), and accelerates onset and propagation of disease (Gerson *et al.,* 2014; Gerson *et al.,* 2016; Sengupta *et al.,* 2015; Shafiei *et al.,* 2017), as well as being implicated in neuronal loss (Berger *et al.,* 2007; Spires *et al.,* 2006). Oligomeric tau can then go on to further aggregate and form fibrils. When applied exogenously, tau fibrils are not internalized by neurons, but in fact to bind to the cell membrane (Puangmalai *et al.,* 2020). Further aggregation of fibrils within neurons can lead to the formation of NFTs (Brion, 1998; Gerson *et al.,* 2014). Tauopathy mouse models have been used to show that although the formation of tangles correlates with neuronal loss and dementia, NFTs do not necessarily cause neuronal death, as the region specific neuronal loss of pathological tau-containing neurons observed can occur before NFTs have formed (in dentate gyrus), and NFTs can form without inducing major cell loss (in striatum) (Spires *et al.,* 2006).

iii. Tau at the Synapse

Damage to synapses occurring as a result of pathological tau aggregation ultimately can lead to both excitatory and inhibitory bipartite synaptic loss (Briel *et al.,* 2021), which is associated with cognitive decline associated with tauopathies such as AD

(DeKosky and Scheff, 1990). The neurotoxicity of oligomeric human tau has been confirmed using *in vivo* subcortical stereotaxic injection into mice, impairing memory consolidation and inducing synaptic dysfunction (Lasagna-Reeves *et al.,* 2011).
Cortical synapse loss has also been shown to be increased in PSP patients with dementia (Bigio *et al.,* 2001), and links have been suggested between synaptic loss and dysfunction (for example, in the frontal cortex) and behavioural changes, cognitive deficits and motor symptoms that can be observed in those with PSP Holland *et al.,* 2023). Positron Emission Tomography has also shown synaptic loss observed in PSP is linked to disease severity (Holland *et al.,* 2020) and may be associated with pathological aggregates such as those in PSP (Holland *et al.,* 2021), though it is not yet understood how. Accumulation of hyperphosphorylated and misfolded tau has been shown in both pre- and post-synapses in AD post-mortem cortices, resulting in dysfunction of the ubiquitin-proteasome system, and therefore dysfunction of the synapse (Tai *et al.,* 2012). AD mouse models have also shown loss of spine-associated synapses containing both pro-aggregate and anti-aggregate mutant tau species, suggesting synapse loss is linked to tau pathology at the synapse, but that aggregation state may not have an effect (Eckermann *et al.,* 2007). Furthermore, synaptic loss has been linked to dysfunctional phagocytosis by microglia in AD brains, with loss of specific secreted phosphoproteins (SPP1) required for microglial synaptic engulfment preventing synaptic loss in mouse models (De Schepper *et al.,* 2023).

There is increasing evidence to suggest that synaptic connections may be key sites of spread of pathological tau to healthy neurons, and ultimately, through the brain. Mouse models expressing pathological human tau in the entorhinal cortex have been utilized to show spread of tau pathology across trans-synaptically connected brain regions (Liu *et al.,* 2012). Furthermore, mouse models overexpressing human tau P301L in layer 2 of the entorhinal cortex (EC) only shows progression of tau pathology from neurons in the EC both neighbouring cells, and downstream neurones within the same synaptic circuit such as the dentate gyrus, cingulate cortex and parts of the hippocampus (de Calignon *et al.,* 2012). Pre-clinical studies have indicated that in PSP and CBD tau spreads across functionally connected neurons in an activity dependent manner (Franzmeier *et al.,* 2021). Additionally, a combination of resting-state fMRI and longitudinal tau-PET in AD cases has indicated that not only do deposition patterns resemble functional networks of the brain, but that connectivity itself is associated with tau spread. For example, areas with greater functional connectivity will be associated with higher rates of tau accumulation (Franzmeier *et al.,* 2020). The synaptic spread of tau across neuronally connected brain regions has been suggested to occur in a ‘prion like’ manner, where aggregated misshapen proteins act as seeds, creating a template and imposing their aberrant structure on their benign counterparts, occurring as in diseases such as Creutzfeldt-Jakob disease (Jucker and Walker, 2013; Zhang *et al.,* 2021a). As has been illustrated in mice, tau aggregates in the extracellular space can be internalized by nearby cells, for example neurons, where their conformational ‘template’ can be imposed on other tau protein, facilitating propagation of tau pathogenesis across the brain (Jucker and Walker, 2013). There is still debate, however, as to what is classed as a ‘seed’ in tau spread; evidence has shown ‘seeds’ from tau monomers (Michel *et al.,* 2014), to trimers (Mirbaha *et al.,* 2015), to fibrils (Frost and Diamond, 2010) can be taken up by a cell to serve as a template for intracellular tau. There is still a limited understanding as to how tau ‘seeds’ are formed, as well as factors within the brain that may contribute to this process, however some therapeutic targets have been identified in AD (Bell *et al.,* 2020).

Steps	Neuronal
1	Globus pallidus Subthalamic nucleus Substantia nigra *Locus coeruleus*
2	Midbrain tegmentum Medulla oblongata Pons base
3	Amygdala Striatum Dentate nucleus
4	Frontal lobe
5	Parietal lobe Temporal lobe
6	Occipital lobe

Steps	Astroglial
1	Striatum
2	Striatum
3	Frontal lobe Thalamus
4	Parietal lobe Temporal lobe Amygdala
5	Occipital lobe Midbrain tegmentum
6	Subtantia nigra Globus pallidus Pons Medulla oblongata Dentate nucleus Hippocampus

Steps	Oligodendroglial
1	Globus pallidus
2	Globus pallidus
3	Thalamus
4	Striatum Cerebellum
5	Frontal lobe Parietal lobe Midbrain Pons Medulla oblongata Amygdala Hippocampus
6	Temporal lobe Occipital lobe

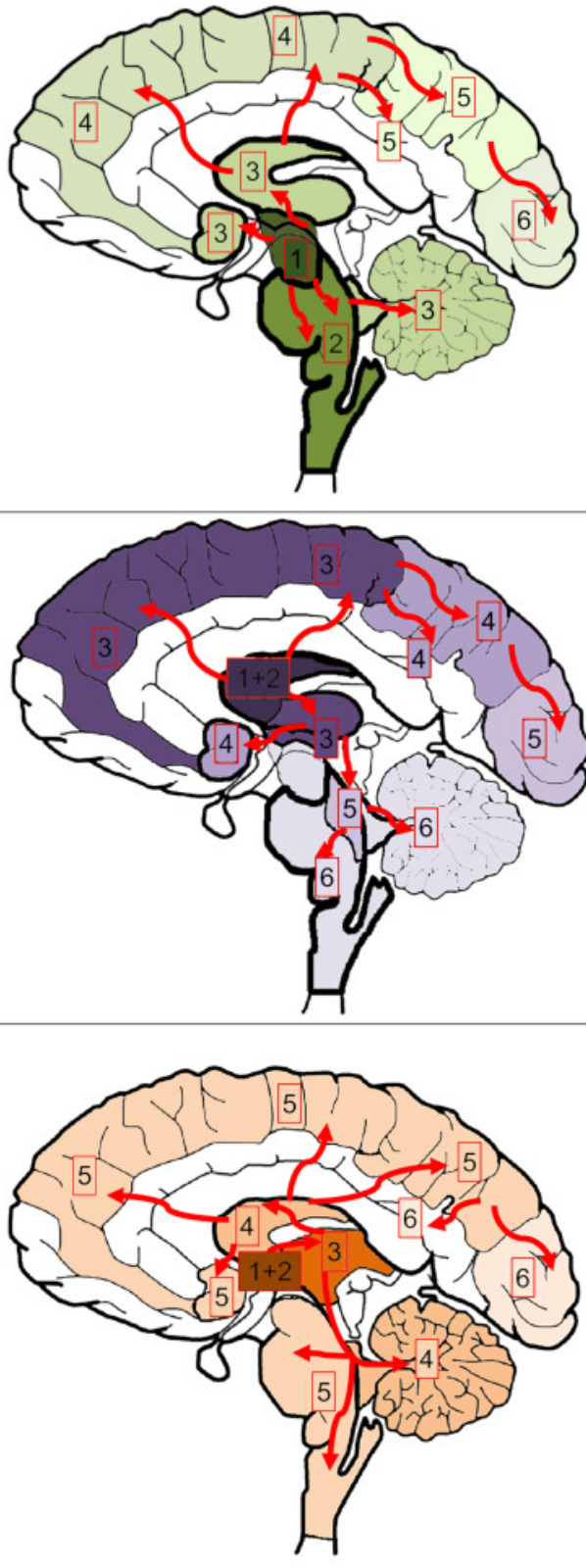

Figure 3: Neuronal, astroglial and oligodendroglial tau spread across the PSP brain (Adapted from Kovacs *et al.,* 2020; CC-BY-4.0)

The activation of astrocytes and microglia as part of the inflammatory response in the central nervous system can be both neuroprotective and neurotoxic. Both astrocytes

and microglia are involved in clearance of pathological proteins (Franklin *et al.,* 2021; Simard *et al.,* 2006), but chronic and uncontrolled inflammatory responses can be detrimental (Singh, 2022). It is unclear if neuroinflammation in cases such as PSP act protectively or cause damage; neuronal injury can be compounded and result in neuronal loss in late stage disease progression where glia are induced to an inflammatory state (Holland *et al.,* 2023; Montalbano *et al.,* 2022). It has been suggested that microglia may play a role in synaptic spread of pathological tau by taking up tau 'seeds', to reduce seeding capability (Hopp *et al.,* 2018). However, this can mean pathological tau taken up by microglia can be spread to healthy neurons via secreted exosomes. Furthermore, evidence suggests actions of microglia to phagocytose synaptic compartments of tau-containing neurons also contributes to synaptic dysfunction (Vogels *et al.,* 2019). There are also contrasting arguments as to the capability of microglia to degrade pathological tau in the diseased brain; evidence suggests some, slow degradation (Hopp *et al.,* 2018).

Astrocytes have long been considered to act to provide metabolic and nutritional support to neurones in distinct brain territories, forming networks across the brain, connected by gap junctions (Reid *et al.,* 2020; Santello *et al.,* 2019), however more recent evidence has revealed their role in neuronal signalling and synaptic transmission. By releasing glutamate to induce an NMDA receptor-mediate neuronal calcium increase (Parpura *et al.,* 1994) in response to neuronal activity, astrocytes form a 'tripartite synapse', inducing neuron-dependent or spontaneous excitation (Volterra and Meldolesi, 2005). The stimulus- and circuit-specific contributions of astrocytes to interactions with synapses appear to be dictated by their biological properties, playing an active role in controlling synaptic function through the exchanges of regulatory signals with neurones (Mariotti *et al.,* 2018; Martín *et al.,* 2015; Santello *et al.,* 2019). It has been acknowledged that in tauopathies astrocytes can accumulate tau, resulting in tauopathy specific characteristic changes to astrocytes, for example tufted astrocytes and astrocytic plaques in PSP and CBD respectively (Kovacs and Budka, 2010). Morphologically and functionally modified astrocytes in response to disease are classed as 'reactive' (Zamanian *et al.,* 2012). Furthermore, through assessing chromatin data of single nuclei of the frontal cortex, molecular changes to astrocytes have been observed that suggests a common signature of phosphorylated tau, reminiscent of an inflammatory response, in PSP (Briel *et al.,* 2022). Similar to the contributions or regulations of spread of tau by microglia, the consequences of astrocytic internalization are still not fully understood. Evidence suggests astrocytes are capable of degrading internalized tau, as well as propagating it neuronally (Martini-Stoica *et al.,* 2018). Data obtained through identification of divergent transcriptional patterns of cell types in PSP compared to controls suggests that aberrant upregulation of microglial transcripts is linked to the increase in astrocytic tau pathology (tufted astrocytes) observed in PSP. The same study also found that astrocytic pathology appears to be linked to a downregulation of synaptic genes, in contrast to upregulation of immune system transcripts and NFT pathology (Allen *et al.,* 2018). Astrocytes have also been shown to contribute to elimination of synapses in hippocampal neurones of a pathological tau transgenic mouse model of AD and other tauopathies (Dejanovic *et al.,* 2022). Furthermore, reactive astrocytes, often observed in close association with neuritic plaques observed in found in AD, have been reported to show some activity of engulfing dystrophic neurites, with the potential to contribute to clearing dysfunctional synapses and synaptic debris (Gomez-Arboledas et al., 2018).

iv. Summary

Our current knowledge of PSP and other tauopathies is limited, but ever expanding. There is growing evidence regarding the links between pathology and resulting clinical presentations of the disease, and the ways in which pathological forms of tau are formed and spread across the brain. To find therapies for treating PSP and other disorders involving pathological tau through countering tau spread and eliminating synapse loss that result in physical and cognitive decline, we must affirm current evidence, and delve deeper to determine mechanisms or pathways which may provide appropriate therapeutic targets. Though evidence has shown synaptic loss is a feature of PSP and other tauopathies, we do not yet understand the mechanisms by which synaptic loss occurs, and how it is associated with pathological tau accumulation in neurons. In this project, we aimed to investigate the accumulation of pathological tau in pre-synapses of the substantia nigra of PSP brains, providing evidence for accumulation of tau at this site in PSP (and potentially other primary tauopathies) and its potential links to synaptic loss. We also investigated colocalization of reactive astrocytes and microglia to pre-synapses and pathological tau in the PSP brain, in both the substantia nigra and frontal cortex (Brodmann area 9, or BA9) with an aim to support hypotheses that glia can contribute to synaptic loss and the propagation of pathological tau, as evidenced by AD models. We hypothesise that there will be an increase in colocalization of pre-synapses with pathological epitopes of tau in the PSP brain compared to controls. We further hypothesise an increase in colocalization of astrocytes and microglia with pre-synapses and hyperphosphorylated tau in PSP cases compared to controls.

Methods

i. Array Tomography Tissue Preparation and Staining

Array tomography was utilised as it provides a more sensitive assessment of synapses when imaging with immunofluorescence, as when studying synapses the lower resolution of traditional light microscopy techniques such as confocal imaging can lead to it being less effective (Kay *et al.,* 2013). For example, when using confocal imaging techniques, a 0.5-1μm resolution across the z plane, and light scatter, can mean synapses imaged in a 3D space will not be resolved due to overlapping fluorophore emission, resulting in them being recorded as a single, large puncta. As in array tomography serial sections at 70nm are taken, this reduces the axial resolution to 70nm; this is smaller than single synaptic puncta, meaning each real synapse will appear in consecutive sections (Sanchez Avila and Henstridge, 2022).

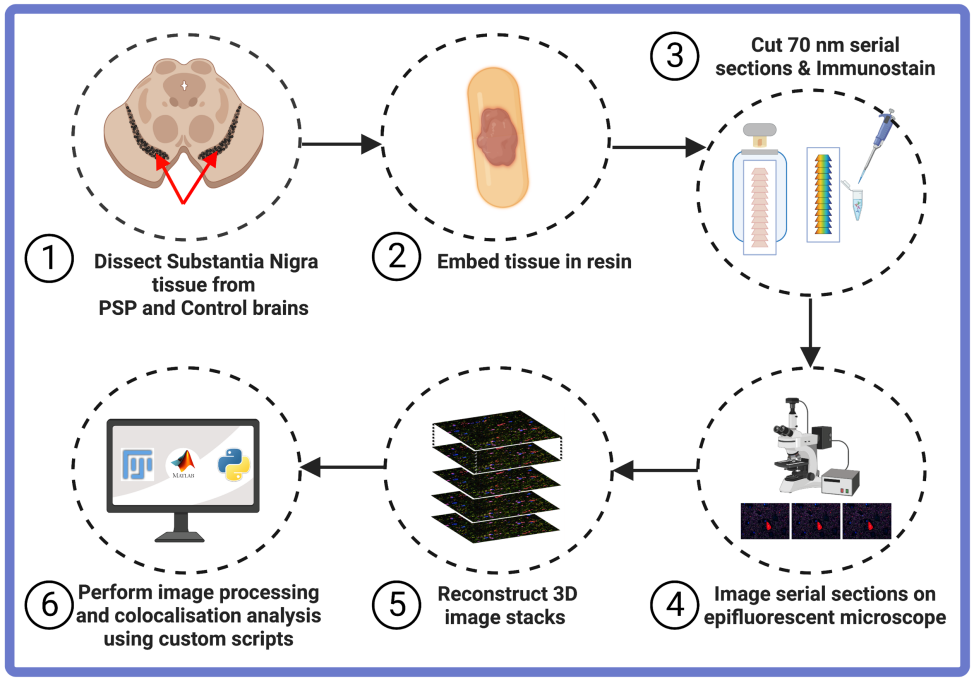

Figure 4: Array tomography methodology, modified from (McGeachan *et al.,* 2022).

Samples from the Substantia Nigra were fixed and embedded for array tomography as described previously (Kay *et al.,* 2013). Fresh tissue samples of ~1mm x 1mm x 6mm were fixed for 3 hours in paraformaldehyde, before subsequent dehydration in ethanol and for incubation overnight in LR white resin at 4°C. Each sample was then cured overnight in LR White in gelatin capsules at 53°C. Two sample blocks were used from each case, in separate staining sessions. Using a Diatome histo Jumbo Diamond knife, and a Leica Ultracut, the embedded samples were then cut into ribbons of ultrathin serial 70nm sections, before mounting on gelatin-coated glass coverslips. After outlining the section ribbons with hydrophobic pen, they were then rehydrated in 50mM glycine (5 min) and blocked for 30 minutes in a solution of 0.1% fish skin gelatin, 0.05% Tween in TBS at room temperature. Ribbons were incubated overnight with primary antibodies to AT8 (MN1020), T22 (courtesy of Rakez Kayed, (Lasagna-Reeves *et al.,* 2012)), and GFAP (ab4674) diluted in blocking buffer at 4 °C at 1:50,

1:50 and 1:100 respectively. Ribbons were washed with TBS before incubation for 30 minutes with secondary antibodies diluted in blocking solution at room temperature; Alexa Fluor Plus 405 labelled goat anti-chicken at 1:100 (A48260), Alexa Fluor 594 labelled goat anti-mouse IgG1 at 1:50 (A21121), Alexa Fluor 647 labelled goat anti-rabbit at 1:50 (A21244). After washing with TBS, ribbons were incubated at room temperature with directly labelled 488 synaptophysin antibody (ab1963794) diluted in blocking solution (1:200) for 1 hour. Ribbons were washed with TBS and distilled water before mounting on glass slides with Vectashield.

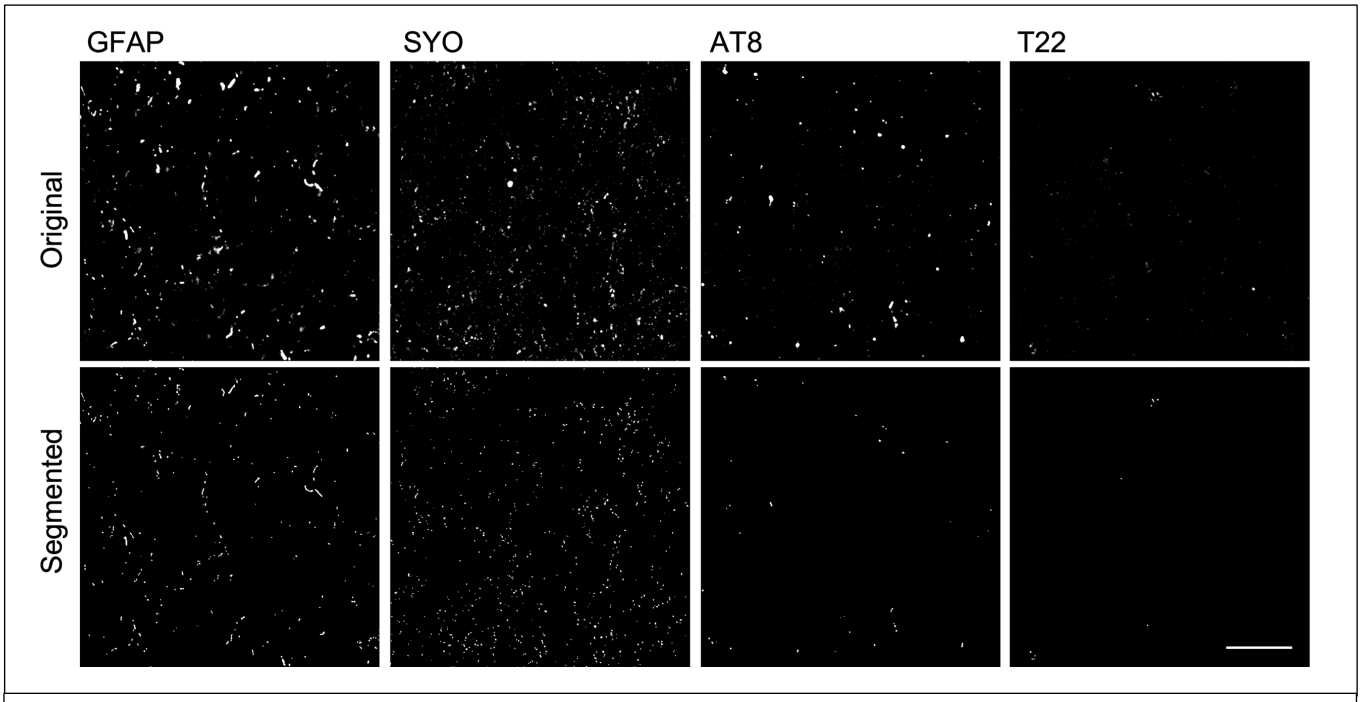

Figure 5: Raw and post-segmentation images from of single section images from 3D stacks of staining channels GFAP (reactive astrocytes), SYO (pre-synapses_, AT8 (hyperphosphorylated tau), and T22 (oligomeric tau) in the substantia nigra.

In each staining session, both control and PSP cases were used. Imaging of stained ribbons was carried out using an Axioimager Z2 with a 63x oil immersion objection (1.4 numerical aperture) and Zen software (Zeiss), acquiring a series of images at the same location in the substantia nigra along ribbons of 25-30 serial sections per ribbon, with 2 ribbons per case. Imaging parameters were kept the same across all imaging batches, with a negative control in each session. Before undertaking image processing, cases were blinded to remove specific case information. Using ImageJ/Fiji and custom batch macros, individual images were then combined into stacks, and a median background filter applied. Custom MATLAB scripts were used to align image stacks. Background staining of each channel was removed through segmentation using an auto-local thresholding algorithm to remove objects detected in single sections (Fig. 5). Parameters for segmentation were shared for each set of slides stained collectively. Analysis of colocalization was undertaken using a separate MATLAB script, with 25% overlap of volume required for classification of colocalization.

In previous experimentation in our group using samples of the frontal vortex (BA9), PSD95 was used to stain excitatory post-synapses, however anatomical differences of the substantia nigra (Zhou and Lee, 2011) meant there was insufficient staining of excitatory post-synapses for analysis, due to their fewer numbers (Fig. 6). We therefore disregarded this antibody and instead stained to observe oligomeric tau with T22.

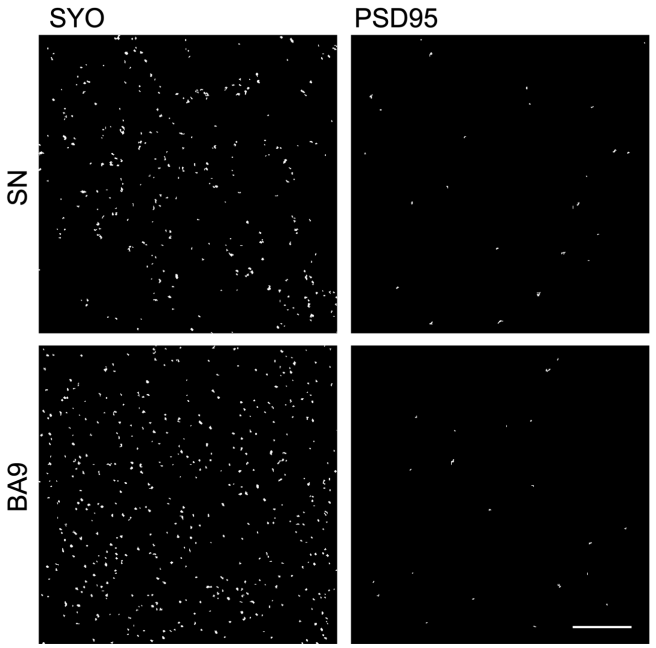

Figure 6: Segmentation images of single sections from 3D stacks obtained from pilot array tomography studies. Synaptophysin (SYO) is a pre-synaptic marker, and PSD95 and Gephyrin were options piloted as post-synaptic markers. All images scaled to 10μm.

ii. Immunohistochemical Staining of Paraffin Embedded Human Post-Mortem Slices

Midbrain and frontal cortex (BA9) slides were dewaxed with xylene and rehydrated from 100% ethanol to 50% ethanol, before washing with water. Slides were pressure cooked for 10 minutes with citrate buffer at pH 6 for antigen retrieval, before washing with water. Slides were washed with 70% ethanol before incubating with Autofluorescence Eliminator Reagent, then washed with 70% ethanol. Slides were then washed with 1xPBS, 0.3% Triton X-100, then with 1xPBS for 5 minutes each, before removing each slide and outlining tissue with wax pen. Slides were incubated with 200ul/slide red blood cell signal quencher (Vector TrueVIEW Autofluorescence Quenching Kit) for 5 minutes, then washed with 1xPBS for 5 minutes. Slides were blocked with 1xPBS, 0.3% TritonX, 10% Normal Donkey Serum (blocking solution) for 1 hour. Slides were incubated overnight at 4^{o}C with primary antibodies (diluted in blocking solution) to GFAP (ab4674) at 1:2000, AT8 (MV1020) at 1:500, and P2RY (HPA014518) at 1:1000. After washing with 1xPBS, 0.3% Triton X-100 then 1xPBS using an aspirator, slides were then incubated with secondary antibodies diluted in PBS for 1 hour; GFAP (Alexa Fluor 405, A48260) Goat anti-chicken, P2Y12 (Alexa Fluor 594, A32787) Donkey anti-rabbit, and AT8 (Alexa Fluor 647, A21207) Goat anti-MsIgG1, all at 1:500. After washing with 1xPBS using an aspirator, sections were then incubated for 1 hour at room temperature with direct label Synaptophysin (ab196379), diluted at 1:1000 in PBS, before washing with 1xPBS using an aspirator. 1xPBS was

then removed from each slide, before mounting with a drop of Immu-Mount and a coverslip.

Slides were imaged using Leica TCS SP8 Confocal microscope using a 63x oil immersion objective, with z-stack size at minimum 11 and maximum 25. Substantia nigra was identified and outlined with marker on each slide to ensure imaging occurred in the correct anatomical area only, as slides included the entire midbrain. For frontal cortex slides, images were taken through all cortical layers. Images were segmented in individual channels using an auto-local thresholding algorithm to remove objects

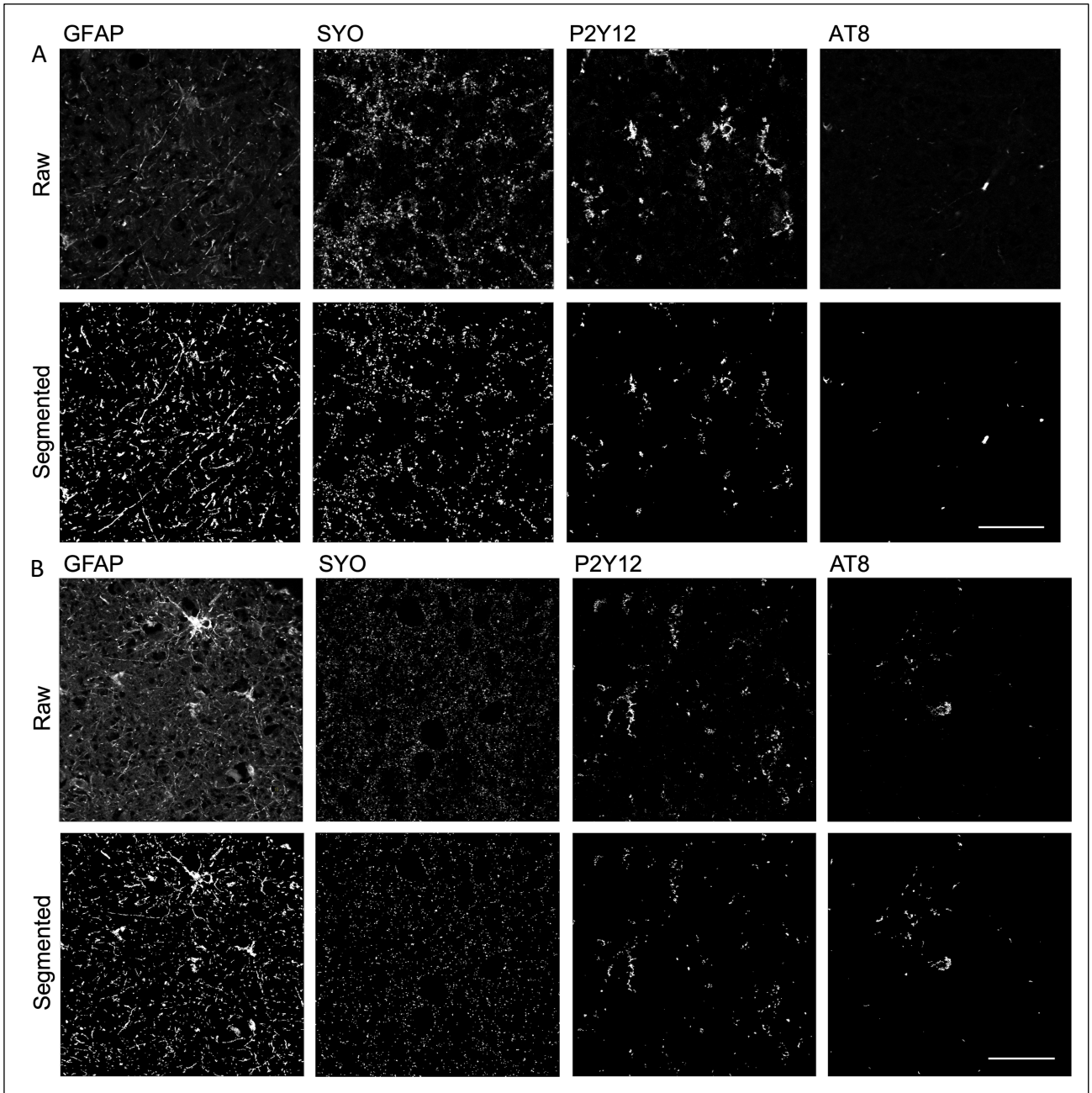

Figure 7: Raw and post-segmentation single section images of 3D stacks of staining channels GFAP (reactive astrocytes), SYO (pre-synapses), P2Y12 (microglia), AT8 (hyperphosphorylated tau) in the (A) substantia nigra and (B) frontal cortex. All images are scaled to 50 μm.

detected in single sections, removing background staining (Fig. 7). After collecting all image stacks into their individual staining channels, segmentation of raw image stacks was undertaken twice, once separating by staining batch, and a second time separating by brain region, to ensure there was no variation between batches. After merging channels, analysis of colocalization was undertaken using custom MATLAB scripts.

iii. DAB staining of phospho-tau

Separately, midbrain and frontal cortex slides were dewaxed with xylene and rehydrated from 100% ethanol to 50% ethanol, before washing with water. Slides were heated in a pressure cooker with citrate buffer for 10 minutes for antigen retrieval, then cooled and rinsed with water. After bordering with hydrophobic pen, tissue was covered with 1x TBS to avoid drying out. After removing 1x TBS, slides were incubated with Peroxidase Block (30 minutes), Protein block (15 minutes), AT8 primary antibody (MV1020) at 1:2000 (30 minutes), Post-Primary Block (30 minutes), and Novolink Polymer Detection (30 minutes) at room temperature, washing with 1x TBS for 5 minutes between each incubation step. After washing for 5 minutes with 1x TBS, slides were incubated with DAB solution (50ul chromagen to every 1ml substrate buffer) for 3 minutes, before washing thoroughly with water. Slides were then counterstained with haematoxylin solution for 30 seconds at room temperature, before washing with water. Midbrain sections were mounted with Immu-mount, frontal cortex sections were dehydrated from 50% ethanol through to 100% ethanol, then xylene, before mounting with DPX.

Stereology was undertaken on slides using Zeiss Axioimager Z2, and raw burden data was calculated with Stereoinvestigator (MicroBrightField) and Neurolucida Explorer software, obtaining values for total area and total area of AT8 stain detected. As Stereoinvestigator software requires a positive stain value for hyperphosphorylated tau to analyse burden across the region of interest, cases were blinded and those with no visible positive tau staining identified as zero tau. Microsoft Excel was used for calculation of percentage burden.

ii. Statistical Analysis

Statistical analyses of colocalization data were undertaken using RStudio. For analysis of array tomography data, a linear mixed effects model with 1|case as a random effect and disease cohort (PSP or control), age and PMI hours as fixed effects was used. Distribution of data was assessed using box plots and assumptions of models tested by examining residual plots and performing Shapiro-Wilks tests on residuals of the models. Where the model did not fit test assumptions, a tukey transformation was used to transform the data. Post-hoc testing was used to determine effect sizes. For analysis of human paraffin immunofluorescent staining, raw colocalization data was analysed using Rstudio. A linear mixed effects model accounting for disease cohort with brain region, and age with disease cohort as fixed effects was chosen for analysis of raw data to ensure the model was biologically relevant, and AIC (Akaike information criterion) value used to compare the fit to other models to ensure it was the most suitable. Distribution of data was assessed using box plots and assumptions of models tested by examining residual plots. Where the

model did not fit test assumptions, an arcsine square-root transformation was used to transform data (this was appropriate as colocalization data was calculated as a percentage of the total volume of the stack, and zero values were present). Post-hoc tests were undertaken to determine effect sizes and provide analysis specific to each brain region. For immunohistochemical staining assessing tau burdens, data was analysed using a linear mixed effects model with 1|case as a random effect and disease cohort and brain region as fixed effects. Post-hoc testing was used to determine effect sizes. Linear mixed effects models and post-hoc testing scripts are illustrated in supplementary materials (Supplementary Tables 1-3). There was no difference in age (Paired t-test, p=0.6683), sex (Fisher's exact test, p=1) or PMI hours (Paired t-test, p=0.2039) between participants from control or PSP groups. The same, larger case pool used for these analyses of participant demographics was used for all 3 studies, though not all cases could be used for each individual study due to availability of tissue. Custom software scripts used in this project are available on GitHub (https://github.com/Spires-Jones-Lab).

Results

i. Tau accumulates in pre-synapses and reactive astrocytes in PSP

Prior to colocalization analysis, images acquired through array tomography were segmented to remove background staining. For analysis of raw data, a linear mixed effects model accounting for Cohort, Age, Sex and PMI hours as fixed effects (with case as a random effect) was used, significant results are indicated as $p < 0.05$. Post hoc testing including effect sizes are reported on the transformed scale; Tukey transformation was used to ensure data fit the assumptions of equal variance and normal distribution. Raw data are presented in Figure 9.

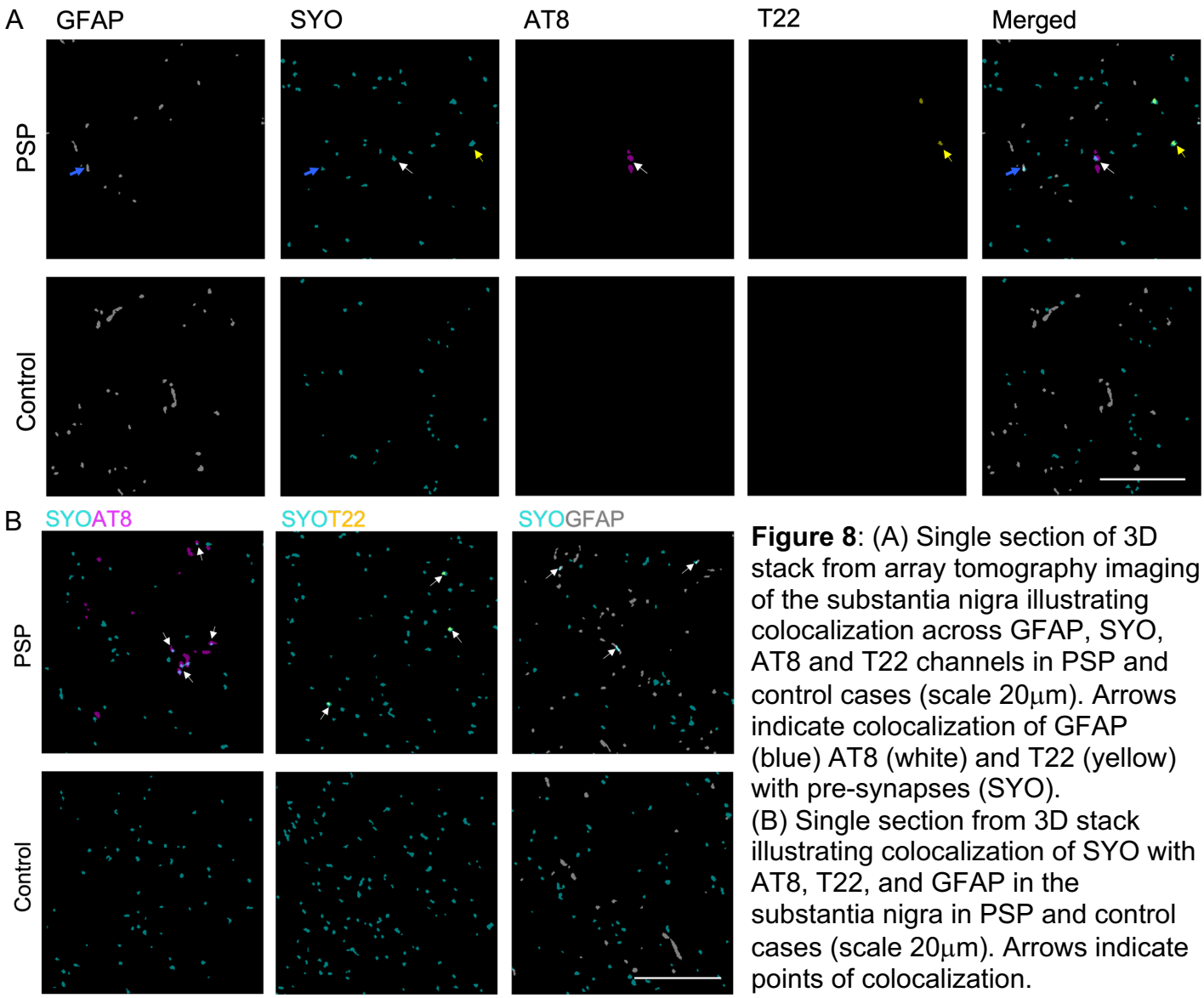

Figure 8: (A) Single section of 3D stack from array tomography imaging of the substantia nigra illustrating colocalization across GFAP, SYO, AT8 and T22 channels in PSP and control cases (scale 20μm). Arrows indicate colocalization of GFAP (blue) AT8 (white) and T22 (yellow) with pre-synapses (SYO).
(B) Single section from 3D stack illustrating colocalization of SYO with AT8, T22, and GFAP in the substantia nigra in PSP and control cases (scale 20μm). Arrows indicate points of colocalization.

To investigate accumulation of pathological tau to synapses we analysed colocalization of hyperphosphorylated and oligomeric tau with pre-synapses, and observed an increase in PSP cases compared to age and sex matched controls (Fig. 8, 9). Colocalization of pre-synapses and hyperphosphorylated tau showed a significant increase in PSP compared to controls, (type 3 ANOVA on linear mixed effects model: $F_{[1,6]}$ =46.1192, p=0.0004989) however colocalization with oligomeric tau was not significant (type 3 ANOVA on linear mixed effects model: $F_{[1,6]}$ =0.7304, p=0.4256). This is likely due to difficulties with the T22 antibody used and subsequent issues this caused for image preparation and segmentation as to avoid inclusion of background staining, we segmented more exclusively and so likely lost a small amount of true staining. We also observed significantly increased colocalization of pre-synapses and reactive astrocytes (type 3 ANOVA on linear mixed effects model: $F_{[1,6]}$ =8.7672, p=0.02525) in PSP compared to controls.

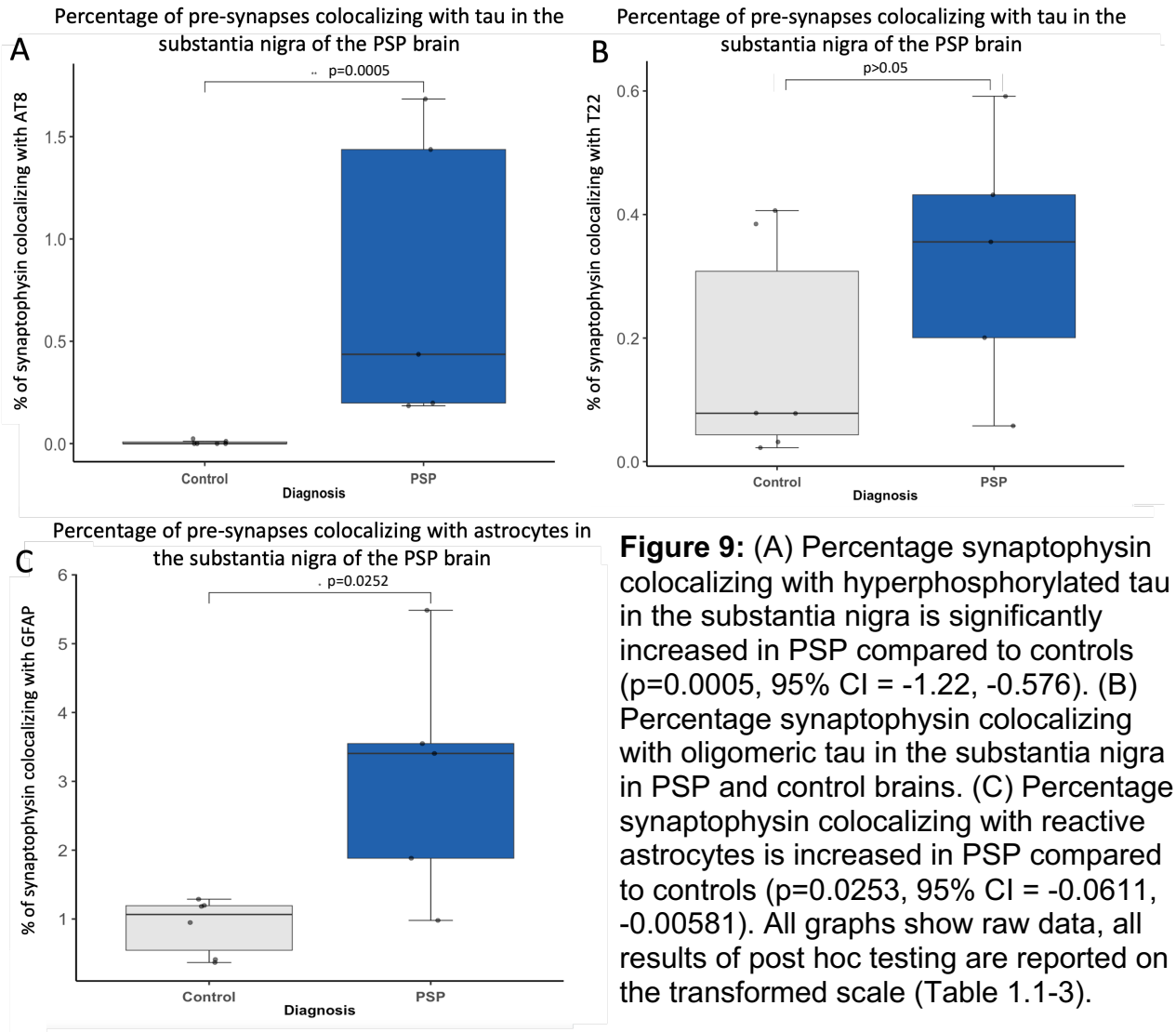

Figure 9: (A) Percentage synaptophysin colocalizing with hyperphosphorylated tau in the substantia nigra is significantly increased in PSP compared to controls (p=0.0005, 95% CI = -1.22, -0.576). (B) Percentage synaptophysin colocalizing with oligomeric tau in the substantia nigra in PSP and control brains. (C) Percentage synaptophysin colocalizing with reactive astrocytes is increased in PSP compared to controls (p=0.0253, 95% CI = -0.0611, -0.00581). All graphs show raw data, all results of post hoc testing are reported on the transformed scale (Table 1.1-3).

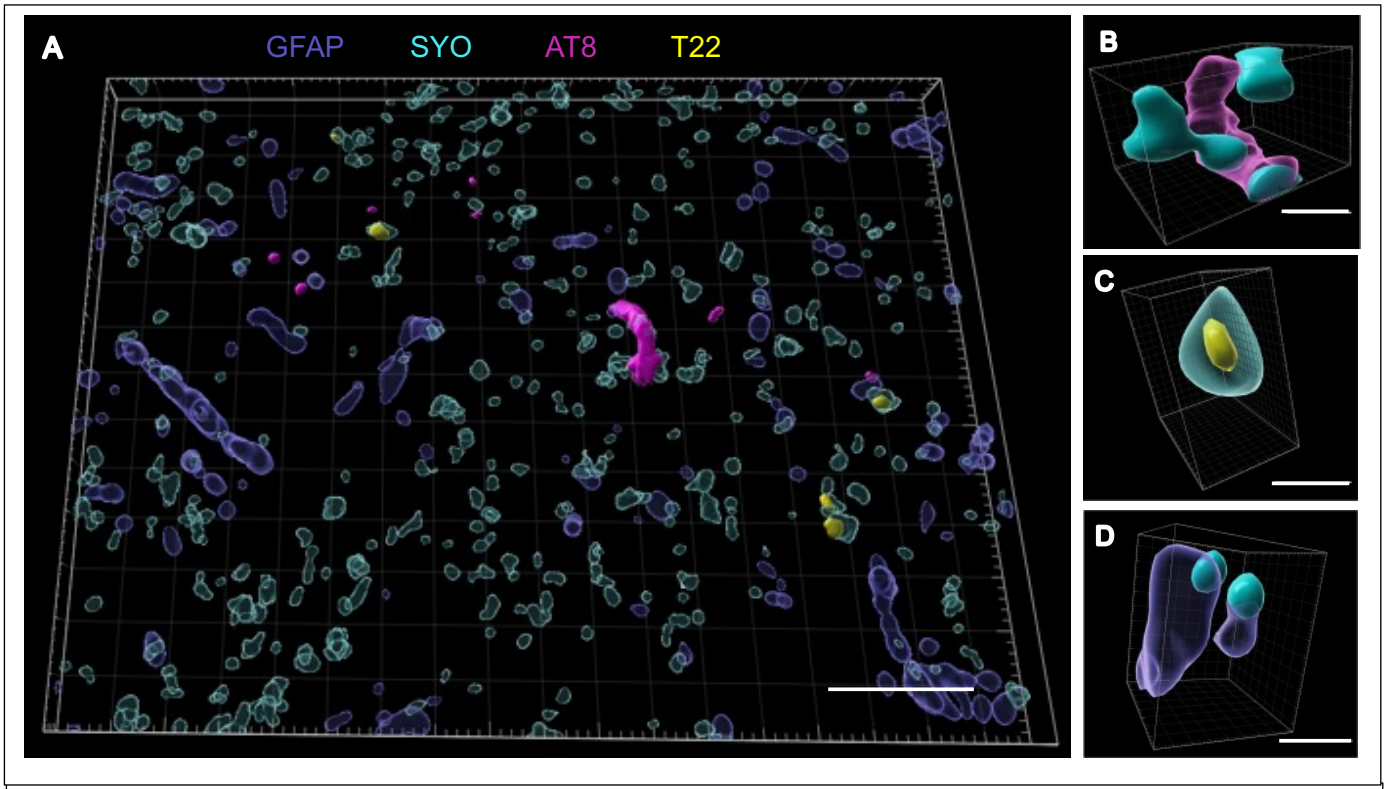

Figure 10: (A) 3D reconstruction of a single stack of images taken through array tomography illustrating colocalization of synaptophysin (SYO) for pre-synapses, with hyperphosphorylated tau (AT8), oligomeric tau (T22) and reactive astrocytes (GFAP) in the substantia nigra of a PSP brain (scale 20um). (B-D) 3D reconstruction illustrating colocalization of SYO staining with (B) AT8 (C) T22 and (D) GFAP (scale 2um).

ii. Analysis of tau colocalization with pre-synapses, reactive astrocytes, and microglia

Only cohort and any significant results indicated as $p<0.05$ will be reported here. Post hoc testing (emmeans, confidence intervals) are reported on the transformed arcsin square root scale; raw data was collected as percentages, making this transformation the most appropriate to ensure data met the assumptions of equal variance and normal distribution. Untransformed data is presented in Figures 14-15.

To investigate accumulation pathological tau at synapses, we undertook analysis of colocalization of pre-synapses with hyperphosphorylated tau (Fig. 11, 12). Results of statistical analysis suggest there is no significant difference between PSP and age and sex matched control, though our p value borders statistical significance (type 3 ANOVA on linear mixed effects model: $F_{[1,16]} =4.4259$, $p=0.05147$). A change with similar, though still not significant statistical significance is also seen with cohort (PSP vs control) and age together (type 3 ANOVA on linear mixed effects model: $F_{[1,16]} =4.1261$, $p=0.05909$), therefore we may consider these results as an effect of both cohort and age. These results do not align with colocalization results concerning AT8 and synaptophysin obtained through array tomography.

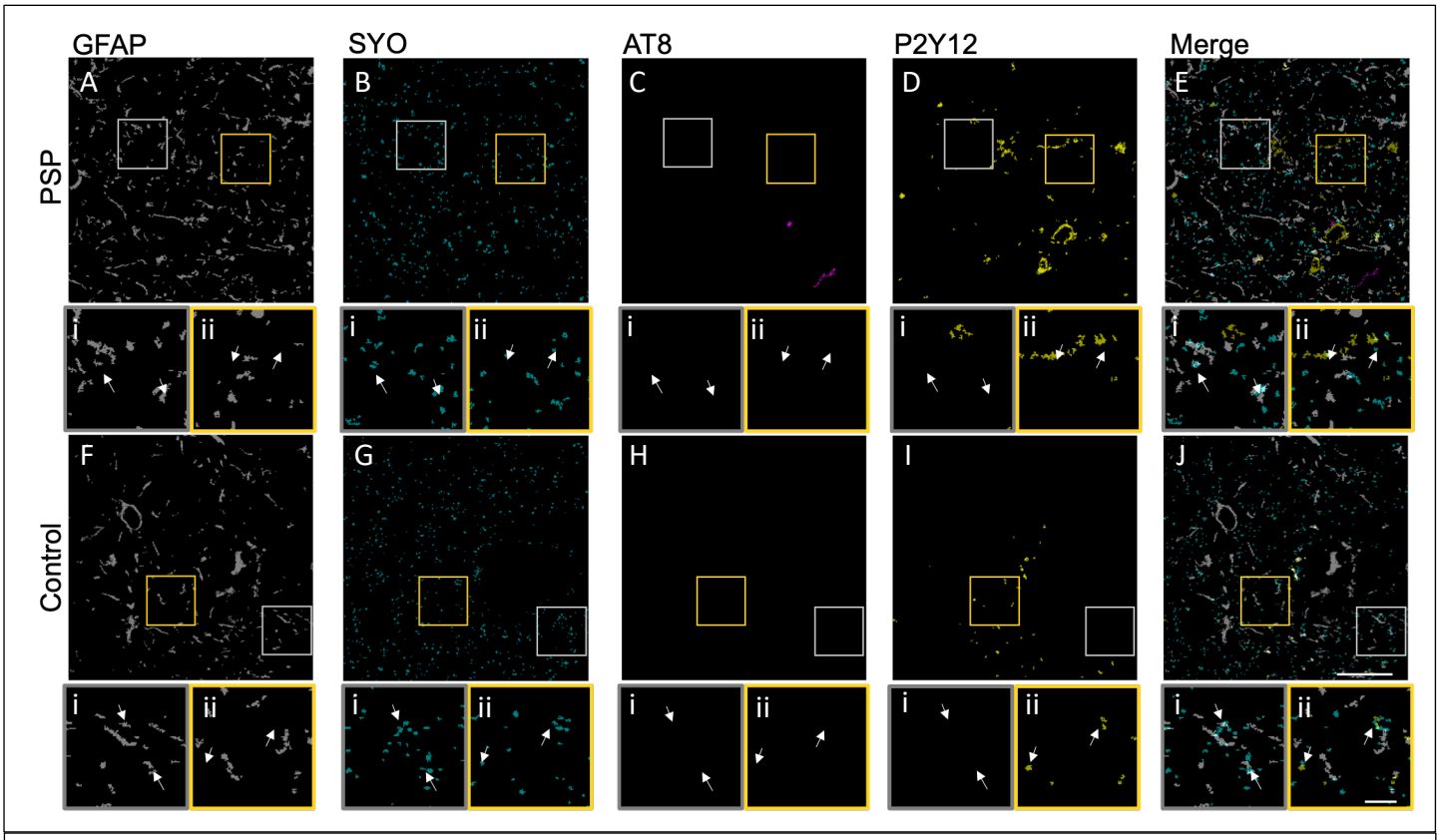

Figure 11: Colocalization of pre-synapses (SYO) with reactive astrocytes (GFAP) and microglia (P2Y12) staining in the frontal cortex of PSP and control brains. Grey boxes illustrate colocalization of pre-synapses with reactive astrocytes, yellow boxes illustrate colocalization of pre-synapses with microglia (white arrows indicate points of colocalization). (A-J) scaled to 20μm, (i/ii marked) all scaled to 5μm.

To investigate synaptic engulfment by astrocytes and microglia we observed colocalization of pre-synapses with reactive astrocytes (GFAP) and microglia (P2Y12). Directly contradicting results obtained through array tomography, results of this analysis of colocalization of percentage volume staining of synaptophysin and GFAP suggest there is a significant decrease between PSP and age and sex matched controls (type 3 ANOVA on linear mixed effects model: $F_{[1,16]}$ =4.9255, p=0.04110). A significant change in colocalization is also seen with cohort and age together (type 3 ANOVA on linear mixed effects model: $F_{[1,16]}$ =5.9180, p=0.02701), therefore we must consider these results as an effect of both cohort and age. The observed change in PSP does not appear to be significant in either substantia nigra (emmeans: p=0.2461, estimate=0.0623, 95%CI= -0.0566, 0.206), or frontal cortex (emmeans: p=0.1870, estimate=0.0435, 95%CI= -0.0322, 0.152). These results contradict those obtained investigating the same colocalization through array tomography. Colocalization of pre-synapses with microglia (P2Y12) shows no significant increase in PSP compared to age and sex matched control (type 3 ANOVA on linear mixed effects model: $F_{[1,16]}$ =3.8787, p=0.6639). Analysis suggests a difference between brain regions bordering statistical significance (type 3 ANOVA on linear mixed effects model: $F_{[1,18]}$ =4.3918, p =0.05025). The observed increase in PSP does not appear to be significant in either substantia nigra (emmeans: p=0.1759, estimate=-0.0248, 95%CI= -0.00445, 0.0555), or frontal cortex (emmeans: p=0.1176, estimate=-0.0335, 95%CI= -0.01323, 0.0486).

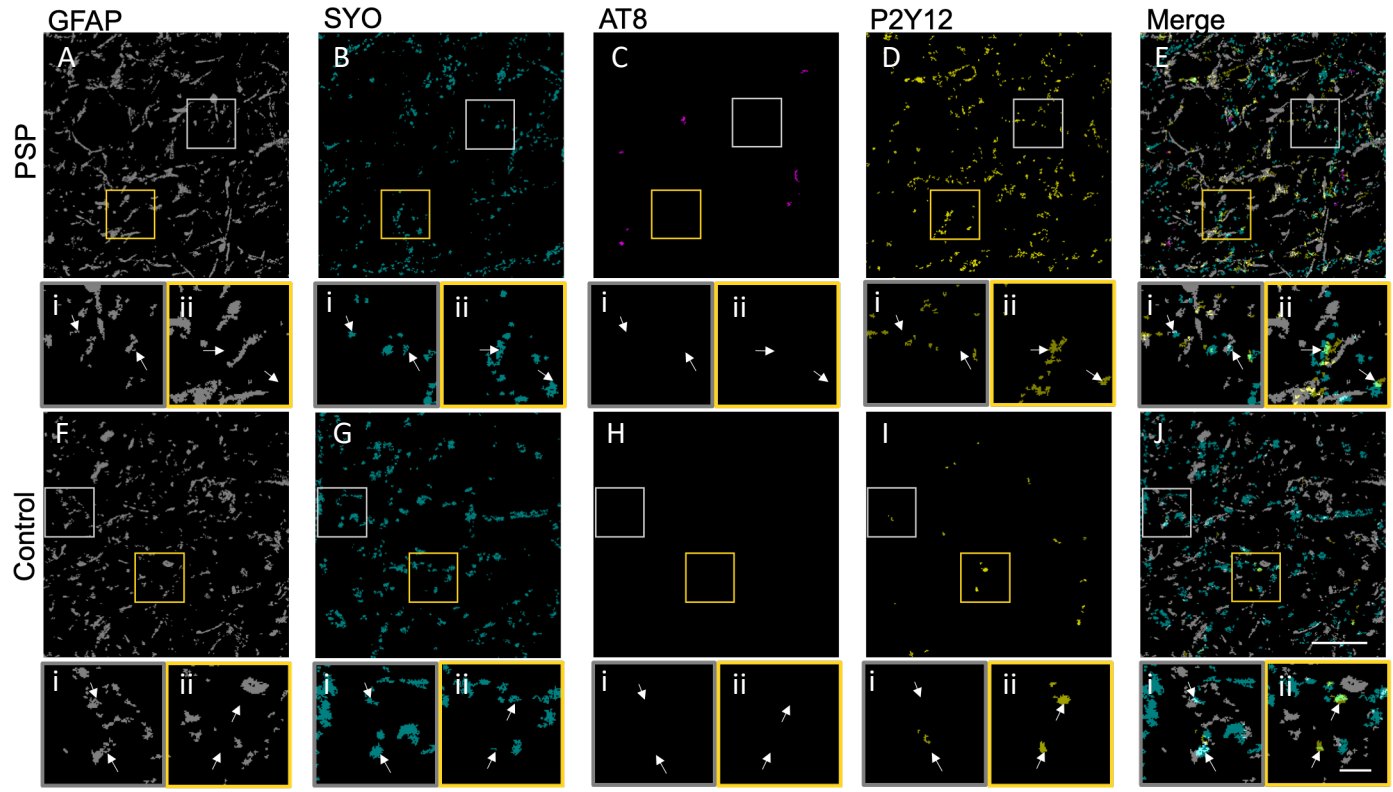

Figure 12: Colocalization of pre-synapses (SYO) with reactive astrocytes (GFAP) and microglia (P2Y12) staining in the substantia nigra of PSP and control brains. Grey boxes illustrate colocalization of pre-synapses with reactive astrocytes, yellow boxes illustrate colocalization of pre-synapses with microglia (white arrows indicate points of colocalization). (A-J) scaled to 20μm, (i/ii marked) all scaled to 5μm.

To investigate glial engulfment of pathological tau we analysed colocalization of hyperphosphorylated tau (stained with AT8) with reactive astrocytes (GFAP) and microglia (P2Y12). Analysis of colocalization of AT8 with GFAP showed no significant difference between PSP and age and sex matched controls, but did show a significant difference between the two brain regions analysed (type 3 ANOVA on linear mixed effects model: $F_{[1,18]}$ =7.9894, p=0.0110); substantia nigra (emmeans: p=0.6132, estimate=-0.0593, 95%CI= -0.0710, 0.117) and frontal cortex (emmeans: p=0.1124, estimate=-0.0593, 95%CI= -0.0155, 0.134). Similarly, colocalization of AT8 with P2Y12 showed no significant difference between PSP and control cohorts, but showed a significant difference in colocalization between brain regions (type 3 ANOVA on linear mixed effects model: $F_{[1,18]}$ =0.2796, p=0.006101); substantia nigra (emmeans: p=0.9049, estimate=0.00371, 95%CI= -0.612, 0.0687), and frontal cortex (emmeans: p=0.4506, estimate=-0.00988, 95%CI= -0.0370, 0.0172).

Analysis of 3-way colocalization of pre-synapses (Synaptophysin), hyperphosphorylated tau (AT8), reactive astrocytes and microglia (GFAP and P2Y12, respectively) was undertaken for investigation of glial engulfment or destruction of pathological tau-containing synapses. Results of both colocalization analysis of synaptophysin, AT8 and GFAP and synaptophysin, AT8 and P2Y12 showed no significant difference between PSP and control cohorts.

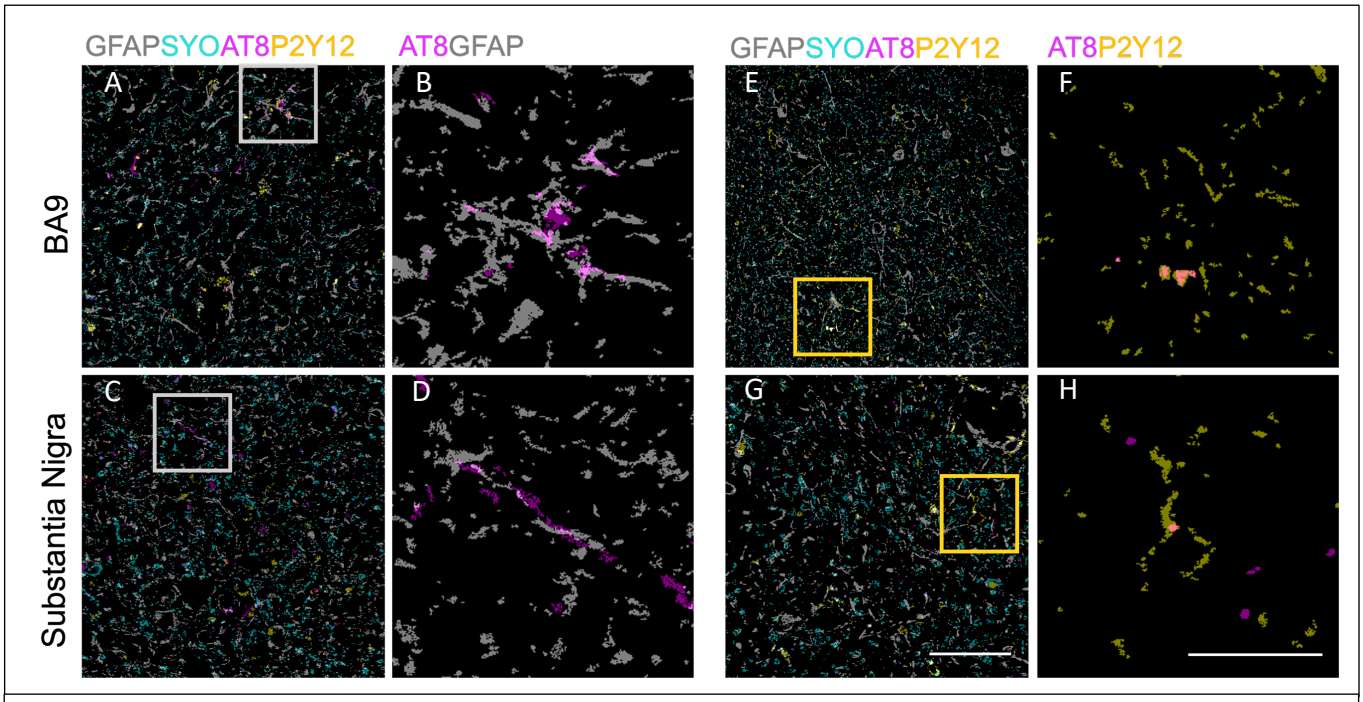

Figure 13: An illustration of colocalization of hyperphosphorylated tau (AT8) with (A) reactive astrocytes (GFAP) and (B) microglia (P2Y12) staining in the frontal cortex and substantia nigra of PSP and control brains. (A, C, E, G) scaled to 50μm, (B, F, D, H) scaled to 20um.

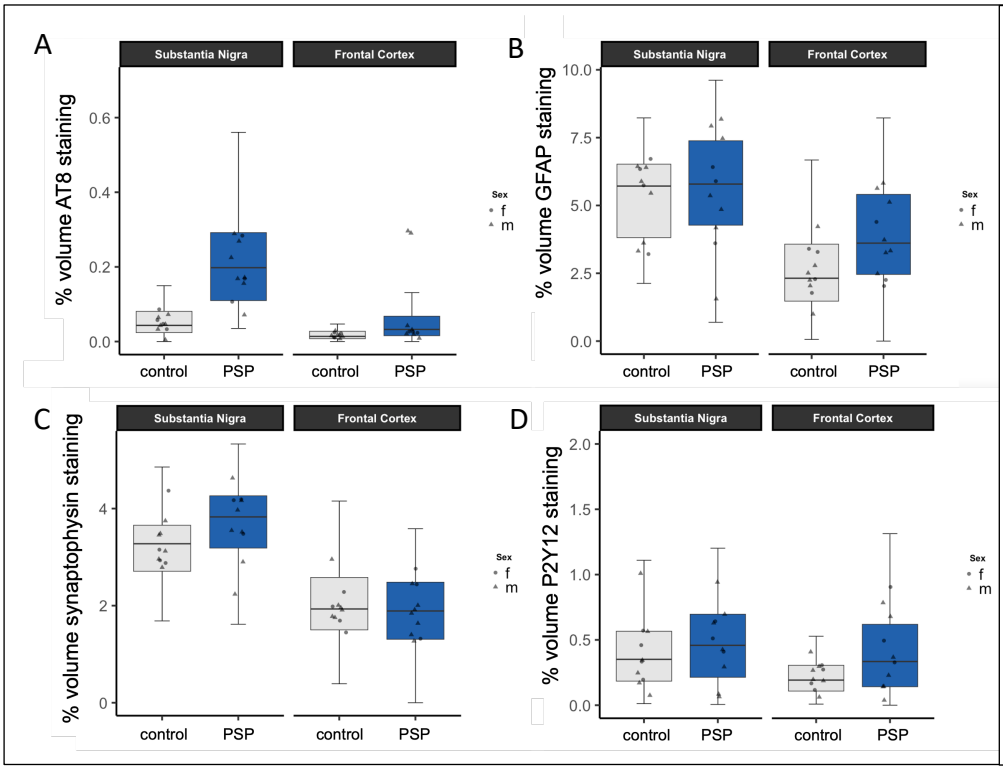

Figure 14: Percentage volume of staining of (A) AT8 (hyperphosphorylated tau) (B) GFAP (reactive astrocytes) (C) SYO (synaptophysin) and (D) P2Y12 (microglia) from 3D image stacks acquired in immunofluorescent staining in substantia nigra and frontal cortex of PSP and control brains. All graphs indicate raw data, results of post hoc are shown on the transformed scale (Table 2.7-11).

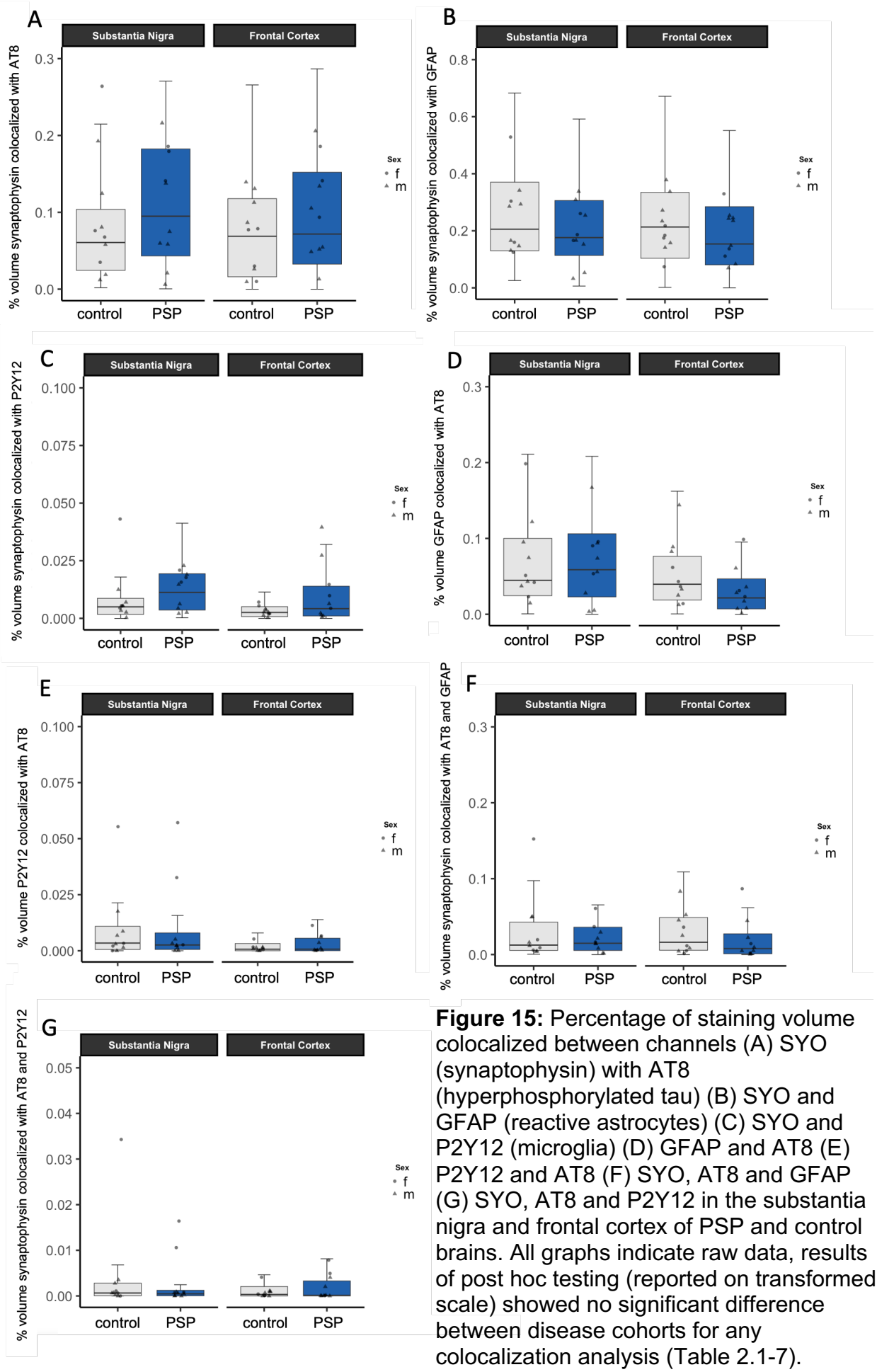

Figure 15: Percentage of staining volume colocalized between channels (A) SYO (synaptophysin) with AT8 (hyperphosphorylated tau) (B) SYO and GFAP (reactive astrocytes) (C) SYO and P2Y12 (microglia) (D) GFAP and AT8 (E) P2Y12 and AT8 (F) SYO, AT8 and GFAP (G) SYO, AT8 and P2Y12 in the substantia nigra and frontal cortex of PSP and control brains. All graphs indicate raw data, results of post hoc testing (reported on transformed scale) showed no significant difference between disease cohorts for any colocalization analysis (Table 2.1-7).

Analysis of DAB (diaminobenzidine) and AT8 staining showed a significant increase in percentage tau burden in PSP cases compared to age and sex matched controls (type 3 ANOVA on linear mixed effects model: $F_{[1,19]} = 13.9033$, $p=0.001435$). Additionally, we observed considerable variation in burden of tau across PSP cases in both substantia nigra and frontal cortex, some showing very high levels of tau, and some with still considerable pathology compared to control brains but a lower tau burden overall (Fig. 16A-F).

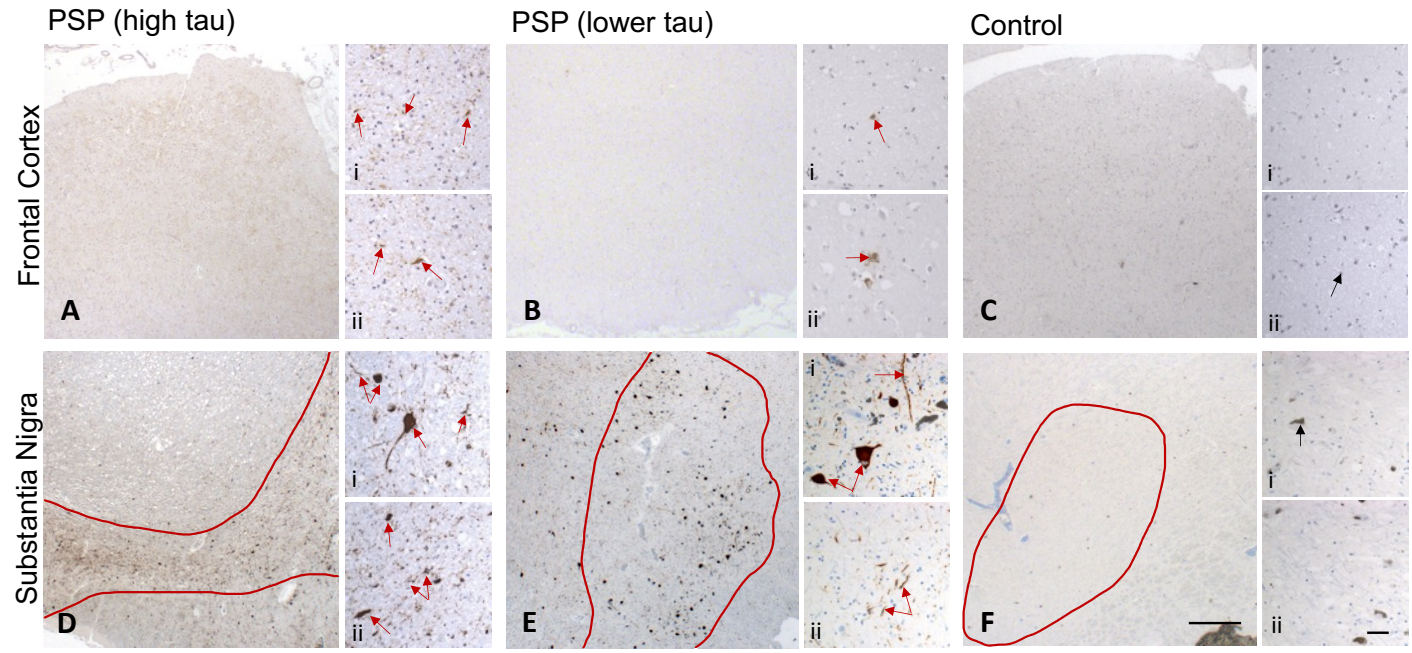

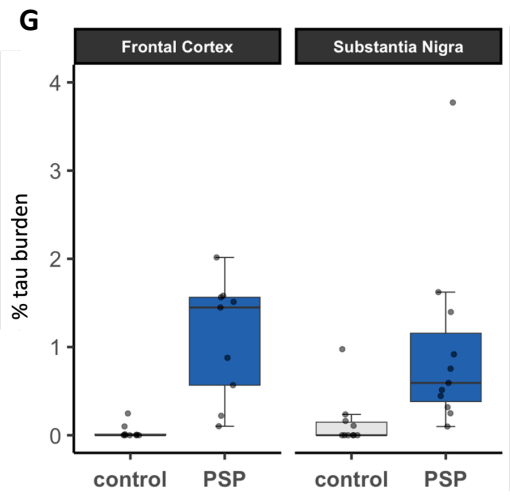

Figure 16: (A-C, respectively) High, lower and minimal to no tau burden in Frontal cortex of PSP and control cases. (D-F, respectively) High, lower and minimal to no tau burden in Substantia Nigra (outlined in red) of PSP and control cases. Red arrows indicate pathological tau staining by AT8, black arrows indicate cell nuclei or artefacts not to be confused with tau. All wide images are scaled to 500μm (F), all zoomed images are scaled to 50μm (Fii). (G) Tau burden in Frontal cortex (emmeans: p=0.0028, 95% CI[-1.64,0.373]) and Substantia Nigra (emmeans: p=0.0078, 95% CI[-1.41,0.232]) of is increased in PSP compared to age and sex matched controls. All results of post hoc testing are reported to the transformed scale (Table 3).

Discussion

Through array tomography we observed significantly greater colocalization of pre-synapses with hyperphosphorylated tau, and reactive astrocytes in the substantia nigra of PSP brains compared to age and sex matched controls. In our second study utilising immunohistochemical staining of human paraffin-embedded tissue, we sought to investigate colocalizations of pre-synapses and hyperphosphorylated tau with reactive astrocytes and microglia, expecting to recapitulate the results obtained through array tomography. However, despite observing a significant increase in colocalization of reactive astrocytes with pre-synapses in PSP brains compared to controls through array tomography, analysis of the same colocalization using immunohistochemical staining of human paraffin embedded slides directly contradicted this. Colocalization of hyperphosphorylated tau with reactive astrocytes and microglia showed significant differences in PSP and control cases across brain regions. However, this effect may simply be due to differential trends of increasing or decreasing colocalization between PSP and control cases in each region analysed. Finally, we examined DAB and AT8 immunohistochemical staining, showing a significant increase in tau burden in PSP cases compared to controls, as well as variation in tau burden levels across both PSP and control cases.

i. Increased Colocalization of Pre-Synapses and Pathological Tau in the PSP Brain

The toxicity of oligomeric tau has been well observed, inhibiting fast axonal transport, propagating disease and inducing neuronal loss (Berger *et al.,* 2007; Gerson *et al.,* 2014; Ward *et al.,* 2012). The 'level' of toxicity and specific consequences of hyperphosphorylated tau accumulation in human conditions such as PSP, however, remains unclear (Rawat *et al.,* 2022). Drosophila models have shown that soluble hyperphosphorylated tau (wild-type human) can induce behavioural deficits through resulting dysfunction of synapses, disruption of axonal transport and destabilization of the cytoskeleton (Cowan and Mudher, 2013). Evidence has also shown that early-stage deficits related to tau may be caused by hyperphosphorylated tau accumulation in dendritic spines, as it can impair glutamate receptor trafficking and synaptic anchoring, disrupting synaptic function and maturation (Hoover *et al.,* 2010; Wu *et al.,* 2021). Further evidence has illustrated the mislocalization of hyperphosphorylated tau to dendrites and dendritic spines due to mechanical injury to neurons, and the resulting dysfunction of synapses (Braun *et al.,* 2020), as well as impairment of pre- and post-synaptic mitochondria through blockage of mitochondrial fission and fusion (DuBoff *et al.,* 2012; Torres *et al.,* 2022). Investigations in AD have indicated c-terminal truncated tau is released from pre-synapses in the cortex (Sokolow et al., 2015). However, there is currently little evidence of the potential contribution of hyperphosphorylated tau at pre-synapses to synaptic loss, tau spread and resulting neuropathology across the brain in PSP. Thus, our projects first aim was to investigate the accumulation of pre-synaptic hyperphosphorylated tau in human PSP tissue, specifically in the substantia nigra, an area of the brain affected early in PSP disease progression (Kovacs *et al.,* 2020).

Isolated synaptosomes obtained from wild-type and tau mutant mouse lines have illustrated an increase in expression of total tau and phosphorylated forms of tau

(Trease et al., 2022). Through illustrating increased colocalized staining using synaptophysin markers to integral membrane glycoproteins of pre-synaptic vesicles (Wiedenmann *et al.,* 1986), with a marker for hyperphosphorylated tau (AT8) in the substantia nigra of PSP brains compared to controls, we have provided new evidence that hyperphosphorylated tau accumulates at pre-synapses in the substantia nigra in human brains with PSP (Fig. 10A). We suggest this accumulation may contribute to transsynaptic pathological tau spread, and could further suggest hyperphosphorylated tau accumulation may contribute to synaptic dysfunction. Our group has previously illustrated an increase in colocalization of both pre- and post-synapses with hyperphosphorylated tau in the frontal cortex in PSP compared to controls (McGeachan *et al.,* 2022). This project expands upon this observation by illustrating the increase in accumulation of hyperphosphorylated tau in pre-synapses of the substantia nigra, an area affected early on and substantially in PSP (Kovacs *et al.,* 2020). We sought to build upon these findings through directly comparing colocalization of hyperphosphorylated tau with pre-synapses in immunostained human post-mortem tissue of both frontal cortex and substantia nigra. Analysis of colocalization of pre-synapses with hyperphosphorylated tau in both substantia nigra and frontal cortex (BA9) showed only bordering statistical significance between PSP and control cohorts. Furthermore, statistical effects encompassing both disease cohort and age showed similar bordering significance, indicating an increase in colocalization of hyperphosphorylated tau with pre-synapses in PSP cohorts compared to controls, but likely with an effect of age, despite cases being age matched (Fig. 14A). Biologically, this is consistent with expectations during development of PSP and other tauopathies, with increasing burden of pathological tau and synaptic spread during later disease progression, (Franzmeier *et al.,* 2020; Kovacs *et al.,* 2020), thus older patients with further PSP progression would show increased burden of pathological tau. Therefore, an increase in pre-synaptic accumulation of hyperphosphorylated, pathological tau in synapses with age as the disease itself progresses is a congruous result.

Issues with clarity of staining of the T22 antibody led to difficulties when analysing images to obtain colocalization data, therefore we must consider the results of pre-synaptic colocalization with oligomeric tau observed through array tomography carefully (Fig. 10B). During segmentation, we excluded anything that could be classed as background or artefactual staining, to include only true staining. Consequentially, there is potential that some true staining may have been excluded, and that had this staining been included for analysis, a significant increase in oligomeric tau colocalization with pre-synapses may have been seen, therefore we should consider the resulting data dubiously. Furthermore, results from Colom-Cadena et al. (2023) suggest that in AD oligomeric tau accumulation at the synapse occurs earlier, followed by hyperphosphorylated or other toxic forms of misfolded tau. This evidence could suggest we may expect to see a greater increase in oligomeric tau colocalization with pre-synapses than that of hyperphosphorylated tau. Considering this and our results pertaining to increased colocalization of hyperphosphorylated tau and pre-synapses in PSP, this may suggest the smaller effect size of the colocalization result of oligomeric tau is in fact due to staining issues as described, as opposed to less colocalization, and therefore, less synaptic accumulation.

ii. Colocalization of Pre-Synapses and Reactive Astrocytes Appears Increased in PSP Brains

Astrocytes support the brain both metabolically and through synaptic interactions (Reid *et al.,* 2020; Mariotti *et al.,* 2018; Martín *et al.,* 2015; Santello *et al.,* 2019; Volterra and Meldolesi, 2005). Reactive astrocytes, such as tufted astrocytes in PSP, are a characteristic gliosis as part of the inflammatory response in tauopathies, and are known to accumulate tau (Kovacs and Budka, 2010). We stained embedded human post-mortem tissue with GFAP, a marker for reactive astrocytes, to observe colocalizations with pre-synapses and hyperphosphorylated tau.

Through array tomography, we observed a significant increase in the colocalization of pre-synapses and reactive GFAP-positive astrocytes in the substantia nigra of PSP cases compared to controls (Fig. 10C). The increased presence of reactive astrocytes colocalized with pre-synapses may suggest more astrocytes are acting to phagocytose pre-synapses in PSP. However this analysis did not also include colocalization of pathological tau, thus, we cannot infer whether astrocytes may be phagocytosing tau containing, dysfunctional pre-synapses. Swollen astrocytes show enhanced labelling with GFAP after lesion of rat optic nerve (Schmidt-Kastner *et al.,* 1993). Swelling of astrocytes may be linked to gliosis through the role of aquaporins in both gliosis and swelling due to neural injury (Lafrenaye and Simard, 2019). Alternatively, this could suggest that in PSP, where gliosis occurs and astrocyte characteristics change (tufted astrocytes), there may be increased labelling of astrocytes due to enhanced swelling. These results suggest that there may be an increase in both gliosis and synaptic engulfment by reactive astrocytes in PSP brains compared to controls.

Percentage volume of staining colocalization analysis of GFAP-positive astrocytes and pre-synapses showed conflicting results to that obtained through array tomography (Fig. 15B), however. These results indicate there is a significant decrease in colocalization of reactive astrocytes and pre-synapses in PSP and controls, with age as a significant factor. For both array tomography and human paraffin studies, the same antibodies were used, and post-mortem tissue obtained from PSP and control brains was from cases that overlapped between both studies, though the human paraffin study had slightly more cases. Previous data has shown that when studying synapses, traditional light microscopy techniques such as confocal imaging can be less effective, with array tomography providing a more sensitive assessment of synapses when imaging with immunofluorescence (Kay *et al.,* 2013). Though we had hoped the use of a second technique could affirm the results we saw through array tomography, considering this, it is likely that the results concerning synaptic colocalization obtained through array tomography are more accurate than data acquired using confocal imaging, as in the human paraffin study. Additionally, increasing evidence suggests astrocytes show heterogeneity not only between brain regions, but also within the same brain (Lafrenaye and Simard, 2019; Zhang and Barres, 2010). Despite many of the same cases being used for array tomography and human paraffin studies, separate parts of substantia nigra tissue were embedded in resin and paraffin for the respective studies, therefore there is also potential for astrocyte variation across the studies.

Previous work using immunohistochemical techniques in AD model mice has shown reactive astrocytes can act to phagocytose pre-synaptic structures, but appear to be acting to clear dysfunctional synapses, and with limited efficiency (Gomez-Arboledas *et al.,* 2018). This could suggest that reactive astrocytes have insufficient activity to phagocytose pre-synaptic structures to cause the larger effect on cognitive ability synaptic loss causes in AD. However, differences in astrocytic morphology, such as the presence of tufted astrocytes in PSP and not AD (Fig. 1), and average nuclear area amongst astrocytes in PSP and AD (32.18μm^2 and 86.32μm^2 respectively, compared to 67.54μm^2 in normal brains) (Montalbano et al., 2022), suggests that the way reactive astrocytes function across these two diseases may not be the same. Considering this, and the resolution limitations of confocal imaging, we suggest it is likely that the significant increase in colocalization of pre-synapses and reactive astrocytes observed in PSP cases (compared to controls) through array tomography is a more reliable conclusion. This could suggest more reactive astrocytes are colocalizing to synapses to phagocytose those that are not functioning appropriately in PSP, for example due to accumulation of oligomeric (Lasagna-Reeves *et al.,* 2011) or hyperphosphorylated tau, as our data have suggested (Fig. 9A).

Astrocytes have been shown to form interactions with synapses, playing active roles in regulation of synaptic function through exchange of regulatory signals with neurones and inducing excitation neurones (Mariotti *et al.,* 2018; Martín *et al.,* 2015; Santello *et al.,* 2019; Volterra and Meldolesi, 2005). In both array tomography and immunohistochemical studies we used GFAP antibodies, which stain reactive astrocytes. An alternative explanation to the increased colocalization of GFAP-positive astrocytes to pre-synapses in PSP we observed, is that astrocytes already associated with synapses are induced to become activated as part of the inflammatory response due to accumulation of pathological tau in PSP. Furthermore, as activation of astrocytes during chronic inflammatory response can be neurotoxic, this could suggest that reactive astrocytes that may already be associated with synapses could directly contribute to their dysfunction, but indirectly lead to synaptic loss through other mechanisms, such as phagocytosis by microglia, though further evidence is required to support this idea.

iii. Reactive astrocytes and pathological tau

Previous evidence from immunostaining of human post-mortem tissue has shown that both tufted and reactive astrocytes can accumulate hyperphosphorylated tau in PSP (Kovacs and Budka, 2010; Togo and Dickson, 2002). We analysed colocalization of GFAP-positive reactive astrocytes and hyperphosphorylated tau in PSP and control brains in the substantia nigra and frontal cortex (BA9) through fluorescent staining of human post-mortem tissue. Our results suggest there was no significant difference between PSP and control cohorts (Fig. 15D), but identified a significant difference in colocalization between brain regions; there is no apparent change between PSP and controls in substantia nigra, but there appeared to be a trend of decreased colocalization in PSP brains in the frontal cortex, compared to controls. By staining with DAB and AT8 to mark hyperphosphorylated tau in both substantia nigra and frontal cortex and analysing the percentage tau burden, we found there was a significant increase in pathological tau burden in PSP cases compared to controls (Fig. 16G). This also allowed us to visualise specific pathological characteristics of PSP

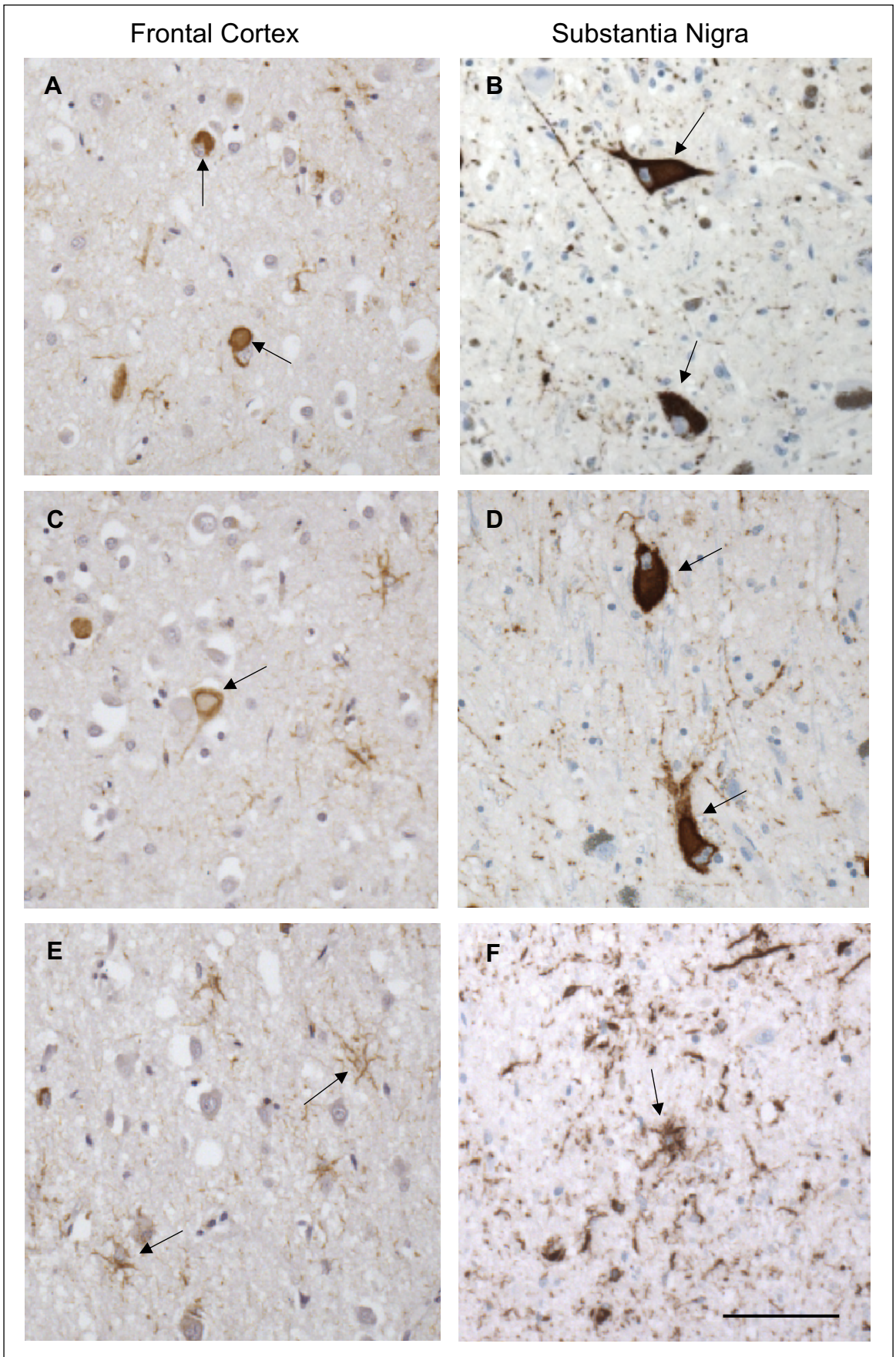

Figure 17: (A-D) Globose neurofibrillary tangles, and (E-F) Tufted astrocytes in PSP brains stained with DAB and AT8. All images are scaled to 50μm.

including tufted astrocytes and NFTs (Fig. 17). This data illustrates the increased burden of hyperphosphorylated tau in PSP, and validates its presence in both NFTs and tufted astrocytes. However, it has also been shown through examination of distribution of tufted astrocytes and gliosis with tau tangles, that the accumulation of tau in astrocytes is a degenerative process, and can occur independently to the reactive process of gliosis (Togo and Dickson, 2002). This suggests astrocytes accumulating tau may be part of the degeneration associated with PSP itself, which may explain the decreasing trend in colocalization of hyperphosphorylated tau we observed in frontal cortex. However, we saw no change in colocalization in the substantia nigra, a region affected markedly and earlier in PSP disease progression, therefore if astrocytes were degenerating in the frontal cortex notably enough to cause the decrease we observed, this would likely also be seen in substantia nigra, potentially to a greater extent. This suggests that either, the change we observed in frontal cortex may be artefactual, or that along with showing heterogeneity in their morphology and physiological properties and functions (Zhang and Barres, 2010), astrocytic response, or susceptibility, to accumulation of pathological tau may also vary across brain regions. Additionally, distribution patterns of tufted astrocytes in the PSP brain have also shown that there are less present in the frontal cortex than areas like the substantia nigra (Hattori *et al.,* 2003), likely due to the lesser tau pathology, depending on disease progression stage, thus, this variation may have also affected our results. However, our staining targeted GFAP-positive reactive astrocytes, and showed there was an increasing trend in this staining in PSP brains compared to controls in both substantia nigra and frontal cortex (Fig. 14B), so this is likely not the case. Furthermore, this would not explain why there was more GFAP-positive astrocyte staining in the frontal cortex control cases.

iv. Colocalization of Microglia with Hyperphosphorylated Tau and Pre-Synapses May Be Region Specific

Microglia, as primary immune cells of the brain, are key regulators of inflammatory responses, such as neuroinflammation associated with neurodegenerative diseases like PSP, where pathogenic tau accumulates. Induction of microglia into an inflammatory state due to tau pathology can result in compounded neuronal injury (Morales *et al.,* 2013). Injury to the brain causes activated microglia to produce interleukin-1 (IL-1), an inflammatory cytokine, which in turn can lead to increased phosphorylation of tau (Demock and Kornguth, 2019; Vogels *et al.,* 2019). Increased expression of IL-1β transcripts in the substantia nigra in PSP has also been observed through evaluation of proinflammatory cytokines (Alster *et al.,* 2020b; Fernández-Botrán *et al.,* 2011). Additionally, mouse models of Alzheimer's Disease, have suggested that tau pathology and its spread through the brain can be driven by microglia (Maphis *et al.,* 2015), though this may not be directly comparable in PSP.

Our results suggest that despite there being an individual increase percentage volume staining of both microglia (P2Y12) and hyperphosphorylated tau (AT8) in PSP compared to controls in both substantia nigra and frontal cortex (Fig. 14A, 14D), increased colocalization of the two is limited to the frontal cortex; there appears to be a trend of more colocalization of microglia and hyperphosphorylated tau in controls compared to PSP in the substantia nigra (Fig. 15E). This impacts effect sizes as a decrease and increase in colocalization are seen in the substantia nigra and frontal

cortex respectively, meaning any significant effect observed is limited to difference between brain regions. Initially, we may consider that microglia may be acting differently in each of these regions in terms of their engulfment of tau, as microglial burden differs across brain regions in PSP (Fernández-Botrán *et al.,* 2011). Microglia have been shown to phagocytose tau containing synpases in AD (Vogels *et al.,* 2019) however it has also been suggested than in cases of an over-reactive inflammatory response due to traumatic injury or disease onset, microglia can become senescent or even undergo cytorrhexis (Greenwood and Brown, 2021; Ng *et al.,* 2023; Streit *et al.,* 2014). Dystrophic microglia have also been proposed as a phenotype exclusive to diseased brains (Shahidehpour *et al.,* 2021). In these neurotoxic phenotypes of senescence or dystrophia microglia exhibit reduced motility and ability to phagocytose (Greenwood and Brown, 2021). This evidence provides an explanation of the differential trends of colocalization of microglial marker P2Y12 and hyperphosphorylated tau in PSP compared to controls in substantia nigra and frontal cortex that result in the significant difference between brain regions we observed (Fig. 15E). We suggest that due to the increased burden of tau pathology in substantia nigra, as an area affected earlier in disease progression of PSP (Kovacs *et al.,* 2020), microglia may become senescent or dystrophic, thus no longer functioning as they should to reduce tau seeding or remove tau-containing synapses (Hopp et al., 2018, Vogels et al., 2019) and so show less colocalization with hyperphosphorylated tau. Whereas, in the frontal cortex, which is affected later and thereby potentially to a lesser extent by tau pathology in PSP, microglia may still be functioning efficiently and so colocalize more with hyperphosphorylated tau in PSP than controls in this region. As some tau accumulation can occur in normal ageing brains (Ziontz et al., 2019), we would expect that microglia would function homeostatically to reduce tau accumulation, and thereby expect to observe some colocalization of microglia and hyperphosphorylated tau in our control cases. The important distinction here, is that the effect of any senescence or dystrophia of microglia as a result of tau pathology in PSP would have to reduce microglial ability to phagocytose hyperphosphorylated tau to a level below that in a normal ageing brain to align with our results. Further investigation into these dysfunctional phenotypes in the PSP brain is required to validate this however, as previous evidence has only shown these effects of disease on microglia in AD brains specifically. Though PSP and AD share changes to gene expression related to inflammatory responses, these occur at different temporal points in disease progression (Iohan et al., 2022), and further, PSP shows glial tau pathology whereas this is mostly neuronal in AD (Chung et al., 2021). Tau itself varies between PSP and AD, with the former showing predominantly 4R tau, whereas in AD the ratio of 3R to 4R tau is 1:1, as is seen in normal brains (Chen *et al.,* 2010; Martínez-Maldonado *et al.,* 2021). Furthermore, analysis of tau fragment concentrations of cerebrospinal fluid has been shown to differ between those with PSP and AD (Wagshal *et al.,* 2015). Additionally, whilst PSP is characterised by tau pathology, AD brains show both tau and, more predominantly, amyloid-β pathology (Zhang *et al.,* 2021b), the interaction of which may influence tau propagation and neuronal uptake, and mediate cognitive dysfunction; the full effects of the interaction and therapeutic opportunities this may provide are not yet fully understood (Tripathi and Khan, 2020; Zhang *et al.,* 2021b). These differences illustrate we can utilise our knowledge of AD to drive investigations in primary tauopathies such as PSP, but results concerning systems that show variation such as microglial action, may not align between the two diseases.

Colocalization levels we observed between microglia and hyperphosphorylated tau appear to be consistent in PSP cohorts across each brain region, however, suggesting that the difference in effect of cohort lies in variation between control cohorts (Fig. 15E). Furthermore, the inflammation response incurred when tau pathology accumulates and propagates involves the activation and migration of microglia to the site of injury, thereby increasing the density of microglia in those regions affected (Alster *et al.,* 2020b; Shields *et al.,* 2020). These activated microglia act to take up pathological tau such as hyperphosphorylated tau, both extra- and intracellular (Hopp *et al.,* 2018). Thus, we could expect to observe increased colocalization of microglia with hyperphosphorylated tau in PSP compared to control, as we did in the frontal cortex, in the substantia nigra. Furthermore, paraffin-embedded human tissue sections can show degradation, due to the processing of the tissue, resulting in degradation of antigens and loss of staining performance (Xie et al., 2011). From this we suggest an alternative explanation, that the higher colocalization in the substantia nigra of controls may be due to staining or segmentation inconsistencies, as opposed to true colocalization representing more microglia taking up hyperphosphorylated tau, in the substantia nigra of controls compared to PSP. We may also determine that this inconsistency could have affected the significance of cohort comparison obtained from statistical testing as both brain regions are included in the analysis, as subdivision of data can hide effects of the population overall according to the statistical theory of Simpson's paradox (Bonovas and Piovani, 2023).

Notably, in our investigation we focused on the hyperphosphorylated epitope of pathological tau. Evidence has suggested that the p38 immune pathway in microglia, which is activated in both PSP and AD amongst other tauopathies (Hartzler *et al.,* 2002; Johnson and Bailey, 2003), is not activated by hyperphosphorylated tau, but by non- and dephosphorylated tau (Perea *et al.,* 2018). This may also explain the lack of significance seen in our results relating to colocalization of hyperphosphorylated tau specifically, and microglia, and could suggest further investigation involving microglial colocalization with other epitopes of pathological tau should be undertaken.

We also investigated colocalization of microglia with pre-synapses, and though initial inspection of the raw data suggested a trend of increased colocalization in PSP compared to controls, in both substantia nigra and frontal cortex, statistical analysis showed this was not significant. Fluorescence microscopy of developing organotypic hippocampal cultures with 3D ultrastructural characterization has shown microglia-synapse interactions span to include selective partial phagocytosis of presynaptic structures, but do not act to prune dendritic spines (Weinhard *et al.,* 2018). However, this was investigated in a neurodevelopmental context. Similarly, previous experimentation has suggested microglia phagocytosing tau-containing synaptic compartments of neurons may contribute to synaptic dysfunction (Vogels *et al.,* 2019). By investigating colocalization of microglia with pre-synapses in PSP compared to controls we hoped to provide evidence of microglial engulfment of synapses, in a neurodegeneration and tauopathy specific context, nevertheless the result was not significant when simply comparing disease cohorts. Interestingly, however, the colocalization of microglia with synapses appears to differ considerably between substantia nigra and frontal cortex, though not quite significantly ($p=0.05025$). This mirroring of effect of brain region on microglia colocalization (with pre-synapses and hyperphosphorylated tau) could further support a hypothesis of differential microglial action between brain regions of PSP and control brains. Conversely, our results of

synaptic staining in control and PSP cohorts (Fig. 14C) show an increase in pre-synaptic staining in the substantia nigra of PSP cases compared to controls. This is likely an artefact as there is no evidence to suggest there would be an increase of pre-synapses in this region in PSP, in fact the opposite (Adams *et al.,* 2023; Briel *et al.,* 2021; Holland *et al.,* 2020). This aberrant increase in pre-synaptic staining may therefore account for the larger increase in microglial-synaptic colocalization in substantia nigra, and therefore the difference in this colocalization between regions.

Though we do not have evidence to discard the 'unexpected' results of colocalization analysis of microglia with hyperphosphorylated tau and pre-synapses, we must consider the evidence proposed here that they may be a result of error, as equally as we consider them to be potentially true effects.

v. Is Hyperphosphorylated Tau Involved in Synaptic Loss in PSP?

Accumulation of hyperphosphorylated tau in synapses in AD has been shown to have cytotoxic effects, both directly and indirectly, to impact signalling cascades, organelle function, and axonal transport, resulting in synaptic loss through activation of immune responses including microglial engulfment (Rajmohan and Reddy, 2017). Engulfment of tau-containing synapses by microglia is often attributed to both AD and PSP (Vogels *et al.,* 2019). Through 3-way colocalization analysis of paraffin stained human post-mortem sections of substantia nigra and frontal cortex (BA9), we expected to see an increase in colocalization of pre-synapses, hyperphosphorylated tau, and microglia in PSP brains to reflect this process, however our results showed no significant difference between PSP and control cases (Fig. 15G).

Microglial engulfment of tau-containing synapses has been shown to occur at higher rates in differential brain regions of AD and PSP. Higher expression of IL-1β in substantia nigra of PSP brains has been observed compared to AD and control, as well as higher expression of IL-1β in parietal cortex and TGFβ in cortical areas of AD brains, compared to PSP or control. Microglial burden has also been shown to differ in a brain-region dependent manner in PSP and AD (Fernández-Botrán *et al.,* 2011). Furthermore, genome wide association studies have highlighted in particular the critical role played by microglia in the immune response in AD, whereas genetic risk factors of PSP were determined to be associated with genes encoding tau protein and oligodendrocyte myelin maintenance (Laurent *et al.,* 2018). As previously described, variation in tau pathology, cytokine expression and resulting immune response between AD and PSP may suggest that despite our knowledge of the impact of tau accumulation on microglial action and resulting synapse loss in AD, there is not yet sufficient evidence that this is mirrored in PSP. It is reasonable to therefore infer that the mechanisms of synapse loss in PSP may differ to AD, or at least at the level of microglial involvement. Our results support this, as we saw no significant difference in colocalization of pre-synapses, hyperphosphorylated tau and microglia, representing no difference in colocalization of tau-containing synapses and microglia acting on them in PSP compared to controls.

As previously described, there is evidence of microglia becoming senescent due to tau pathology in AD, and ageing, as opposed to activated, resulting in loss of function and, in disease, microglia becoming dystrophic (Streit *et al.,* 2009; Vogels *et al.,* 2019).

We suggest that our 3-way colocalization data of microglial markers, pre-synapses and hyperphosphorylated tau may also evidence this in PSP, as it illustrated similar trends to that of the colocalization of microglial markers and hyperphosphorylated tau alone. Initial observation of raw colocalization data suggests a small trends of a decrease in our 3-way colocalization in substantia nigra, and a small increase in frontal cortex (BA9) (Fig. 15G), though this was not found to be statistically significant. These trends could suggest microglia may have become dysfunctional and therefore may have stopped acting to phagocytose tau containing pre-synapses due to the earlier emergence of disease effects in substantia nigra, whilst retaining some functionality in the lesser affected frontal cortex. However, unlike the 2-way colocalization data focusing on microglia and hyperphosphorylated tau, analysis of the 3-way colocalization with the addition of pre-synapses did not show any significance of brain region, therefore here we can only comment on the similarity of trends observed in the two analyses. Furthermore, as previously discussed, further evidence is required to support the hypothesis of microglial senescence and phagocytosis of synapses to cause synaptic loss in PSP, as much of the evidence currently available in the literature relates to AD.

Previous evidence in mouse AD models with both amyloid-β and tau pathology, has indicated astrocytes contribute to elimination of inhibitory synapses surrounding plaques, pathology specific to AD, via the C1q complement pathway (Dejanovic *et al.,* 2022). Through our investigation of colocalization of reactive astrocytes with both pre-synapses and hyperphosphorylated tau, we sought to determine if astrocytes may act similarly in PSP. Analysis of 3-way colocalization of GFAP-positive astrocytes, hyperphosphorylated tau, and pre-synapses indicated a trend of decreasing colocalization in PSP brains compared to controls in both brain regions, though neither change was statistically significant (Fig. 15F). This may suggest that reactive astrocytes do not act to phagocytose tau-containing pre-synapses. Investigations into synaptic loss surrounding tau-containing tufted astrocytes in human PSP tissue have indicated that there is little difference in synapse number compared to control astrocytes from non-diseased subjects in the same brain region (Briel et al., 2021), aligning with our results.

Overall, our investigations into the the role of hyperphosphorylated tau in the activation of glia and resulting synaptic loss have provided interesting insights, but are insufficient to make conclusions. Further investigation into senescence, dysfunction and activation of microglia and astrocytes due to the accumulation of tau pathology in a brain region specific manner is required to build upon what we have presented here.

vi. Tau Burden is varied in both PSP and control cases

We observed a significantly increased burden of hyperphosphorylated tau in PSP cases compared to controls in both substantia nigra (Fig. 16G). However, as illustrated in Figure 16 (A-F) we also observed a considerable amount of variation in tau burden within PSP cases, and some variation within control cases. Previous studies of tau burden in Frontotemporal lobar degeneration with *MAPT* pathogenic variants (a group of disorders of which FTD is one subgroup) showed that within a group with only the 4R tau isoform, tau burden appeared more severe compared to the 3R-only isoform group. However, they also observed less neuronal degeneration in the 4R group than

the 3R group, as well as most frequent tau inclusions (Giannini et al., 2022). Results from our second study, whereby we saw no significant increase in colocalization of astrocytes or microglia with pre-synapses, could suggest the action of these glia to engulf synapses and neuronal structures was not changed in PSP cases compared to controls. This could suggest that by staining for hyperphosphorylated tau in our PSP (which would only present with 4R tau) and control cases, the increased burden of hyperphosphorylated tau we observed may not necessarily correlate with an increase in degeneration of synapses due to glial engulfment specifically. As with many of our results we found greater variance in tau burden than anticipated, we suggest this may be due to inherent variation of disease progression of the human cases available to us.

vii. Limitations

We suggest that our immunofluorescence study on human paraffin-embedded tissue, whilst providing some interesting insights and possibilities in the context of the literature, was likely impacted by limits of confocal imaging and further, may have been underpowered. This research would benefit from repeats to confirm our observations and further conclusions we do not yet have the data to affirm. Further, repetition utilising array tomography, with the same antibodies and analysis parameters, would provide useful evidence as to which of our data may have been impacted by the resolution limits of confocal imaging. It is likely that colocalizations concerning pre-synapses were affected, as we know array tomography is more precise in this aspect (Kay *et al.,* 2013), but it could be academically useful to compare the effect of these two techniques on analysis of colocalizations with larger structures such as astrocytes and microglia Furthermore, formalin-fixed paraffin embedded tissue can show degeneration, thus leading to degeneration of antigens and impacting the performance of staining (Xie *et al.,* 2011). Therefore, repeating our studies with another technique such as array tomography, which has been shown to yield good quality imaging over multiple staining rounds (Sanchez Avila and Henstridge, 2022) could clarify if tissue sample degeneration impacted our results, and could allow us to investigate synaptic loss in PSP further. As this project focused on using human post-mortem tissue, our sample sizes were therefore limited by the cases and donated tissue available to us. This may have impacted the clarity of effects observed, and furthering this research with a greater sample size and therefore greater power for statistical testing would help support our findings and potentially provide further insight to the conclusions we have made.

For our all analyses we used the maximum number of cases available to us, whilst ensuring experimentation would be balanced and matched for age and sex. However, the results from our immunohistochemical analysis of human paraffin-embedded sections, and the results conflicting with those obtained in our array tomography study, may suggest this study was underpowered. After the fact, using mean and standard deviation values from colocalization analysis, a power value of 80%, group number of 2 and $p < 0.05$, we calculated the optimal sample size for this study was n=126. Utilising the maximum number of cases available to us, with 20 samples per region (frontal cortex and substantia nigra), per cohort (PSP and control) to total n=80, we likely therefore had a power level of ~60%. Studies with low statistical power have reduced chances of detecting true effects, and furthermore lower powered studies can

lead to inflated effect sizes (Button et al., 2013). This suggests that as well as being underpowered, we may be obtaining outputs of inflated effect sizes for this part of the project.

Furthermore, this study involved two separate brain regions that we intended to use for comparison, substantia nigra and frontal cortex. In statistical comparison utilising post-hoc testing to focus beyond the initial comparison of simply PSP vs control, we were able to see significant differences in colocalizations of hyperphosphorylated tau with reactive astrocytes and microglia by brain region. Furthermore, age was identified as a significant effect between PSP and control groups in relation to colocalization of pre-synapses with reactive astrocytes, despite the groups being age matched. According to the statistical phenomenon Simpson's paradox, associations between two variables can be affected by subdivision of the population (Bonovas and Piovani, 2023), such as we have done by utilising two separate brain regions. This may explain why we could not see significant increases in colocalizations that we may have expected due to previous array tomography data when simply comparing PSP and control groups. It may therefore also indicate that these emerging significant changes specific to brain region or age are important findings.

As previously discussed, there are multiple epitopes of pathological tau, however there is also heterogeneity within epitopes (Dujardin *et al.,* 2020). Phosphorylation of tau, for example, can occur at numerous sites including serine, threonine and tyrosine sites (Noble *et al.,* 2013). Additionally, previous data obtained through bioactivity assays has suggested that this molecular diversity within tau epitopes may contribute to the variation observed between patients with AD (Dujardin *et al.,* 2020). The AT8 antibody utilised here has been reported to bind to hyperphosphorylated tau with phosphorylation sites at serine-202 and -208, and threonine-205, plus combinations of those sites (Malia *et al.,* 2016). From this, we can elucidate that though this antibody provides reliable evidence for identifying colocalizations of hyperphosphorylated tau, it may not show us the whole picture. Furthermore, data obtained using array tomography showed that in PSP approximately 1% of pre-synapses are colocalizing with hyperphosphorylated tau, compared to essentially none in controls (Fig. 9A). Despite showing a significant increase in colocalization, it must be contemplated as to whether 1% of synapses accumulating tau is a significant enough proportion, considering the number of synapses within the region, to aid spread of pathological tau.

Due to the anatomy of the substantia nigra (Zhou and Lee, 2011) we opted not to use antibodies for post-synaptic structures as the staining was insufficient. However, it is also important to consider the effects of the anatomical variation within the substantia nigra, which can be separated into the substantia nigra pars compacta and pars reticulata (Sonne *et al.,* 2023). The former contains dopaminergic and glutamatergic neurons, indirectly inhibiting target cells of the striatum via activation of g-aminobutyric acid (GABA) receptors (Melani and Tritsch, 2022; Yamaguchi *et al.,* 2013), whereas the latter contains mostly inhibitory GABAergic neurons (Sonne *et al.,* 2023), and some glutamatergic neurons (Yamaguchi *et al.,* 2013). Previous work utilising organoids with tau mutations has shown that as well as upregulated expression of *MAPT*, glutamatergic signalling pathways and their regulators such as ELAVL4 are also upregulated. This is important to consider, as we did not separate our investigations between the two major divisions of substantia nigra, which have

differing anatomies and inclusion of glutamatergic neurons, as it is possible mutations leading to pathological tau accumulation may affect these areas to a greater or lesser extent depending on the inclusions of these glutamatergic pathways.

viii. Conclusions

Our evidence indicates new evidence that in the PSP brain, there is accumulation of pathological, hyperphosphorylated tau at pre-synapses in the substantia nigra, an area of the brain markedly affected in PSP. This accumulation may play a role in the dysfunction and loss of synapses observed in PSP brains, resulting in the symptomatic loss of motor and cognitive function experienced by those with PSP and other tauopathies, however this requires further investigation to be validated. We also indicate an increased colocalization of reactive astrocytes with pre-synapses in PSP cases compared to controls. This result was obtained through array tomography, however results from our second study utilising human paraffin embedded post-mortem slides were contradictory. Overall, we determined this was likely due to the resolution of confocal imaging being insufficient to identify single synapses, and so determined the results obtained through array tomography were more accurate. These results could suggest reactive astrocytes are acting to phagocytose pre-synapses in PSP, or alternatively that astrocytes associated with neuronal and synaptic function are becoming reactive, and potentially contributing the synaptic dysfunction itself. As 3-way colocalization analysis of reactive astrocytes, pre-synapses and hyperphosphorylated tau showed no significant difference between PSP and control cohorts in either substantia nigra or frontal cortex, we deduce that we have insufficient evidence to conclude whether astrocytes contribute to synaptic loss in PSP, and further investigation is required.

By immunostaining with microglial and hyperphosphorylated tau markers, we indicate that there may be regional differences in microglial function in PSP through senescence or degradation of microglia in brain regions affected markedly by tau pathology, such as the substantia nigra, lessening microglial phagocytosis and motility. This is concurrent with existing research, and aligns with our observation of a decreasing trend of colocalization of microglial markers with hyperphosphorylated tau in the substantia, compared to an increasing trend of colocalization in frontal cortex. Investigations into microglial engulfment of synapses gleaned similar, statistically insignificant results, with further indication of regional differences of colocalization of microglia, here with pre-synapses. We also provide evidence that these results are unexpected in the context of current evidence of microglial function in PSP, and as the only statistically significant effect found in these analyses was region, suggest these results may be due to tissue degradation due to the process of paraffin embedding and the reduced staining performance as a result. However, we suggest further investigation into potential effects of tau accumulation on microglial function and resulting senescence and degradation could aid our understanding of the role of microglia in synaptic loss in PSP.

Power analysis indicates our experimentation utilising immunofluorescent staining of human paraffin embedded tissue was likely under-powered to observe significant differences between PSP and controls in colocalization of reactive astrocytes and microglia with tau-containing pre-synapses. Therefore, we suggest repeating our

investigations with greater a sample size, and with techniques such as array tomography to ensure imaging is undertaken with sufficient resolution to reflect the structures of the brain we are investigating, would be a useful next step.

Our investigation pertaining to the burden of pathological, hyperphosphorylated tau indicated a significantly greater burden in PSP brains compared to controls, but also illustrated the variation of the burden of pathological tau, not only in PSP brains, but also in healthy ageing control brains. This provided a useful context for our more unexpected data concerning colocalizations of hyperphosphorylated tau with reactive astrocytes and microglia, suggesting that the burden of this isoform of tau may not be itself related to the mechanisms of synaptic loss by microglia and astrocytes, and we suggest that similar investigations involving other pathological forms of tau could be useful to further our understanding.

We also indicate here that utilising our current knowledge of mechanisms of synaptic loss other tauopathies such as Alzheimer's disease can contribute to our investigations in PSP. However, we must undertake our investigations with a consideration of the system specific similarities and differences between these diseases, with the understanding that although tauopathies may share pathological traits, each are distinguishable and require individual investigation. Building upon our results indicating increased accumulation of hyperphosphorylated tau and presence of reactive astrocytes at pre-synapses, we believe further investigation into the mechanisms by which the accumulation of pathological forms of tau in synapses may lead to both the dysfunction and loss of synapses is required. Beyond that, further investigation of the roles of astrocytes and microglia in this synaptic loss is required to validate ideas put forth here surrounding their ability to phagocytose tau-containing synapses in a PSP brain with increasing tau pathology, and whether this differs from our current knowledge of their function in other tauopathies. By improving our understanding of these mechanisms, we may find potential therapeutic targets to treat those with PSP, however from the evidence presented here and our current knowledge of these mechanisms, our understanding requires further development to reach this target.

Supplementary Tables

Table 1.1: Statistical analysis output of percent colocalization of pre-synapses and hyperphosphorylated tau

transformTukey(SYO_AT8) ~ Cohort + Age_years + Sex + PMI_Hours + (1|SD_number)						
Anova (lmerTest) output – Tukey transformed						
	Sum Sq	Mean Sq	NumDF	DenDF	F value	Pr(>F)
Cohort	0.95173	0.95173	1	6	46.1192	**0.0004989**
Age (Years)	0.03685	0.03685	1	6	1.7859	0.2298708
Sex	0.02661	0.02661	1	6	1.2895	0.2994604
PMI (Hours)	0.05212	0.05212	1	6	2.5256	0.1631156

emmeans (lmVOI, “Cohort”, type=”response”)						
emmeans (Tukey transformed scale), pairs, confint output (back transformed scale)						
Contrast	Estimate	SE	DF	95% CI	t.ratio	p.value
PSP - Control	-0.9	0.133	6	-1.22, 0.576	-6.791	**0.0005**

Table 1.2: Statistical analysis output of percent colocalization of pre-synapses and oligomeric tau

transformTukey(SYO_T22) ~ Cohort + Age_years + Sex + PMI_Hours + (1|SD_number)						
Anova (lmerTest) output – Tukey transformed						
	Sum Sq	Mean Sq	NumDF	DenDF	F value	Pr(>F)
Cohort	0.0087871	0.0087871	1	6	0.7304	**0.4256**
Age (Years)	0.0001101	0.0001101	1	6	0.0092	0.9269
Sex	0.0162423	0.0162423	1	6	1.3501	0.2894
PMI (Hours)	0.0001682	0.0001682	1	6	0.0140	0.9097

emmeans (lmVOI, “Cohort”, type=”response”)						
emmeans (Tukey transformed scale), pairs, confint output (back transformed scale)						
Contrast	Estimate	SE	DF	95% CI	t.ratio	p.value
PSP - Control	-0.138	0.162	6	-0.535, 0.258	-0.855	0.4256

Table 1.3: Statistical analysis output of percent colocalization of pre-synapses and reactive astrocytes

transformTukey(SYO_GFAP) ~ Cohort + Age_years + Sex + PMI_Hours + (1|SD_number)						
Anova (lmerTest) output – Tukey transformed						
	Sum Sq	Mean Sq	NumDF	DenDF	F value	Pr(>F)
Cohort	0.00226398	0.00226398	1	6	8.7672	**0.02525**
Age (Years)	0.00008201	0.00008201	1	6	0.3176	0.59348
Sex	0.00007956	0.00007956	1	6	0.3081	0.59891
PMI (Hours)	0.00027867	0.00027867	1	6	1.0791	0.33893

emmeans (lmVOI, “Cohort”, type=”response”)						
emmeans (Tukey transformed scale), pairs, confint output (back transformed scale)						
Contrast	Estimate	SE	DF	95% CI	t.ratio	p.value
PSP - Control	-0.0334	0.0113	6	-0.0611, -0.00581	-2.961	**0.02525**

Table 2.1: Statistical analysis output of percent colocalization of pre-synapses and hyperphosphorylated tau

Asin(sqrt(SYOAT8_percent_area) ~ Cohort*Brain_region + Age*Cohort + (Brain_region|Case) Anova (lmerTest) output – arcsin square root transformed						
	Sum Sq	Mean Sq	NumDF	DenDF	F value	Pr(>F)
Cohort	0.052842	0.052842	1	16.099	4.4259	0.05147
Brain region	0.005486	0.005486	1	18.206	0.4595	0.50638
Age	0.020605	0.020605	1	16.082	1.7258	0.20738
Cohort:Brain region	0.001369	0.001369	1	18.206	0.1147	0.73874
Cohort:Age	0.049263	0.049263	1	16.082	4.1261	0.05909

emmeans (SYOAT8_Cohort, pairwise, ~ Cohort | Brain_region) emmeans, confint output – arcsin square root transformed						
Contrast (Control – PSP)	Estimate	SE	DF	95% CI	t.ratio	p.value
Substantia Nigra	-0.0249	0.0505	16.5	-0.132, 0.0819	-0.493	0.6284
Frontal Cortex	-0.0435	0.0441	16.2	-0.137, 0.0499	-0.986	0.3387

Table 2.2: Statistical analysis output of percent colocalization of pre-synapses and reactive astrocytes

Asin(sqrt(SYOGFAP_percent_area) ~ Cohort*Brain_region + Age*Cohort + (Brain_region|Case) Anova (lmerTest) output – arcsin square root transformed						
	Sum Sq	Mean Sq	NumDF	DenDF	F value	Pr(>F)
Cohort	0.136345	0.136345	1	16.178	4.9255	**0.04110**
Brain region	0.022575	0.022575	1	18.311	0.8155	0.37822
Age	0.013139	0.013139	1	16.102	0.4747	0.50066
Cohort:Brain region	0.001151	0.001151	1	18.311	0.0416	0.84069
Cohort:Age	0.163818	0.163818	1	16.102	5.9180	**0.02701**

emmeans (SYOGFAP_Cohort, pairwise, ~ Cohort | Brain_region) emmeans, confint output – arcsin square root transformed						
Contrast (Control – PSP)	Estimate	SE	DF	95% CI	t.ratio	p.value
Substantia Nigra	0.0748	0.0623	16.9	-0.0566, 0.206	1.201	0.2461
Frontal Cortex	0.0600	0.0435	16.2	-0.0322, 0.152	1.378	0.1870

Table 2.3: Statistical analysis output of percent colocalization of pre-synapses and microglia

Asin(sqrt(SYOP2RY_percent_area) ~ Cohort*Brain_region + Age*Cohort + (Brain_region|Case) Anova (lmerTest) output – arcsin square root transformed						
	Sum Sq	Mean Sq	NumDF	DenDF	F value	Pr(>F)
Cohort	0.0064853	0.0064853	1	16.069	3.8787	0.6639
Brain region	0.0073432	0.0073432	1	18.339	4.3918	0.05025
Age	0.002330	0.002330	1	16.055	0.1394	0.71379
Cohort:Brain region	0.0003168	0.0003168	1	18.339	0.1895	0.66844
Cohort:Age	0.0053979	0.0053979	1	16.055	3.2284	0.09121

emmeans (SYOP2RY_Cohort, pairwise, ~ Cohort | Brain_region) emmeans, confint output – arcsin square root transformed						
Contrast (Control – PSP)	Estimate	SE	DF	95% CI	t.ratio	p.value
Substantia Nigra	-0.0248	0.0175	16.1	-0.00445, 0.0555	-1.416	0.1759
Frontal Cortex	-0.0335	0.0203	16.4	-0.01323, 0.0486	-1.652	0.1176

Table 2.4: Statistical analysis output of percent colocalization of reactive astrocytes and hyperphosphorylated tau

Asin(sqrt(GFAPAT8_percent_area) ~ Cohort*Brain_region + Age*Cohort + (Brain_region|Case)						
Anova (lmerTest) output – arcsin square root transformed						
	Sum Sq	Mean Sq	NumDF	DenDF	F value	Pr(>F)
Cohort	0.007238	0.007238	1	16.128	0.6514	0.4314
Brain region	0.088773	0.088773	1	18.433	7.9894	**0.0110**
Age	0.025596	0.025596	1	16.090	2.3035	0.1485
Cohort:Brain region	0.008211	0.008211	1	18.433	0.7390	0.4010
Cohort:Age	0.009922	0.009922	1	16.090	0.8930	0.3586

emmeans (GFAPAT8_Cohort, pairwise, ~ Cohort | Brain_region)						
emmeans, confint output – arcsin square root transformed						
Contrast (Control – PSP)	Estimate	SE	DF	95% CI	t.ratio	p.value
Substantia Nigra	0.0229	0.0444	16.5	-0.0710, 0.117	0.515	0.6132
Frontal Cortex	0.0593	0.0353	16.1	-0.0155, 0.134	1.679	0.1124

Table 2.5: Statistical analysis output of percent colocalization of microglia and hyperphosphorylated tau

Asin(sqrt(P2RYAT8_percent_area) ~ Cohort*Brain_region + Age*Cohort + (Brain_region|Case)						
Anova (lmerTest) output – arcsin square root transformed						
	Sum Sq	Mean Sq	NumDF	DenDF	F value	Pr(>F)
Cohort	0.0004883	0.0004883	1	16.552	0.2796	0.603983
Brain region	0.0167940	0.0167940	1	18.220	9.6155	**0.006101**
Age	0.0000002	0.0000002	1	15.950	0.0001	0.991542
Cohort:Brain region	0.0005303	0.0005303	1	18.220	0.3036	0.588299
Cohort:Age	0.0004591	0.0004591	1	15.950	0.2629	0.615178

emmeans (P2RYAT8_Cohort, pairwise, ~ Cohort | Brain_region)						
emmeans, confint output – arcsin square root transformed						
Contrast (Control – PSP)	Estimate	SE	DF	95% CI	t.ratio	p.value
Substantia Nigra	0.00371	0.0308	17.4	-0.0612, 0.0687	0.121	0.9049
Frontal Cortex	-0.00988	0.0128	16	-0.0370, 0.0172	-0.773	0.4506

Table 2.6: Statistical analysis output of percent colocalization of pre-synapses, hyperphosphorylated tau and reactive astrocytes

Asin(sqrt(SYOAT8GFAP_percent_area) ~ Cohort*Brain_region + Age*Cohort + (Brain_region|Case)						
Anova (lmerTest) output – arcsin square root transformed						
	Sum Sq	Mean Sq	NumDF	DenDF	F value	Pr(>F)
Cohort	0.0046558	0.0046558	1	16.117	0.6960	0.41633
Brain region	0.0016134	0.0016134	1	18.607	0.2412	0.62910
Age	0.0247983	0.0247983	1	16.107	3.7070	0.07203
Cohort:Brain region	0.0005353	0.0005353	1	18.607	0.0800	0.78039
Cohort:Age	0.0062476	0.0062476	1	16.107	0.9339	0.34813

emmeans (SYOAT8GFAP_Cohort, pairwise, ~ Cohort | Brain_region)						
emmeans, confint output – arcsin square root transformed						
Contrast (Control – PSP)	Estimate	SE	DF	95% CI	t.ratio	p.value
Substantia Nigra	0.0272	0.0334	16.3	-0.0435, 0.098	0.815	0.4269
Frontal Cortex	0.0377	0.0324	16.3	-0.0309, 0.106	1.164	0.2613

Table 2.7: Statistical analysis output of percent colocalization of pre-synapses, hyperphosphorylated tau and microglia

Asin(sqrt(SYOAT8P2RY_percent_area) ~ Cohort*Brain_region + Age*Cohort + (Brain_region|Case)						
Anova (lmerTest) output – arcsin square root transformed						
	Sum Sq	Mean Sq	NumDF	DenDF	F value	Pr(>F)
Cohort	0.00000607	0.00000607	1	16.247	0.0068	0.9352
Brain region	0.00178578	0.00178578	1	18.535	2.0064	0.1732
Age	0.00035705	0.00035705	1	16.075	0.4012	0.5354
Cohort:Brain region	0.00083666	0.00083666	1	18.535	0.9400	0.3447
Cohort:Age	0.00000560	0.00000560	1	16.075	0.0063	0.9378

emmeans (SYOAT8P2RY_Cohort, pairwise, ~ Cohort | Brain_region)						
emmeans, confint output – arcsin square root transformed						
Contrast (Control – PSP)	Estimate	SE	DF	95% CI	t.ratio	p.value
Substantia Nigra	0.00822	0.0201	16.9	-0.0343, 0.0507	0.408	0.6884
Frontal Cortex	-0.00722	0.0120	16.0	-0.0327, 0.0182	-0.602	0.5556

Table 2.8: Statistical analysis output of percentage area of hyperphosphorylated tau

Asin(sqrt(AT8_percent_area) ~ Cohort*Brain_region + Age*Cohort + (Brain_region|Case)						
Anova (lmerTest) output – arcsin square root transformed						
	Sum Sq	Mean Sq	NumDF	DenDF	F value	Pr(>F)
Cohort	0.06810	0.06810	1	16.049	7.2500	**0.015982**
Brain region	0.37695	0.37695	1	18.080	40.1326	**0.000005599**
Age	0.00739	0.00739	1	15.995	0.7873	0.388074
Cohort:Brain region	0.07937	0.07937	1	18.080	8.4508	**0.009371**
Cohort:Age	0.04463	0.04463	1	15.995	4.7519	**0.044553**

emmeans (AT8_Cohort, pairwise, ~ Cohort | Brain_region)						
emmeans, confint output – arcsin square root transformed						
Contrast (Control – PSP)	Estimate	SE	DF	95% CI	t.ratio	p.value
Substantia Nigra	-0.255	0.0370	16.1	-0.334, -0.17682	-6.893	**<0.0001**
Frontal Cortex	-0.133	0.0522	16.7	-0.223, -0.00284	-2.167	**0.0450**

Table 2.9: Statistical analysis output of percentage area of reactive astrocytes

Asin(sqrt(GFAP_percent_area) ~ Cohort*Brain_region + Age*Cohort + (Brain_region|Case)						
Anova (lmerTest) output – no transformation						
	Sum Sq	Mean Sq	NumDF	DenDF	F value	Pr(>F)
Cohort	8.299	8.299	1	16.065	5.0995	**0.03819**
Brain region	68.079	68.079	1	18.221	41.8337	**0.000004133**
Age	3.466	3.466	1	15.942	2.1301	0.16386
Cohort:Brain region	2.067	2.067	1	18.221	1.2704	0.27432
Cohort:Age	7.096	7.096	1	15.942	4.3606	0.05318

emmeans (GFAP_Cohort, pairwise, ~ Cohort | Brain_region)						
emmeans, confint output – no transformation						
Contrast (Control – PSP)	Estimate	SE	DF	95% CI	t.ratio	p.value
Substantia Nigra	-0.481	0.748	16.9	-2.06, 1.098	-0.643	0.5287
Frontal Cortex	-1.235	0.463	16.0	-2.22, -0.255	-2.670	**0.0168**

Table 2.10: Statistical analysis output of percentage area of pre-synapses

Asin(sqrt(SYO_percent_area) ~ Cohort*Brain_region + Age*Cohort + (Brain_region|Case)						
Anova (lmerTest) output – no transformation						
	Sum Sq	Mean Sq	NumDF	DenDF	F value	Pr(>F)
Cohort	1.471	1.471	1	15.903	2.7911	0.11435
Brain region	54.966	54.966	1	18.084	104.2663	**0.000000006176**
Age	0.020	0.020	1	15.842	0.0387	0.84664
Cohort:Brain region	2.358	2.358	1	18.084	4.4728	**0.04858**
Cohort:Age	1.339	1.339	1	15.842	2.5391	0.13081

emmeans (SYO_Cohort, pairwise, ~ Cohort | Brain_region)						
emmeans, confint output – no transformation						
Contrast (Control – PSP)	Estimate	SE	DF	95% CI	t.ratio	p.value
Substantia Nigra	-0.450	0.255	16.8	-0.987, 0.0878	-1.767	0.0954
Frontal Cortex	0.149	0.188	16.2	-0.250, 0.5478	0.790	0.4409

Table 2.11: Statistical analysis output of percentage area of microglia

Asin(sqrt(P2RY_percent_area) ~ Cohort*Brain_region + Age*Cohort + (Brain_region|Case)						
Anova (lmerTest) output – arcsin square root transformed						
	Sum Sq	Mean Sq	NumDF	DenDF	F value	Pr(>F)
Cohort	0.105988	0.105988	1	16.064	3.4496	0.08170
Brain region	0.225437	0.225437	1	17.497	7.3372	**0.01463**
Age	0.006656	0.006656	1	16.017	0.2166	0.64789
Cohort:Brain region	0.024198	0.024198	1	17.497	0.7876	0.38687
Cohort:Age	0.093423	0.093423	1	16.017	3.0406	0.10036

emmeans (P2RY_Cohort, pairwise, ~ Cohort | Brain_region)						
emmeans, confint output – arcsin square root transformed						
Contrast (Control – PSP)	Estimate	SE	DF	95% CI	t.ratio	p.value
Substantia Nigra	-0.1591	0.0939	16.1	-0.358, 0.0399	-1.695	0.1094
Frontal Cortex	-0.0783	0.1181	16.4	-0.328, 0.1715	-0.663	0.5163

Table 3: Statistical analysis output of percentage burden of hyperphosphorylated tau

(burden) ~ cohort*region + (1|Case)						
Anova (lmerTest) output						
	Sum Sq	Mean Sq	NumDF	DenDF	F value	Pr(>F)
Cohort	3.8748	3.8748	1	18.887	13.9033	**0.001435**
Region	0.0021	0.0021	1	17.648	0.0075	0.932074
Cohort:Brain region	0.0800	0.0800	1	17.648	0.2869	0.598882

emmeans (P2RY_Cohort, pairwise, ~ Cohort | Brain_region)						
emmeans, confint output – arcsin square root transformed						
Contrast (Control – PSP)	Estimate	SE	DF	95% CI	t.ratio	p.value
Substantia Nigra	-0.823	0.290	31.2	-1.41, 0.232	-2.842	**0.0078**
Frontal Cortex	-1.007	0.311	32.9	-1.64, 0.373	-3.233	**0.0028**

Bibliography

Adams, N.E., Jafarian, A., Perry, A., Rouse, M.A., Shaw, A.D., Murley, A.G., Cope, T.E., Bevan-Jones, W.R., Passamonti, L., Street, D., Holland, N., Nesbitt, D., Hughes, L.E., Friston, K.J., Rowe, J.B., 2023. Neurophysiological consequences of synapse loss in progressive supranuclear palsy. Brain 146, 2584–2594. https://doi.org/10.1093/brain/awac471

Ahmed, T., Van der Jeugd, A., Blum, D., Galas, M.-C., D'Hooge, R., Buee, L., Balschun, D., 2014. Cognition and hippocampal synaptic plasticity in mice with a homozygous tau deletion. Neurobiol Aging 35, 2474–2478. https://doi.org/10.1016/j.neurobiolaging.2014.05.005

Allen, M., Wang, X., Serie, D.J., Strickland, S.L., Burgess, J.D., Koga, S., Younkin, C.S., Nguyen, T.T., Malphrus, K.G., Lincoln, S.J., Alamprese, M., Zhu, K., Chang, R., Carrasquillo, M.M., Kouri, N., Murray, M.E., Reddy, J.S., Funk, C., Price, N.D., Golde, T.E., Younkin, S.G., Asmann, Y.W., Crook, J.E., Dickson, D.W., Ertekin-Taner, N., 2018. Divergent brain gene expression patterns associate with distinct cell-specific tau neuropathology traits in progressive supranuclear palsy. Acta Neuropathol 136, 709–727. https://doi.org/10.1007/s00401-018-1900-5

Alster, P., Madetko, N., Koziorowski, D., Friedman, A., 2020a. Progressive Supranuclear Palsy—Parkinsonism Predominant (PSP-P)—A Clinical Challenge at the Boundaries of PSP and Parkinson's Disease (PD). Frontiers in Neurology 11.

Alster, P., Madetko, N., Koziorowski, D., Friedman, A., 2020b. Microglial Activation and Inflammation as a Factor in the Pathogenesis of Progressive Supranuclear Palsy (PSP). Front Neurosci 14, 893. https://doi.org/10.3389/fnins.2020.00893

Armstrong, M.J., Castellani, R.J., Reich, S.G., 2014. "Rapidly" Progressive Supranuclear Palsy. Mov Disord Clin Pract 1, 70–72. https://doi.org/10.1002/mdc3.12011

Armstrong, R.A., Lantos, P.L., Cairns, N.J., 2007. Progressive supranuclear palsy (PSP): a quantitative study of the pathological changes in cortical and subcortical regions of eight cases. J Neural Transm 114, 1569–1577. https://doi.org/10.1007/s00702-007-0796-3

Avila, J., Lucas, J.J., Pérez, M., Hernández, F., 2004. Role of Tau Protein in Both Physiological and Pathological Conditions. Physiological Reviews 84, 361–384. https://doi.org/10.1152/physrev.00024.2003

Bell, B.J., Malvankar, M.M., Tallon, C., Slusher, B.S., 2020. Sowing the Seeds of Discovery: Tau-Propagation Models of Alzheimer's Disease. ACS chemical neuroscience 11, 3499. https://doi.org/10.1021/acschemneuro.0c00531

Berger, Z., Roder, H., Hanna, A., Carlson, A., Rangachari, V., Yue, M., Wszolek, Z., Ashe, K., Knight, J., Dickson, D., Andorfer, C., Rosenberry, T.L., Lewis, J., Hutton, M., Janus, C., 2007. Accumulation of Pathological Tau Species and Memory Loss in a Conditional Model of Tauopathy. J. Neurosci. 27, 3650–3662. https://doi.org/10.1523/JNEUROSCI.0587-07.2007

Bigio, E.H., Brown, D.F., White, C.L., 1999. Progressive supranuclear palsy with dementia: cortical pathology. J Neuropathol Exp Neurol 58, 359–364. https://doi.org/10.1097/00005072-199904000-00006

Bigio, E.H., Vono, M.B., Satumtira, S., Adamson, J., Sontag, E., Hynan, L.S., White, C.L., III, Baker, M., Hutton, M., 2001. Cortical Synapse Loss in progressive

Supranuclear palsy. Journal of Neuropathology & Experimental Neurology 60, 403–410. https://doi.org/10.1093/jnen/60.5.403
Bonovas, S., Piovani, D., 2023. Simpson's Paradox in Clinical Research: A Cautionary Tale. J Clin Med 12, 1633. https://doi.org/10.3390/jcm12041633
Braun, N.J., Yao, K.R., Alford, P.W., Liao, D., 2020. Mechanical injuries of neurons induce tau mislocalization to dendritic spines and tau-dependent synaptic dysfunction. Proceedings of the National Academy of Sciences 117, 29069–29079. https://doi.org/10.1073/pnas.2008306117
Briel, N., Pratsch, K., Roeber, S., Arzberger, T., Herms, J., 2021. Contribution of the astrocytic tau pathology to synapse loss in progressive supranuclear palsy and corticobasal degeneration. Brain Pathol 31, e12914. https://doi.org/10.1111/bpa.12914
Briel, N., Ruf, V.C., Pratsch, K., Roeber, S., Widmann, J., Mielke, J., Dorostkar, M.M., Windl, O., Arzberger, T., Herms, J., Struebing, F.L., 2022. Single-nucleus chromatin accessibility profiling highlights distinct astrocyte signatures in progressive supranuclear palsy and corticobasal degeneration. Acta Neuropathol 144, 615–635. https://doi.org/10.1007/s00401-022-02483-8
Brion, J.-P., 1998. Neurofibrillary Tangles and Alzheimer's Disease. European neurology 40, 130–40. https://doi.org/10.1159/000007969
Button, K.S., Ioannidis, J.P.A., Mokrysz, C., Nosek, B.A., Flint, J., Robinson, E.S.J., Munafò, M.R., 2013. Power failure: why small sample size undermines the reliability of neuroscience. Nat Rev Neurosci 14, 365–376. https://doi.org/10.1038/nrn3475
Chen, Q., Zhou, Z., Zhang, L., Wang, Y., Zhang, Y., Zhong, M., Xu, S., Chen, C., Li, L., Yu, Z., 2012. Tau protein is involved in morphological plasticity in hippocampal neurons in response to BDNF. Neurochem Int 60, 233–242. https://doi.org/10.1016/j.neuint.2011.12.013
Chen, S., Townsend, K., Goldberg, T.E., Davies, P., Conejero-Goldberg, C., 2010. MAPT Isoforms: Differential Transcriptional Profiles Related to 3R and 4R Splice Variants. J Alzheimers Dis 22, 1313–1329. https://doi.org/10.3233/JAD-2010-101155
Chung, D.C., Roemer, S., Petrucelli, L., Dickson, D.W., 2021. Cellular and pathological heterogeneity of primary tauopathies. Molecular Neurodegeneration 16, 57. https://doi.org/10.1186/s13024-021-00476-x
Chung, S.-H., 2009. Aberrant phosphorylation in the pathogenesis of Alzheimer's disease. BMB Rep 42, 467–474. https://doi.org/10.5483/bmbrep.2009.42.8.467
Clerici, I., Ferrazzoli, D., Maestri, R., Bossio, F., Zivi, I., Canesi, M., Pezzoli, G., Frazzitta, G., 2017. Rehabilitation in progressive supranuclear palsy: Effectiveness of two multidisciplinary treatments. PLoS One 12, e0170927. https://doi.org/10.1371/journal.pone.0170927
Colom-Cadena, M., Davies, C., Sirisi, S., Lee, J.-E., Simzer, E.M., Tzioras, M., Querol-Vilaseca, M., Sánchez-Aced, É., Chang, Y.Y., Holt, K., McGeachan, R.I., Rose, J., Tulloch, J., Wilkins, L., Smith, C., Andrian, T., Belbin, O., Pujals, S., Horrocks, M.H., Lleó, A., Spires-Jones, T.L., 2023. Synaptic oligomeric tau in Alzheimer's disease - A potential culprit in the spread of tau pathology through the brain. Neuron S0896-6273(23)00305–7. https://doi.org/10.1016/j.neuron.2023.04.020

Coughlin, D.G., Litvan, I., 2020. Progressive Supranuclear Palsy: Advances in Diagnosis and Management. Parkinsonism Relat Disord 73, 105–116. https://doi.org/10.1016/j.parkreldis.2020.04.014
Cowan, C., Mudher, A., 2013. Are Tau Aggregates Toxic or Protective in Tauopathies? Frontiers in Neurology 4.
de Calignon, A., Polydoro, M., Suárez-Calvet, M., William, C., Adamowicz, D.H., Kopeikina, K.J., Pitstick, R., Sahara, N., Ashe, K.H., Carlson, G.A., Spires-Jones, T.L., Hyman, B.T., 2012. Propagation of tau pathology in a model of early Alzheimer's disease. Neuron 73, 685–697. https://doi.org/10.1016/j.neuron.2011.11.033
De Schepper, S., Ge, J.Z., Crowley, G., Ferreira, L.S.S., Garceau, D., Toomey, C.E., Sokolova, D., Rueda-Carrasco, J., Shin, S.-H., Kim, J.-S., Childs, T., Lashley, T., Burden, J.J., Sasner, M., Sala Frigerio, C., Jung, S., Hong, S., 2023. Perivascular cells induce microglial phagocytic states and synaptic engulfment via SPP1 in mouse models of Alzheimer's disease. Nat Neurosci 26, 406–415. https://doi.org/10.1038/s41593-023-01257-z
Dejanovic, B., Wu, T., Tsai, M.-C., Graykowski, D., Gandham, V.D., Rose, C.M., Bakalarski, C.E., Ngu, H., Wang, Y., Pandey, S., Rezzonico, M.G., Friedman, B.A., Edmonds, R., De Mazière, A., Rakosi-Schmidt, R., Singh, T., Klumperman, J., Foreman, O., Chang, M.C., Xie, L., Sheng, M., Hanson, J.E., 2022. Complement C1q-dependent excitatory and inhibitory synapse elimination by astrocytes and microglia in Alzheimer's disease mouse models. Nat Aging 2, 837–850. https://doi.org/10.1038/s43587-022-00281-1
DeKosky, S.T., Scheff, S.W., 1990. Synapse loss in frontal cortex biopsies in Alzheimer's disease: correlation with cognitive severity. Ann Neurol 27, 457–464. https://doi.org/10.1002/ana.410270502
Demock, M., Kornguth, S., 2019. A Mechanism for the Development of Chronic Traumatic Encephalopathy From Persistent Traumatic Brain Injury. J Exp Neurosci 13, 1179069519849935. https://doi.org/10.1177/1179069519849935
Dickson, D.W., Rademakers, R., Hutton, M.L., 2007. Progressive Supranuclear Palsy: Pathology and Genetics. Brain Pathology 17, 74–82. https://doi.org/10.1111/j.1750-3639.2007.00054.x
DuBoff, B., Götz, J., Feany, M.B., 2012. Tau promotes neurodegeneration via DRP1 mislocalization in vivo. Neuron 75, 618–632. https://doi.org/10.1016/j.neuron.2012.06.026
Dujardin, S., Commins, C., Lathuiliere, A., Beerepoot, P., Fernandes, A.R., Kamath, T.V., De Los Santos, M.B., Klickstein, N., Corjuc, D.L., Corjuc, B.T., Dooley, P.M., Viode, A., Oakley, D.H., Moore, B.D., Mullin, K., Jean-Gilles, D., Clark, R., Atchison, K., Moore, R., Chibnik, L.B., Tanzi, R.E., Frosch, M.P., Serrano-Pozo, A., Elwood, F., Steen, J.A., Kennedy, M.E., Hyman, B.T., 2020. Tau molecular diversity contributes to clinical heterogeneity in Alzheimer's disease. Nat Med 26, 1256–1263. https://doi.org/10.1038/s41591-020-0938-9
Eckermann, K., Mocanu, M.-M., Khlistunova, I., Biernat, J., Nissen, A., Hofmann, A., Schönig, K., Bujard, H., Haemisch, A., Mandelkow, E., Zhou, L., Rune, G., Mandelkow, E.-M., 2007. The β-Propensity of Tau Determines Aggregation and Synaptic Loss in Inducible Mouse Models of Tauopathy*. Journal of Biological Chemistry 282, 31755–31765. https://doi.org/10.1074/jbc.M705282200
Fernández-Botrán, R., Ahmed, Z., Crespo, F.A., Gatenbee, C., Gonzalez, J., Dickson, D.W., Litvan, I., 2011. Cytokine expression and microglial activation

in progressive supranuclear palsy. Parkinsonism & Related Disorders 17, 683–688. https://doi.org/10.1016/j.parkreldis.2011.06.007
Ferrer, I., López-González, I., Carmona, M., Arregui, L., Dalfó, E., Torrejón-Escribano, B., Diehl, R., Kovacs, G.G., 2014. Glial and Neuronal Tau Pathology in Tauopathies:Characterization of Disease-Specific Phenotypes and Tau Pathology Progression. Journal of Neuropathology & Experimental Neurology 73, 81–97. https://doi.org/10.1097/NEN.0000000000000030
Franklin, H., Clarke, B.E., Patani, R., 2021. Astrocytes and microglia in neurodegenerative diseases: Lessons from human in vitro models. Prog Neurobiol 200, 101973. https://doi.org/10.1016/j.pneurobio.2020.101973
Franzmeier, N., Brendel, M., Beyer, L., Arzberger, T., Kovacs, G.G., Rubinski, A., Palleis, C., Katzdobler, S., Finze, A., Song, M., Biechele, G., Kern, M., Scheifele, M., Rauchmann, B.-S., Perneczky, R., Rullmann, M., Schildan, A., Barthel, H., Sabri, O., Classen, J., Lukic, M.J., Irwin, D.J., Lee, E.B., Coughlin, D., Giese, A., Grossman, M., Kurz, C., McMillan, C.T., Gelpi, E., Compta, Y., Swieten, J.C., Troakes, C., Al-Sarraj, S., Roeber, S., Xie, S.X., Lee, V.M.-Y., Herms, J., Bartenstein, P., Haass, C., Dichgans, M., Trojanowski, J.Q., Levin, J., Höglinger, G., Ewers, M., 2021. Tau spreads across connected brain regions in progressive supranuclear palsy and corticobasal syndrome. Alzheimer's & Dementia 17, e051668. https://doi.org/10.1002/alz.051668
Franzmeier, N., Neitzel, J., Rubinski, A., Smith, R., Strandberg, O., Ossenkoppele, R., Hansson, O., Ewers, M., 2020. Functional brain architecture is associated with the rate of tau accumulation in Alzheimer's disease. Nat Commun 11, 347. https://doi.org/10.1038/s41467-019-14159-1
Frost, B., Diamond, M.I., 2010. Prion-like mechanisms in neurodegenerative diseases. Nat Rev Neurosci 11, 155–159. https://doi.org/10.1038/nrn2786
Gao, Y.-L., Wang, N., Sun, F.-R., Cao, X.-P., Zhang, W., Yu, J.-T., 2018. Tau in neurodegenerative disease. Ann Transl Med 6, 175. https://doi.org/10.21037/atm.2018.04.23
Gerson, J., Castillo-Carranza, D.L., Sengupta, U., Bodani, R., Prough, D.S., DeWitt, D.S., Hawkins, B.E., Kayed, R., 2016. Tau Oligomers Derived from Traumatic Brain Injury Cause Cognitive Impairment and Accelerate Onset of Pathology in Htau Mice. Journal of Neurotrauma 33, 2034–2043. https://doi.org/10.1089/neu.2015.4262
Gerson, J.E., Sengupta, U., Lasagna-Reeves, C.A., Guerrero-Muñoz, M.J., Troncoso, J., Kayed, R., 2014. Characterization of tau oligomeric seeds in progressive supranuclear palsy. Acta Neuropathologica Communications 2, 73. https://doi.org/10.1186/2051-5960-2-73
Giannini, L.A.A., Ohm, D.T., Rozemuller, A.J.M., Dratch, L., Suh, E., van Deerlin, V.M., Trojanowski, J.Q., Lee, E.B., van Swieten, J.C., Grossman, M., Seelaar, H., Irwin, D.J., 2022. Isoform-specific patterns of tau burden and neuronal degeneration in MAPT-associated frontotemporal lobar degeneration. Acta Neuropathol 144, 1065–1084. https://doi.org/10.1007/s00401-022-02487-4
Gilley, J., Seereeram, A., Ando, K., Mosely, S., Andrews, S., Kerschensteiner, M., Misgeld, T., Brion, J.-P., Anderton, B., Hanger, D.P., Coleman, M.P., 2012. Age-dependent axonal transport and locomotor changes and tau hypophosphorylation in a "P301L" tau knockin mouse. Neurobiol Aging 33, 621.e1-621.e15. https://doi.org/10.1016/j.neurobiolaging.2011.02.014
Gomez-Arboledas, A., Davila, J.C., Sanchez-Mejias, E., Navarro, V., Nuñez-Diaz, C., Sanchez-Varo, R., Sanchez-Mico, M.V., Trujillo-Estrada, L., Fernandez-

Valenzuela, J.J., Vizuete, M., Comella, J.X., Galea, E., Vitorica, J., Gutierrez, A., 2018. Phagocytic clearance of presynaptic dystrophies by reactive astrocytes in Alzheimer's disease. Glia 66, 637–653. https://doi.org/10.1002/glia.23270

Greenwood, E.K., Brown, D.R., 2021. Senescent Microglia: The Key to the Ageing Brain? Int J Mol Sci 22, 4402. https://doi.org/10.3390/ijms22094402

Guillozet-Bongaarts, A.L., Cahill, M.E., Cryns, V.L., Reynolds, M.R., Berry, R.W., Binder, L.I., 2006. Pseudophosphorylation of tau at serine 422 inhibits caspase cleavage: in vitro evidence and implications for tangle formation in vivo. J Neurochem 97, 1005–1014. https://doi.org/10.1111/j.1471-4159.2006.03784.x

Han, H.J., Kim, H., Park, J.-H., Shin, H.-W., Kim, G.U., Kim, D.S., Lee, E.J., Oh, H.E., Park, S.-H., Kim, Y.J., 2010. Behavioral changes as the earliest clinical manifestation of progressive supranuclear palsy. J Clin Neurol 6, 148–151. https://doi.org/10.3988/jcn.2010.6.3.148

Hanger, D.P., Anderton, B.H., Noble, W., 2009. Tau phosphorylation: the therapeutic challenge for neurodegenerative disease. Trends Mol Med 15, 112–119. https://doi.org/10.1016/j.molmed.2009.01.003

Hartzler, A.W., Zhu, X., Siedlak, S.L., Castellani, R.J., Avilá, J., Perry, G., Smith, M.A., 2002. The p38 pathway is activated in Pick disease and progressive supranuclear palsy: a mechanistic link between mitogenic pathways, oxidative stress, and tau. Neurobiology of Aging, Brain Aging: Identifying the Brakes and Accelerators 23, 855–859. https://doi.org/10.1016/S0197-4580(02)00029-5

Hasegawa, M., 2019. Structure of NFT: Biochemical Approach. Advances in experimental medicine and biology 1184. https://doi.org/10.1007/978-981-32-9358-8_2

Hattori, M., Hashizume, Y., Yoshida, M., Iwasaki, Y., Hishikawa, N., Ueda, R., Ojika, K., 2003. Distribution of astrocytic plaques in the corticobasal degeneration brain and comparison with tuft-shaped astrocytes in the progressive supranuclear palsy brain. Acta Neuropathol 106, 143–149. https://doi.org/10.1007/s00401-003-0711-4

Höglinger, G.U., Respondek, G., Stamelou, M., Kurz, C., Josephs, K.A., Lang, A.E., Mollenhauer, B., Müller, U., Nilsson, C., Whitwell, J.L., Arzberger, T., Englund, E., Gelpi, E., Giese, A., Irwin, D.J., Meissner, W.G., Pantelyat, A., Rajput, A., van Swieten, J.C., Troakes, C., Antonini, A., Bhatia, K.P., Bordelon, Y., Compta, Y., Corvol, J.-C., Colosimo, C., Dickson, D.W., Dodel, R., Ferguson, L., Grossman, M., Kassubek, J., Krismer, F., Levin, J., Lorenzl, S., Morris, H.R., Nestor, P., Oertel, W.H., Poewe, W., Rabinovici, G., Rowe, J.B., Schellenberg, G.D., Seppi, K., van Eimeren, T., Wenning, G.K., Boxer, A.L., Golbe, L.I., Litvan, I., Movement Disorder Society-endorsed PSP Study Group, 2017. Clinical diagnosis of progressive supranuclear palsy: The movement disorder society criteria. Mov Disord 32, 853–864. https://doi.org/10.1002/mds.26987

Holland, N., Jones, P.S., Savulich, G., Naessens, M., Malpetti, M., Whiteside, D.J., Street, D., Swann, P., Hong, Y.T., Fryer, T.D., Rittman, T., Mulroy, E., Aigbirhio, F.I., Bhatia, K.P., O'Brien, J.T., Rowe, J.B., 2023. Longitudinal Synaptic Loss in Primary Tauopathies: An In Vivo [11C]UCB-J Positron Emission Tomography Study. Movement Disorders n/a. https://doi.org/10.1002/mds.29421

Holland, N., Jones, P.S., Savulich, G., Wiggins, J.K., Hong, Y.T., Fryer, T.D., Manavaki, R., Sephton, S.M., Boros, I., Malpetti, M., Hezemans, F.H., Aigbirhio, F.I., Coles, J.P., O'Brien, J., Rowe, J.B., 2020. Synaptic loss in primary tauopathies revealed by [11C]UCB-J positron emission tomography. Mov Disord 35, 1834–1842. https://doi.org/10.1002/mds.28188

Holland, N., Malpetti, M., Rittman, T., Mak, E.E., Passamonti, L., Kaalund, S.S., Hezemans, F.H., Jones, P.S., Savulich, G., Hong, Y.T., Fryer, T.D., Aigbirhio, F.I., O'Brien, J.T., Rowe, J.B., 2021. Molecular pathology and synaptic loss in primary tauopathies: an 18F-AV-1451 and 11C-UCB-J PET study. Brain 145, 340–348. https://doi.org/10.1093/brain/awab282

Hoover, B.R., Reed, M.N., Su, J., Penrod, R.D., Kotilinek, L.A., Grant, M.K., Pitstick, R., Carlson, G.A., Lanier, L.M., Yuan, L.-L., Ashe, K.H., Liao, D., 2010. Tau mislocalization to dendritic spines mediates synaptic dysfunction independently of neurodegeneration. Neuron 68, 1067–1081. https://doi.org/10.1016/j.neuron.2010.11.030

Hopp, S.C., Lin, Y., Oakley, D., Roe, A.D., DeVos, S.L., Hanlon, D., Hyman, B.T., 2018. The role of microglia in processing and spreading of bioactive tau seeds in Alzheimer's disease. J Neuroinflammation 15, 269. https://doi.org/10.1186/s12974-018-1309-z

Houlden, H., Baker, M., Morris, H.R., MacDonald, N., Pickering-Brown, S., Adamson, J., Lees, A.J., Rossor, M.N., Quinn, N.P., Kertesz, A., Khan, M.N., Hardy, J., Lantos, P.L., St George-Hyslop, P., Munoz, D.G., Mann, D., Lang, A.E., Bergeron, C., Bigio, E.H., Litvan, I., Bhatia, K.P., Dickson, D., Wood, N.W., Hutton, M., 2001. Corticobasal degeneration and progressive supranuclear palsy share a common tau haplotype. Neurology 56, 1702–1706. https://doi.org/10.1212/wnl.56.12.1702

Ikeda, C., Yokota, O., Nagao, S., Ishizu, H., Oshima, E., Hasegawa, M., Okahisa, Y., Terada, S., Yamada, N., 2016. The Relationship Between Development of Neuronal and Astrocytic Tau Pathologies in Subcortical Nuclei and Progression of Argyrophilic Grain Disease. Brain Pathol 26, 488–505. https://doi.org/10.1111/bpa.12319

Iohan, L. da C.C., Lambert, J.-C., Costa, M.R., 2022. Analysis of modular gene co-expression networks reveals molecular pathways underlying Alzheimer's disease and progressive supranuclear palsy. PLoS One 17, e0266405. https://doi.org/10.1371/journal.pone.0266405

Ittner, L.M., Götz, J., 2011. Amyloid-β and tau — a toxic pas de deux in Alzheimer's disease. Nat Rev Neurosci 12, 67–72. https://doi.org/10.1038/nrn2967

Johnson, G.V.W., Bailey, C.D.C., 2003. The p38 MAP kinase signaling pathway in Alzheimer's disease. Experimental Neurology 183, 263–268. https://doi.org/10.1016/S0014-4886(03)00268-1

Josephs, K.A., Duffy, J.R., Strand, E.A., Whitwell, J.L., Layton, K.F., Parisi, J.E., Hauser, M.F., Witte, R.J., Boeve, B.F., Knopman, D.S., Dickson, D.W., Jack, C.R., Petersen, R.C., 2006a. Clinicopathological and imaging correlates of progressive aphasia and apraxia of speech. Brain 129, 1385–1398. https://doi.org/10.1093/brain/awl078

Josephs, K.A., Katsuse, O., Beccano-Kelly, D.A., Lin, W.-L., Uitti, R.J., Fujino, Y., Boeve, B.F., Hutton, M.L., Baker, M.C., Dickson, D.W., 2006b. Atypical progressive supranuclear palsy with corticospinal tract degeneration. J Neuropathol Exp Neurol 65, 396–405. https://doi.org/10.1097/01.jnen.0000218446.38158.61

Jucker, M., Walker, L.C., 2013. Self-propagation of pathogenic protein aggregates in neurodegenerative diseases. Nature 501, 45–51. https://doi.org/10.1038/nature12481
Kay, K.R., Smith, C., Wright, A.K., Serrano-Pozo, A., Pooler, A.M., Koffie, R., Bastin, M.E., Bak, T.H., Abrahams, S., Kopeikina, K.J., McGuone, D., Frosch, M.P., Gillingwater, T.H., Hyman, B.T., Spires-Jones, T.L., 2013. Studying synapses in human brain with array tomography and electron microscopy. Nat Protoc 8, 1366–1380. https://doi.org/10.1038/nprot.2013.078
Kent, S.A., Spires-Jones, T.L., Durrant, C.S., 2020. The physiological roles of tau and Aβ: implications for Alzheimer's disease pathology and therapeutics. Acta Neuropathol 140, 417–447. https://doi.org/10.1007/s00401-020-02196-w
Kimura, T., Whitcomb, D.J., Jo, J., Regan, P., Piers, T., Heo, S., Brown, C., Hashikawa, T., Murayama, M., Seok, H., Sotiropoulos, I., Kim, E., Collingridge, G.L., Takashima, A., Cho, K., 2014. Microtubule-associated protein tau is essential for long-term depression in the hippocampus. Philos Trans R Soc Lond B Biol Sci 369, 20130144. https://doi.org/10.1098/rstb.2013.0144
Kovacs, G.G., 2020. Astroglia and Tau: New Perspectives. Front Aging Neurosci 12, 96. https://doi.org/10.3389/fnagi.2020.00096
Kovacs, G. G., Budka, H., 2010. Current concepts of neuropathological diagnostics in practice: neurodegenerative diseases. Clin Neuropathol 29, 271–288. https://doi.org/10.5414/npp29271
Kovacs, G.G., Lukic, M.J., Irwin, D.J., Arzberger, T., Respondek, G., Lee, E.B., Coughlin, D., Giese, A., Grossman, M., Kurz, C., McMillan, C.T., Gelpi, E., Compta, Y., van Swieten, J.C., Laat, L.D., Troakes, C., Al-Sarraj, S., Robinson, J.L., Roeber, S., Xie, S.X., Lee, V.M.-Y., Trojanowski, J.Q., Höglinger, G.U., 2020. Distribution patterns of tau pathology in progressive supranuclear palsy. Acta Neuropathol 140, 99–119. https://doi.org/10.1007/s00401-020-02158-2
Lafrenaye, A.D., Simard, J.M., 2019. Bursting at the Seams: Molecular Mechanisms Mediating Astrocyte Swelling. Int J Mol Sci 20, 330. https://doi.org/10.3390/ijms20020330
Lasagna-Reeves, C.A., Castillo-Carranza, D.L., Sengupta, U., Clos, A.L., Jackson, G.R., Kayed, R., 2011. Tau oligomers impair memory and induce synaptic and mitochondrial dysfunction in wild-type mice. Mol Neurodegener 6, 39. https://doi.org/10.1186/1750-1326-6-39
Lasagna-Reeves, C.A., Castillo-Carranza, D.L., Sengupta, U., Sarmiento, J., Troncoso, J., Jackson, G.R., Kayed, R., 2012. Identification of oligomers at early stages of tau aggregation in Alzheimer's disease. FASEB J 26, 1946–1959. https://doi.org/10.1096/fj.11-199851
Laurent, C., Buée, L., Blum, D., 2018. Tau and neuroinflammation: What impact for Alzheimer's Disease and Tauopathies? Biomedical Journal 41, 21–33. https://doi.org/10.1016/j.bj.2018.01.003
Lee, S.E., Rabinovici, G.D., Mayo, M.C., Wilson, S.M., Seeley, W.W., DeArmond, S.J., Huang, E.J., Trojanowski, J.Q., Growdon, M.E., Jang, J.Y., Sidhu, M., See, T.M., Karydas, A.M., Gorno-Tempini, M.-L., Boxer, A.L., Weiner, M.W., Geschwind, M.D., Rankin, K.P., Miller, B.L., 2011. Clinicopathological correlations in corticobasal degeneration. Ann Neurol 70, 327–340. https://doi.org/10.1002/ana.22424

Lei, P., Ayton, S., Finkelstein, D.I., Spoerri, L., Ciccotosto, G.D., Wright, D.K., Wong, B.X.W., Adlard, P.A., Cherny, R.A., Lam, L.Q., Roberts, B.R., Volitakis, I., Egan, G.F., McLean, C.A., Cappai, R., Duce, J.A., Bush, A.I., 2012. Tau deficiency induces parkinsonism with dementia by impairing APP-mediated iron export. Nat Med 18, 291–295. https://doi.org/10.1038/nm.2613

Li, X., Feng, X., Sun, X., Hou, N., Han, F., Liu, Y., 2022. Global, regional, and national burden of Alzheimer's disease and other dementias, 1990–2019. Front Aging Neurosci 14, 937486. https://doi.org/10.3389/fnagi.2022.937486

Liu, L., Drouet, V., Wu, J.W., Witter, M.P., Small, S.A., Clelland, C., Duff, K., 2012. Trans-Synaptic Spread of Tau Pathology In Vivo. PLoS One 7, e31302. https://doi.org/10.1371/journal.pone.0031302

Lopes, S., Lopes, A., Pinto, V., Guimarães, M.R., Sardinha, V.M., Duarte-Silva, S., Pinheiro, S., Pizarro, J., Oliveira, J.F., Sousa, N., Leite-Almeida, H., Sotiropoulos, I., 2016. Absence of Tau triggers age-dependent sciatic nerve morphofunctional deficits and motor impairment. Aging Cell 15, 208–216. https://doi.org/10.1111/acel.12391

Lu, M., Kosik, K.S., 2001. Competition for Microtubule-binding with Dual Expression of Tau Missense and Splice Isoforms. Mol Biol Cell 12, 171–184.

Malia, T.J., Teplyakov, A., Ernst, R., Wu, S.-J., Lacy, E.R., Liu, X., Vandermeeren, M., Mercken, M., Luo, J., Sweet, R.W., Gilliland, G.L., 2016. Epitope mapping and structural basis for the recognition of phosphorylated tau by the anti-tau antibody AT8. Proteins 84, 427–434. https://doi.org/10.1002/prot.24988

Maphis, N., Xu, G., Kokiko-Cochran, O.N., Jiang, S., Cardona, A., Ransohoff, R.M., Lamb, B.T., Bhaskar, K., 2015. Reactive microglia drive tau pathology and contribute to the spreading of pathological tau in the brain. Brain 138, 1738–1755. https://doi.org/10.1093/brain/awv081

Marciniak, E., Leboucher, A., Caron, E., Ahmed, T., Tailleux, A., Dumont, J., Issad, T., Gerhardt, E., Pagesy, P., Vileno, M., Bournonville, C., Hamdane, M., Bantubungi, K., Lancel, S., Demeyer, D., Eddarkaoui, S., Vallez, E., Vieau, D., Humez, S., Faivre, E., Grenier-Boley, B., Outeiro, T.F., Staels, B., Amouyel, P., Balschun, D., Buee, L., Blum, D., 2017. Tau deletion promotes brain insulin resistance. J Exp Med 214, 2257–2269. https://doi.org/10.1084/jem.20161731

Mariotti, L., Losi, G., Lia, A., Melone, M., Chiavegato, A., Gómez-Gonzalo, M., Sessolo, M., Bovetti, S., Forli, A., Zonta, M., Requie, L.M., Marcon, I., Pugliese, A., Viollet, C., Bettler, B., Fellin, T., Conti, F., Carmignoto, G., 2018. Interneuron-specific signaling evokes distinctive somatostatin-mediated responses in adult cortical astrocytes. Nat Commun 9, 82. https://doi.org/10.1038/s41467-017-02642-6

Martín, R., Bajo-Grañeras, R., Moratalla, R., Perea, G., Araque, A., 2015. Circuit-specific signaling in astrocyte-neuron networks in basal ganglia pathways. Science 349, 730–734. https://doi.org/10.1126/science.aaa7945

Martínez-Maldonado, A., Ontiveros-Torres, M.Á., Harrington, C.R., Montiel-Sosa, J.F., Prandiz, R.G.-T., Bocanegra-López, P., Sorsby-Vargas, A.M., Bravo-Muñoz, M., Florán-Garduño, B., Villanueva-Fierro, I., Perry, G., Garcés-Ramírez, L., de la Cruz, F., Martínez-Robles, S., Pacheco-Herrero, M., Luna-Muñoz, J., 2021. Molecular Processing of Tau Protein in Progressive Supranuclear Palsy: Neuronal and Glial Degeneration. J Alzheimers Dis 79, 1517–1531. https://doi.org/10.3233/JAD-201139

Martini-Stoica, H., Cole, A.L., Swartzlander, D.B., Chen, F., Wan, Y.-W., Bajaj, L., Bader, D.A., Lee, V.M.Y., Trojanowski, J.Q., Liu, Z., Sardiello, M., Zheng, H., 2018. TFEB enhances astroglial uptake of extracellular tau species and reduces tau spreading. J Exp Med 215, 2355–2377. https://doi.org/10.1084/jem.20172158

Massey, L.A., Micallef, C., Paviour, D.C., O'Sullivan, S.S., Ling, H., Williams, D.R., Kallis, C., Holton, J.L., Revesz, T., Burn, D.J., Yousry, T., Lees, A.J., Fox, N.C., Jäger, H.R., 2012. Conventional magnetic resonance imaging in confirmed progressive supranuclear palsy and multiple system atrophy. Mov Disord 27, 1754–1762. https://doi.org/10.1002/mds.24968

McGeachan, R., Spires-Jones, M., Gillmore, M., Rose, J., Spires-Jones, T., 2022. Tau accumulates in synaptogyrin-3 positive synapses in Progressive Supranuclear Palsy. https://doi.org/10.1101/2022.09.20.22280086

Melani, R., Tritsch, N.X., 2022. Inhibitory co-transmission from midbrain dopamine neurons relies on presynaptic GABA uptake. Cell Reports 39, 110716. https://doi.org/10.1016/j.celrep.2022.110716

Michel, C.H., Kumar, S., Pinotsi, D., Tunnacliffe, A., St. George-Hyslop, P., Mandelkow, E., Mandelkow, E.-M., Kaminski, C.F., Kaminski Schierle, G.S., 2014. Extracellular Monomeric Tau Protein Is Sufficient to Initiate the Spread of Tau Protein Pathology. J Biol Chem 289, 956–967. https://doi.org/10.1074/jbc.M113.515445

Mirbaha, H., Holmes, B.B., Sanders, D.W., Bieschke, J., Diamond, M.I., 2015. Tau Trimers Are the Minimal Propagation Unit Spontaneously Internalized to Seed Intracellular Aggregation. J Biol Chem 290, 14893–14903. https://doi.org/10.1074/jbc.M115.652693

Mochizuki, A., Ueda, Y., Komatsuzaki, Y., Tsuchiya, K., Arai, T., Shoji, S., 2003. Progressive supranuclear palsy presenting with primary progressive aphasia--clinicopathological report of an autopsy case. Acta Neuropathol 105, 610–614. https://doi.org/10.1007/s00401-003-0682-5

Montalbano, M., Majmundar, L., Sengupta, U., Fung, L., Kayed, R., 2022. Pathological tau signatures and nuclear alterations in neurons, astrocytes and microglia in Alzheimer's disease, progressive supranuclear palsy, and dementia with Lewy bodies. Brain Pathol 33, e13112. https://doi.org/10.1111/bpa.13112

Morales, I., Jiménez, J.M., Mancilla, M., Maccioni, R.B., 2013. Tau oligomers and fibrils induce activation of microglial cells. J Alzheimers Dis 37, 849–856. https://doi.org/10.3233/JAD-131843

Ng, P.Y., McNeely, T.L., Baker, D.J., 2023. Untangling senescent and damage-associated microglia in the aging and diseased brain. The FEBS Journal 290, 1326–1339. https://doi.org/10.1111/febs.16315

Niewidok, B., Igaev, M., Sündermann, F., Janning, D., Bakota, L., Brandt, R., 2016. Presence of a carboxy-terminal pseudorepeat and disease-like pseudohyperphosphorylation critically influence tau's interaction with microtubules in axon-like processes. Mol Biol Cell 27, 3537–3549. https://doi.org/10.1091/mbc.E16-06-0402

Noble, W., Hanger, D.P., Miller, C.C.J., Lovestone, S., 2013. The Importance of Tau Phosphorylation for Neurodegenerative Diseases. Front Neurol 4, 83. https://doi.org/10.3389/fneur.2013.00083

Pallas-Bazarra, N., Jurado-Arjona, J., Navarrete, M., Esteban, J.A., Hernández, F., Ávila, J., Llorens-Martín, M., 2016. Novel function of Tau in regulating the

effects of external stimuli on adult hippocampal neurogenesis. EMBO J 35, 1417–1436. https://doi.org/10.15252/embj.201593518
Panda, D., Goode, B.L., Feinstein, S.C., Wilson, L., 1995. Kinetic stabilization of microtubule dynamics at steady state by tau and microtubule-binding domains of tau. Biochemistry 34, 11117–11127. https://doi.org/10.1021/bi00035a017
Parpura, V., Basarsky, T.A., Liu, F., Jeftinija, K., Jeftinija, S., Haydon, P.G., 1994. Glutamate-mediated astrocyte–neuron signalling. Nature 369, 744–747. https://doi.org/10.1038/369744a0
Perea, J.R., Ávila, J., Bolós, M., 2018. Dephosphorylated rather than hyperphosphorylated Tau triggers a pro-inflammatory profile in microglia through the p38 MAPK pathway. Experimental Neurology 310, 14–21. https://doi.org/10.1016/j.expneurol.2018.08.007
Pîrscoveanu, D.F.V., Pirici, I., Tudoric, V., 2017. Tau protein in neurodegenerative diseases – a review.
Puangmalai, N., Bhatt, N., Montalbano, M., Sengupta, U., Gaikwad, S., Ventura, F., McAllen, S., Ellsworth, A., Garcia, S., Kayed, R., 2020. Internalization mechanisms of brain-derived tau oligomers from patients with Alzheimer's disease, progressive supranuclear palsy and dementia with Lewy bodies. Cell Death Dis 11, 314. https://doi.org/10.1038/s41419-020-2503-3
Quattrone, A., Nicoletti, G., Messina, D., Fera, F., Condino, F., Pugliese, P., Lanza, P., Barone, P., Morgante, L., Zappia, M., Aguglia, U., Gallo, O., 2008. MR imaging index for differentiation of progressive supranuclear palsy from Parkinson disease and the Parkinson variant of multiple system atrophy. Radiology 246, 214–221. https://doi.org/10.1148/radiol.2453061703
Rajmohan, R., Reddy, P.H., 2017. Amyloid-Beta and Phosphorylated Tau Accumulations Cause Abnormalities at Synapses of Alzheimer's disease Neurons. Journal of Alzheimer's Disease 57, 975–999. https://doi.org/10.3233/JAD-160612
Rawat, P., Sehar, U., Bisht, J., Selman, A., Culberson, J., Reddy, P.H., 2022. Phosphorylated Tau in Alzheimer's Disease and Other Tauopathies. Int J Mol Sci 23, 12841. https://doi.org/10.3390/ijms232112841
Regan, P., Piers, T., Yi, J.-H., Kim, D.-H., Huh, S., Park, S.J., Ryu, J.H., Whitcomb, D.J., Cho, K., 2015. Tau phosphorylation at serine 396 residue is required for hippocampal LTD. J Neurosci 35, 4804–4812. https://doi.org/10.1523/JNEUROSCI.2842-14.2015
Reid, M.J., Beltran-Lobo, P., Johnson, L., Perez-Nievas, B.G., Noble, W., 2020. Astrocytes in Tauopathies. Frontiers in Neurology 11.
Robbins, M., Clayton, E., Kaminski Schierle, G.S., 2021. Synaptic tau: A pathological or physiological phenomenon? Acta Neuropathologica Communications 9, 149. https://doi.org/10.1186/s40478-021-01246-y
Sanchez Avila, A., Henstridge, C.M., 2022. Array tomography: 15 years of synaptic analysis. Neuronal Signal 6, NS20220013. https://doi.org/10.1042/NS20220013
Santello, M., Toni, N., Volterra, A., 2019. Astrocyte function from information processing to cognition and cognitive impairment. Nat Neurosci 22, 154–166. https://doi.org/10.1038/s41593-018-0325-8
Schmidt, M.L., Huang, R., Martin, J.A., Henley, J., Mawal-Dewan, M., Hurtig, H.I., Lee, V.M.-Y., Trojanowski, J.Q., 1996. Neurofibrillary Tangles in Progressive Supranuclear Palsy Contain the Same Tau Epitopes Identified in Alzheimer's

Disease PHFtau. Journal of Neuropathology & Experimental Neurology 55, 534–539. https://doi.org/10.1097/00005072-199605000-00006
Schmidt-Kastner, R., Wietasch, K., Weigel, H., Eysel, U.T., 1993. Immunohistochemical staining for glial fibrillary acidic protein (GFAP) after deafferentation or ischemic infarction in rat visual system: features of reactive and damaged astrocytes. Int J Dev Neurosci 11, 157–174. https://doi.org/10.1016/0736-5748(93)90076-p
Sengupta, U., Guerrero-Muñoz, M.J., Castillo-Carranza, D.L., Lasagna-Reeves, C.A., Gerson, J.E., Paulucci-Holthauzen, A.A., Krishnamurthy, S., Farhed, M., Jackson, G.R., Kayed, R., 2015. Pathological Interface Between Oligomeric Alpha-Synuclein and Tau in Synucleinopathies. Biological Psychiatry, Transdiagnosticpathological Mechanisms in Aging 78, 672–683. https://doi.org/10.1016/j.biopsych.2014.12.019
Shafiei, S.S., Guerrero-Muñoz, M.J., Castillo-Carranza, D.L., 2017. Tau Oligomers: Cytotoxicity, Propagation, and Mitochondrial Damage. Frontiers in Aging Neuroscience 9.
Shahidehpour, R.K., Higdon, R.E., Crawford, N.G., Neltner, J.H., Ighodaro, E.T., Patel, E., Price, D., Nelson, P.T., Bachstetter, A.D., 2021. Dystrophic microglia are associated with neurodegenerative disease and not healthy aging in the human brain. Neurobiol Aging 99, 19–27. https://doi.org/10.1016/j.neurobiolaging.2020.12.003
Shields, D.C., Haque, A., Banik, N.L., 2020. Neuroinflammatory responses of microglia in central nervous system trauma. J Cereb Blood Flow Metab 40, S25–S33. https://doi.org/10.1177/0271678X20965786
Simard, A.R., Soulet, D., Gowing, G., Julien, J.-P., Rivest, S., 2006. Bone marrow-derived microglia play a critical role in restricting senile plaque formation in Alzheimer's disease. Neuron 49, 489–502. https://doi.org/10.1016/j.neuron.2006.01.022
Singh, D., 2022. Astrocytic and microglial cells as the modulators of neuroinflammation in Alzheimer's disease. J Neuroinflammation 19, 206. https://doi.org/10.1186/s12974-022-02565-0
Sokolow, S., Henkins, K.M., Bilousova, T., Gonzalez, B., Vinters, H.V., Miller, C.A., Cornwell, L., Poon, W.W., Gylys, K.H., 2015. Pre-synaptic C-terminal truncated tau is released from cortical synapses in Alzheimer's disease. J Neurochem 133, 368–379. https://doi.org/10.1111/jnc.12991
Sonne, J., Reddy, V., Beato, M.R., 2023. Neuroanatomy, Substantia Nigra, in: StatPearls. StatPearls Publishing, Treasure Island (FL).
Sotiropoulos, I., Lopes, A.T., Pinto, V., Lopes, S., Carlos, S., Duarte-Silva, S., Neves-Carvalho, A., Pinto-Ribeiro, F., Pinheiro, S., Fernandes, R., Almeida, A., Sousa, N., Leite-Almeida, H., 2014. Selective impact of Tau loss on nociceptive primary afferents and pain sensation. Exp Neurol 261, 486–493. https://doi.org/10.1016/j.expneurol.2014.07.008
Spires, T.L., Orne, J.D., SantaCruz, K., Pitstick, R., Carlson, G.A., Ashe, K.H., Hyman, B.T., 2006. Region-specific Dissociation of Neuronal Loss and Neurofibrillary Pathology in a Mouse Model of Tauopathy. The American Journal of Pathology 168, 1598–1607. https://doi.org/10.2353/ajpath.2006.050840
Spires-Jones, T.L., Kopeikina, K.J., Koffie, R.M., de Calignon, A., Hyman, B.T., 2011. Are Tangles as Toxic as They Look? J Mol Neurosci 45, 438–444. https://doi.org/10.1007/s12031-011-9566-7

Streit, W.J., Braak, H., Xue, Q.-S., Bechmann, I., 2009. Dystrophic (senescent) rather than activated microglial cells are associated with tau pathology and likely precede neurodegeneration in Alzheimer's disease. Acta Neuropathol 118, 475–485. https://doi.org/10.1007/s00401-009-0556-6
Streit, W.J., Xue, Q.-S., Tischer, J., Bechmann, I., 2014. Microglial pathology. Acta Neuropathol Commun 2, 142. https://doi.org/10.1186/s40478-014-0142-6
Tai, H.-C., Serrano-Pozo, A., Hashimoto, T., Frosch, M.P., Spires-Jones, T.L., Hyman, B.T., 2012. The Synaptic Accumulation of Hyperphosphorylated Tau Oligomers in Alzheimer Disease Is Associated With Dysfunction of the Ubiquitin-Proteasome System. The American Journal of Pathology 181, 1426–1435. https://doi.org/10.1016/j.ajpath.2012.06.033
Togo, T., Dickson, D.W., 2002. Tau accumulation in astrocytes in progressive supranuclear palsy is a degenerative rather than a reactive process. Acta Neuropathol 104, 398–402. https://doi.org/10.1007/s00401-002-0569-x
Torres, A.K., Rivera, B.I., Polanco, C.M., Jara, C., Tapia-Rojas, C., 2022. Phosphorylated tau as a toxic agent in synaptic mitochondria: implications in aging and Alzheimer's disease. Neural Regen Res 17, 1645–1651. https://doi.org/10.4103/1673-5374.332125
Trease, A.J., George, J.W., Roland, N.J., Lichter, E.Z., Emanuel, K., Totusek, S., Fox, H.S., Stauch, K.L., 2022. Hyperphosphorylated Human Tau Accumulates at the Synapse, Localizing on Synaptic Mitochondrial Outer Membranes and Disrupting Respiration in a Mouse Model of Tauopathy. Frontiers in Molecular Neuroscience 15.
Tripathi, T., Khan, H., 2020. Direct Interaction between the β-Amyloid Core and Tau Facilitates Cross-Seeding: A Novel Target for Therapeutic Intervention. Biochemistry 59, 341–342. https://doi.org/10.1021/acs.biochem.9b01087
Violet, M., Delattre, L., Tardivel, M., Sultan, A., Chauderlier, A., Caillierez, R., Talahari, S., Nesslany, F., Lefebvre, B., Bonnefoy, E., Buée, L., Galas, M.-C., 2014. A major role for Tau in neuronal DNA and RNA protection in vivo under physiological and hyperthermic conditions. Front Cell Neurosci 8, 84. https://doi.org/10.3389/fncel.2014.00084
Vogels, T., Murgoci, A.-N., Hromádka, T., 2019. Intersection of pathological tau and microglia at the synapse. Acta Neuropathol Commun 7, 109. https://doi.org/10.1186/s40478-019-0754-y
Volterra, A., Meldolesi, J., 2005. Astrocytes, from brain glue to communication elements: the revolution continues. Nat Rev Neurosci 6, 626–640. https://doi.org/10.1038/nrn1722
Wagshal, D., Sankaranarayanan, S., Guss, V., Hall, T., Berisha, F., Lobach, I., Karydas, A., Voltarelli, L., Scherling, C., Heuer, H., Tartaglia, M.C., Miller, Z., Coppola, G., Ahlijanian, M., Soares, H., Kramer, J.H., Rabinovici, G.D., Rosen, H.J., Miller, B.L., Meredith, J., Boxer, A.L., 2015. Divergent CSF tau alterations in two common tauopathies: Alzheimer's disease and Progressive Supranuclear Palsy. J Neurol Neurosurg Psychiatry 86, 244–250. https://doi.org/10.1136/jnnp-2014-308004
Wang, X., Allen, M., İş, Ö., Reddy, J.S., Tutor-New, F.Q., Castanedes Casey, M., Carrasquillo, M.M., Oatman, S.R., Min, Y., Asmann, Y.W., Funk, C., Nguyen, T., Ho, C.C.G., Malphrus, K.G., Seyfried, N.T., Levey, A.I., Younkin, S.G., Murray, M.E., Dickson, D.W., Price, N.D., Golde, T.E., Ertekin-Taner, N., 2022. Alzheimer's disease and progressive supranuclear palsy share similar

transcriptomic changes in distinct brain regions. J Clin Invest 132, e149904. https://doi.org/10.1172/JCI149904
Wang, Y., Mandelkow, E., 2016. Tau in physiology and pathology. Nat Rev Neurosci 17, 22–35. https://doi.org/10.1038/nrn.2015.1
Ward, S.M., Himmelstein, D.S., Lancia, J.K., Binder, L.I., 2012. Tau oligomers and tau toxicity in neurodegenerative disease. Biochemical Society Transactions 40, 667–671. https://doi.org/10.1042/BST20120134
Weinhard, L., di Bartolomei, G., Bolasco, G., Machado, P., Schieber, N.L., Neniskyte, U., Exiga, M., Vadisiute, A., Raggioli, A., Schertel, A., Schwab, Y., Gross, C.T., 2018. Microglia remodel synapses by presynaptic trogocytosis and spine head filopodia induction. Nat Commun 9, 1228. https://doi.org/10.1038/s41467-018-03566-5
Wiedenmann, B., Franke, W.W., Kuhn, C., Moll, R., Gould, V.E., 1986. Synaptophysin: a marker protein for neuroendocrine cells and neoplasms. Proceedings of the National Academy of Sciences of the United States of America 83, 3500. https://doi.org/10.1073/pnas.83.10.3500
Williams, D.R., de Silva, R., Paviour, D.C., Pittman, A., Watt, H.C., Kilford, L., Holton, J.L., Revesz, T., Lees, A.J., 2005. Characteristics of two distinct clinical phenotypes in pathologically proven progressive supranuclear palsy: Richardson's syndrome and PSP-parkinsonism. Brain 128, 1247–1258. https://doi.org/10.1093/brain/awh488
Wu, M., Zhang, M., Yin, X., Chen, K., Hu, Z., Zhou, Q., Cao, X., Chen, Z., Liu, D., 2021. The role of pathological tau in synaptic dysfunction in Alzheimer's diseases. Transl Neurodegener 10, 45. https://doi.org/10.1186/s40035-021-00270-1
Xie, R., Chung, J.-Y., Ylaya, K., Williams, R.L., Guerrero, N., Nakatsuka, N., Badie, C., Hewitt, S.M., 2011. Factors influencing the degradation of archival formalin-fixed paraffin-embedded tissue sections. J Histochem Cytochem 59, 356–365. https://doi.org/10.1369/0022155411398488
Yamaguchi, T., Wang, H.-L., Morales, M., 2013. Glutamate neurons in the substantia nigra compacta and retrorubral field. Eur J Neurosci 38, 3602–3610. https://doi.org/10.1111/ejn.12359
Yoshida, M., 2014. Astrocytic inclusions in progressive supranuclear palsy and corticobasal degeneration. Neuropathology 34, 555–570. https://doi.org/10.1111/neup.12143
Zamanian, J.L., Xu, L., Foo, L.C., Nouri, N., Zhou, L., Giffard, R.G., Barres, B.A., 2012. Genomic Analysis of Reactive Astrogliosis. J. Neurosci. 32, 6391–6410. https://doi.org/10.1523/JNEUROSCI.6221-11.2012
Zhang, H., Cao, Y., Ma, L., Wei, Y., Li, H., 2021a. Possible Mechanisms of Tau Spread and Toxicity in Alzheimer's Disease. Front Cell Dev Biol 9, 707268. https://doi.org/10.3389/fcell.2021.707268
Zhang, H., Wei, W., Zhao, M., Ma, L., Jiang, X., Pei, H., Cao, Y., Li, H., 2021b. Interaction between Aβ and Tau in the Pathogenesis of Alzheimer's Disease. Int J Biol Sci 17, 2181–2192. https://doi.org/10.7150/ijbs.57078
Zhang, Y., Barres, B.A., 2010. Astrocyte heterogeneity: an underappreciated topic in neurobiology. Curr Opin Neurobiol 20, 588–594. https://doi.org/10.1016/j.conb.2010.06.005
Zhang, Y., Wu, K.-M., Yang, L., Dong, Q., Yu, J.-T., 2022. Tauopathies: new perspectives and challenges. Mol Neurodegener 17, 28. https://doi.org/10.1186/s13024-022-00533-z

Zhou, F.-M., Lee, C.R., 2011. Intrinsic and integrative properties of substantia nigra pars reticulata neurons. Neuroscience 198, 69–94. https://doi.org/10.1016/j.neuroscience.2011.07.061
Ziontz, J., Bilgel, M., Shafer, A.T., Moghekar, A., Elkins, W., Helphrey, J., Gomez, G., June, D., McDonald, M.A., Dannals, R.F., Azad, B.B., Ferrucci, L., Wong, D.F., Resnick, S.M., 2019. Tau pathology in cognitively normal older adults. Alzheimers Dement (Amst) 11, 637–645. https://doi.org/10.1016/j.dadm.2019.07.007